SELF-ASSEMBLY OF AZULENIC MONOLAYER FILMS ON METALLIC GOLD SURFACES

By

Brad Michael Neal

Submitted to the graduate degree program in the Department of Chemistry and the Graduate Faculty of the University of Kansas in partial fulfillment of the requirements for the degree of Doctor of Philosophy.

_____

Chairperson, Dr. Mikhail V. Barybin

_____

Chairperson, Dr. Cindy. L. Berrie

_____

Dr. Kyle V. Camarda

_____

Dr. Timothy A. Jackson

_____

Dr. Shenqiang Ren

Date Defended: June 28, 2012

The Dissertation Committee for Brad Michael Neal

certifies that this is the approved version of the following dissertation:

SELF-ASSEMBLY OF AZULENIC MONOLAYER FILMS ON METALLIC GOLD SURFACES

_____

Chairperson Dr. Mikhail V. Barybin

_____

Chairperson Dr. Cindy L. Berrie

Date approved: July 27, 2012

Abstract

Derivatives of azulene, an unusual nonbenzenoid aromatic hydrocarbon featuring fused five- and seven-membered sp^2 carbon rings, are of substantial current interest in the design of advanced functional materials such as organic electronics. The overarching theme of this dissertation is the chemistry of new hybrid metal/azulene platforms featuring azulenic monolayer films anchored to the atomically flat metallic gold via isocyanide or thiolate junctions. One of the key aspects of this work addresses the influence of the junction group's nature on the formation, stability, reactivity, and physicochemical characteristics of azulenic self-assembled monolayer (SAM) films on the Au(111) surface. Both isocyanide and thiolate "alligator clips" in these SAMs were shown to induce approximately upright orientation of the azulenic framework with respect to the gold surface. The films' properties were evaluated by various means including surface-enhanced infrared spectroscopy and optical ellipsometry.

Of particular significance are the initial examples of molecular films involving all three possible linear biazulenic scaffolds. These SAMs feature isocyanide junction groups and exhibit good stability toward ambient lighting and, in some cases, air atmosphere. Characterization of certain isocyano- and mercaptoazulenic molecular films reported herein was greatly facilitated by incorporation of ancillary nitrile infrared spectroscopic reporters into the azulenic scaffold. Such an approach constitutes a novel strategy in the surface chemistry of organic thiols, to the best of the author's knowledge. In addition, the thesis describes, among other isocyanide/thiol competitive binding investigations, the first monolayer film displacement studies involving the RSH and RNC species with identical substituents R that underscore the higher affinity of the thiolate versus isocyanide junctions for metallic gold. Accessibility of the new monolayer films

reported in this dissertation paves the way for future experimental validation of the theoretically predicted low resistivity of the linear 2,6-azulenic framework.

Acknowledgements

First, allow me to thank my "bosses." Without them, none of the work found herein would have been possible. More importantly, I would not be the chemist or person I am today. With their guidance, I have become a much improved scientist and, through their friendship, a much enriched person. I cannot imagine my graduate career being any better and they are owed much of that credit. Both have pushed, and sometimes pulled, me to heights I never thought I'd see. Misha and Cindy, it has been an honor to work with you and I look forward to our continued friendship in the days ahead. I hope to be as wonderful mentor and dedicated educator as you are.

I would like to thank my lab mates in both the Barybin and Berrie groups, current and past. Andy, thanks for laughing at many of my poorer jokes and pointing out the really bad ones. Anna, it was a pleasure working with you and I hope you learned at least a fraction as much as I did that summer. Chris, you've earned your star permanently in my book. Dave DuBose, thanks for showing me the ropes in the Berrie lab. Dave McGinnis, you are an amazing friend and I've missed you greatly since you've graduated. Greg, thanks for the questions in group meetings that stumped me flat as they've helped me get where I am today. Jen, thanks for all the help and support over the years and telling me I could do it. John, I meant what I said at your wedding, every word. Kolbe, you are a truly honorable man that has my deepest respect. Sasha, without your synthetic skills, where would this chemistry be today? Tiffany, thanks for showing me the ins and outs of the Barybin lab when I first started. Tina, friend, I have immensely enjoyed our conversations over the years. Toshi, you are an amazing chemist, my friend.

Without the love and support of family and friends, where would any of us be? Mom, I love you, but I think I'll keep this degree for myself if you don't mind. Dad, thanks for the encouragement throughout my time here in Kansas. Jason and Stephen, I love you both. Kieran,

I am more appreciative of your love and support than I can express. Grandpa, you inspire me to push myself every day to be better and you mean the world to me.

I'd like to thank the Chemistry Department at the University of Kansas for providing facilities necessary for this work, financial support but most so for the opportunity to develop my teaching skills. Dr. Roderick Black has been especially supportive of my growth in teaching and I am indebted to him for his encouragement and words of wisdom. Tangentially, I'd like to thank my committee members, Dr. Kyle Camarda, Dr. Timothy Jackson, and Dr. Shenqiang Ren, for their time and service toward my defense.

I am grateful for the funding of my research by the NSF CAREER Award (CHE-0548212) and the DuPont Young Professor Award awarded to Dr. Misha Barybin.

To the faculty and staff at Bellarmine University, I give my heartfelt thanks. The chemistry department was exceptionally kind to me and fostered my learning, especially Bob Bernauer. Bob, working for you may have been the most fun job I've ever had and your tutelage was amazing and it is something I hope to emulate in my own career.

Scott, our friendship has been one of my most prized and dear. Through thick and thin, you've been the friend I've needed, and I hope I've been there for you in the same way. I hope that our good times so far have just been a prelude to the future.

The most significant person in my success and work indubitably is my fiancé, Mandi. I can't count the number of times I would have quit chemistry to become a sheep herder in Montana were it not for her love and refusal to allow me to quit on myself. My life has been enhanced through our relationship in ways I did not know were possible. Mandi, I love you and this Thesis is for you. And my degree requirements. But mostly for you.

Table of Contents

List of Tables

List of Figures

List of Schemes

Abbreviations Used in this Thesis

CP-AFM – Conductive Probe – Atomic Force Microscopy

CV – Cyclic Voltammetry

DFT- Density Functional Theory

FMOs – Frontier Molecular Orbitals

HOMO – Highest Occupied Molecular Orbital

HREELS – High Resolution Electron Energy Loss Spectroscopy

HRMS – High Resolution Mass Spectroscopy

LUMO – Lowest Unoccupied Molecular Orbital

MCBJ – Mechanically Controllable Break Junction

ML – Monolayer

NEGF – Non-Equilibrium Green's Function

NEXAFS – Near Edge X-ray Adsorption Fine Structure

SAM – Self-Assemble Monolayer

SERS – Surface Enhanced Raman Spectroscopy

SFG – Sum Frequency Generation

STM – Scanning Tunneling Microscopy

TOF – Time of Flight

TPD – Temperature Programmed Desoprtion

UHV –Ultra High Vacuum

UPS – Ultraviolet Photoelectron Spectroscopy

XPS – X-ray Photoelectron Spectroscopy

CHAPTER I

I. Self-Assembly of Organic Isocyanides and Thiols on Metal Surfaces: Background, Methods, and Analytical Techniques

Portions of this work have been published in:

Barybin, M. V.; Meyers, J. J., Jr.; Neal, B. M. Renaissance of Isocyanoarenes as Ligands in Low-Valent Organometallic Chemistry. In *Isocyanide Chemistry: Applications in Synthesis and Material Science*. Nenajdenko, V., Ed. Wiley-VCH: Weinheim, 2012, pp 493-529. (ISBN-10: 3-527-33043-7).

I.1 Introduction: Background and experimental methods employed in this Thesis

Azulene is a blue, nonbenzenoid aromatic hydrocarbon isomer of naphthalene composed of edge sharing five- and seven-membered rings. The electronic properties of the azulenic motif are intriguing due to its non-mirror related frontier molecular orbitals, intrinsic dipole, and narrow HOMO-LUMO gap, all of which make it attractive for applications in organic nanoelectronics.

This Thesis is focused on the formation, characterization, and properties of novel azulene-based molecular films on metallic gold. To set the stage for the research discussed in the following Chapters, several relevant experimental methods and techniques are introduced herein. These include optical ellipsometry and surface enhanced grazing angle infrared spectroscopy.

I.1.1 Optical Ellipsometry

Ellipsometry is an optical technique that relies on changes in the polarization of plane-polarized light impinged on a surface to assess certain properties of a thin film on that surface. [1-5] Ellipsometric measurements provide important and accurate information regarding thickness of very thin films on surfaces. The nondestructive nature of an ellipsometric experiment makes ellipsometry a powerful tool for self-assembled monolayer (SAM) characterization that offers angstrom level sensitivity to thickness heights when appropriate wavelength and intensity of the laser are used.

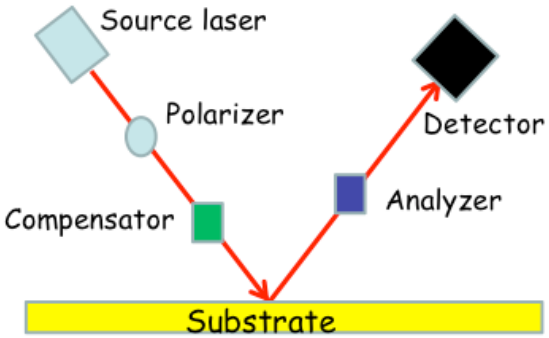

Figure I.1 - Schematic representation of a nulling ellipsometric experiment

Figure I.1 shows the basic schematic of a nulling ellipsometer. [2] The source laser is often a HeNe laser, which produces a nearly monochromatic light. The light from the laser first passes through a polarizer, where it is linearly plane-polarized before entering the compensator. In the compensator, the phases of the light are shifted with respect to one another. [1-4] For a typical, single-wavelength ellipsometer, a quarter-wave plate is used, which results in the two phases being 90° with respect to each other, thus causing the light to become elliptically polarized. [2] The elliptically polarized light then hits and is reflected off the surface, thereby changing the polarization of the light further through interaction of the light with the material that the light was transmitted through at the interface. Subsequently, the light enters an analyzer and passes through to the detector, often a photomultiplier tube. At this point, the analyzer is rotated until a null, a minimum of the signal, is found. By considering the alignments of the polarizer, the compensator, and the analyzer when the null is found, it is possible to calculate optical properties of the surface substrate. [3]

At the beginning of an ellipsometric experiment, it is important to determine optical properties of the substrate. Of particular importance are its index of refraction, n, and its extinction coefficient, k. These two parameters are related by the equation for the complex index of refraction, given by Equation 1, where i is an imaginary number. [4]

$$\tilde{N} = n - ik \quad (1)$$

The index of refraction is defined as

$$n = c/s \quad (2)$$

where n is the index of refraction, c is the speed of light in a vacuum, and s is the speed of light in the particular medium of interest. [5] As evident, if the value of n is high, the speed of light in a particular medium is slow. The extinction coefficient, *k*, measures exactly how quickly the intensity of the light decreases as the light passes through a material. [4] The absorption coefficient, α, can be related to *k* by

$$\alpha = (4\pi k)/\lambda \quad (3)$$

where λ is the wavelength of light in a vacuum.

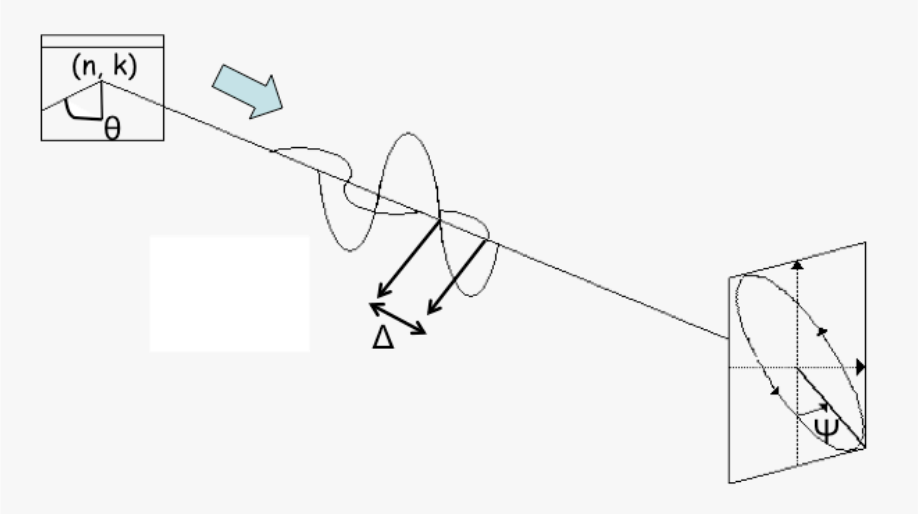

Figure I.2 – Schematic representation of the change in phase and amplitude in an ellipsometric experiment

Figure I.2 illustrates the basic principle of ellipsometry with respect to the changes experienced by the polarized light. Once the elliptically polarized light reflects off the surface at

an angle θ, the two polarizations that make up the plane-polarized light become out of phase and amplitude, measured by Δ and Ψ, respectively. [5] By determining these changes, it is possible to obtain the values of n and k experimentally. Once n and k, the optical constants, are determined, the thickness of a film on the surface can be calculated. While such calculations can, in principle, be done by hand, they are usually automated by a computer. Additionally, a good model of the structure of the film is necessary to calculate the thickness of the film on the surface.

I.1.2 Surface-enhanced Infrared Spectroscopy

While the premise is the same, Reflection Absorption Infrared Spectroscopy (RAIRS) has many acronyms such as RAIR, IRRS, IRRAS, FT-IRAS, RAS, GIR, IR-ERS, ERIR, and FT-IRRAS. [6] The selection rules for infrared spectroscopy have been addressed in numerous literature sources. [6,7] In the case of SAM films and other species on surfaces, these rules must take into consideration additional factors, such as molecular orientation on the surface and polarization of the incident radiation. For these systems, the intensity of the absorption will be proportional to the square of the product of

$$E_j * \mu' = |\mathrm{E}|\,|\mu'|\cos\theta \qquad (4)$$

where θ is the angle between μ', the direction of the dipole of the vibration, and E, the vector of the incident radiation. [6] Thus, the polarized component of the incident radiation that is properly aligned with the dipole of the vibration will result in a much greater observed signal than that arising from a non-aligned polarized component. This phenomenon, illustrated in Figure 3, is behind the surface IR selection rules on metal surfaces.

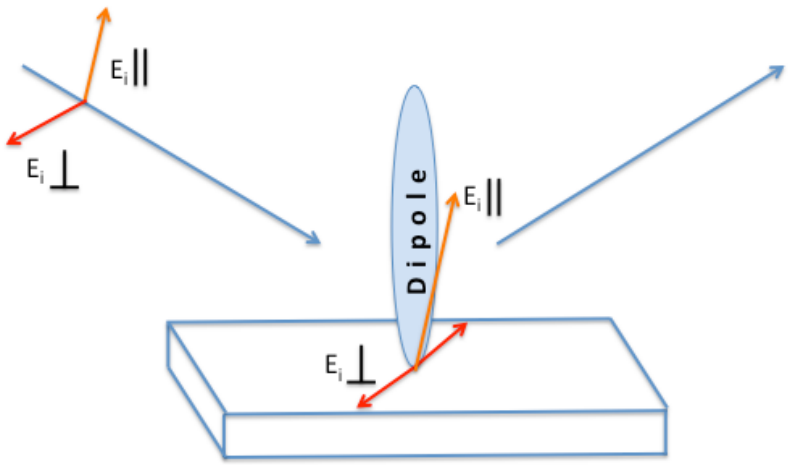

Figure I.3 - The incident radiation, E_i, featuring two polarizations. The parallel and perpendicular (with respect to the surface) components both reach the surface but only the parallel component enhances the dipole on the surface.

As shown in Figure I.3, it is, therefore, possible to distinguish between the parallel and perpendicular orientations of a dipole on the surface. If the dipole is parallel, the metal will form a image dipole in the metal at the interface, thereby effectively decreasing the expected signal. If the dipole is perpendicular, the formed image in the metal will be additive and the observed signal will be amplified, as shown in Figure I.4. [6] This phenomenon has been used extensively to study SAMs of organic isocyanides adsorbed on metal surfaces to determine their molecular orientations, as summarized in Table I.1 found later in this Chapter.

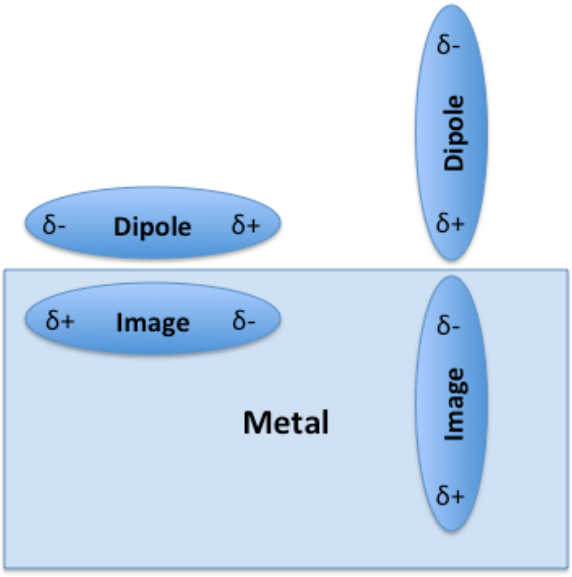

Figure I.4 - The dipole, and its corresponding image formed in the metal at the interface. Left: The dipole's signal is effectively canceled by its image in the metal. Right: The dipole's signal is enhanced by its image in the metal. [6]

I.1.3 Au(111) substrates and methods for preparation thereof

Many of the experiments described herein involved Au(111) substrates. The term Au(111) denotes the (111) face, a particular packing slice, or plane, of gold's crystalline lattice. It is ideal to use substrates that have a single crystal face so that coordination of the ligands may be understood with respect to a particular orientation defined by the available adsorption sites. Single crystalline gold adopts a face-centered cubic crystal structure. [8] The Miller indeces indicate where the plane of the surface will intercept on the x-, y- and z- coordinates of the unit cell [9], as illustrated in Figure 5.

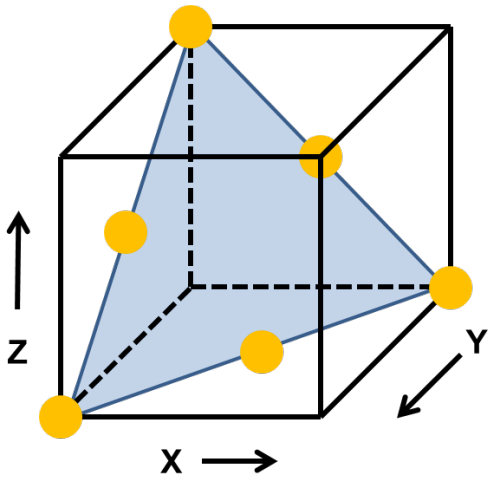

Figure I.5 - Representation of the (111) plane in an fcc crystal [9].

As shown in Figure I.5, the fcc crystal packing structure can be sliced by a plane to include the (100), (010), and (001) positions, shown as the three atoms in shown in the corners of the cube, points in the unit cell. This is the (111) plane exhibited by single crystalline gold depicted in Figure I.5.

While there are a variety of methods to prepare Au(111) substrates, the samples used in the experiments reported in this Thesis were obtained by vapor deposition techniques, either on freshly cleaved mica or on silicon substrates coated with an adhesion layer of titanium metal prior to gold coating. The vapor deposition of gold on mica is a well-understood process that has been employed throughout the literature. [10-12] Simply put, pure gold wire is placed in an evaporator much like the one shown in Figure 6.

Figure I.6 - Edwards Rotary Evaporator used for coating substrates

The chamber pressure is reduced to very low pressures, such as 1.0×10^{-7} torr, while the chamber is being heated. Once sufficiently low vacuum and adequately high temperatures are achieved, a current is run through the gold wire which begins melting and quickly vaporizes. The gaseous gold is then deposited onto the substrate until the desired thickness is reached, as measured by a the change in resonance frequency of the quartz crystal due to the mass change in a quartz crystal microbalance. In the case of silicon substrates, a similar process is used to deposit a coating of gold onto films of titanium previously coated on the silicon. The titanium adhesion layer is necessary for proper formation of gold-coated silicon substrates because gold coated directly onto silicon results in poor adhesion of the gold, which is prone to flaking of the gold off the silicon.

I.2 Self-Assembled Monolayer Films of Nonbenzenoid Isocyano- and Diisocyanoarenes on Gold Surfaces

This section constitutes excerpts from a book chapter recently co-authored by the author of the Thesis: Barybin, M. V.; Meyers, J. J., Jr.; Neal, B. M. Renaissance of Isocyanoarenes as Ligands in Low-Valent Organometallic Chemistry. In *Isocyanide Chemistry: Applications in Synthesis and Material Science*. Nenajdenko, V., Ed. Wiley-VCH: Weinheim, 2012, pp 493-529. (ISBN-10: 3-527-33043-7). It provides a brief introduction to the investigations of self-assembled monolayers formed from these interesting new systems.

Chemisorption of isocyanoarenes on metal surfaces to yield the corresponding self-assembled monolayer (SAM) films provides valuable initial platforms for a variety of potential nanotechnological applications, including organic electronics. [13-20] A recent review by Angelici and Lasar [21] gives a detailed account of adsorption of organic isocyanides on gold, silver, copper, platinum, palladium, nickel, rhodium, and chromium metal surfaces. [21] Adsorption of isocyanides on various gold surfaces, including Au(111) films, gold powder, and gold nanoparticles, is of particular practical interest due to the oxidative stability of gold in ambient atmosphere. A large body of experimental and theoretical studies indicates that organic isocyanides adsorb on gold in the terminal upright (η^1) fashion with only the isocyanide carbon atom interacting with the surface.[21] Upon adsorption of a benzenoid isocyanide molecule to a gold surface, the energy of the ν_{NC} band shifts to higher energy, typically by 50 – 80 cm^{-1}, compared to that of free isocyanide, seen in Table 1 *vide infra.* [22] This is a consequence of the isocyanide carbon's lone pair, which interacts with Au, being somewhat antibonding with respect to the C≡NR π-bond.

Self-assembly of many benzenoid isocyanoarenes on gold surfaces requires sample handling and storage under inert atmosphere to avoid marked deterioration of the isocyanide

groups to isocyanates, RN=C=O, which give a characteristic stretching band at around 2270 cm^{-1} in their infrared spectra. [10, 12] Polydentate isocyanoarenes that can adsorb to the gold surface via multiple isocyanide junctions constitute a notable exception in this regard. For example, SAMs of tetraisocyano-*meta*-cyclophane (TIMC), the structure of which is shown in Figure 1, exhibit enhanced kinetic stability toward gold-promoted oxidation. The reflection-absorption IR spectra of the SAMs of this tetraisocyanide, which are prepared and stored in air without exclusion of ambient lighting, indicate the absorption of TIMC to the Au(111) surface via all four of its isocyanide groups (Figure I.7) and lack any features that could be attributed to isocyanate formation. [23]

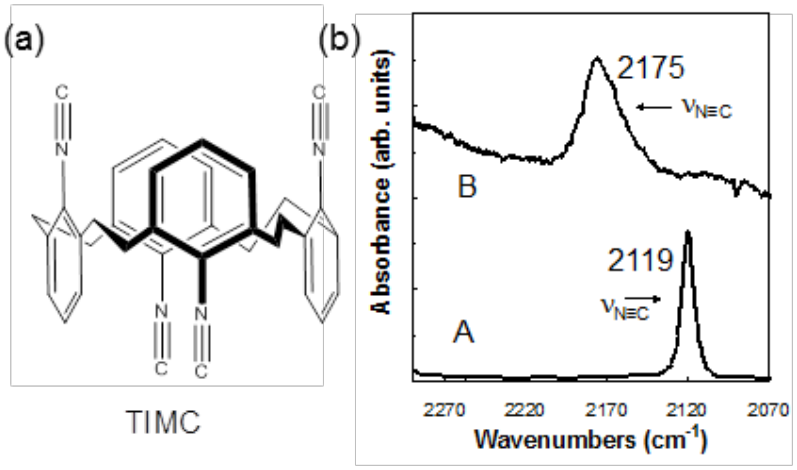

Figure I.7 - (a) Structure of TIMC. (b) IR spectrum of TIMC in CH_2Cl_2 solution (bottom) and reflection-absorption IR spectrum of a SAM film of TIMC on Au(111). [23]

With the exception of isocyanoferrocene, all isocyanoarenes known until the early 2000's possessed benzenoid aryl substituents. [24] Recently, we have established a new class of isocyanoarenes incorporating the nonbenzenoid aromatic system of azulene. [24] Azulene is an unusual hydrocarbon composed of fused 5- and 7-membered rings (Figure I.8). Figure I.9 shows

isocyanoazulene compounds, together with their corresponding abbreviations, reported by our group to date. [25-29] Given the polar nature of the azulenic scaffold (Figure I.8), these species can be considered stable derivatives of the hypothetical isocyanocyclopentadienide anion or isocyanotropylium cation. [24] The isocyanoazulenes in Figure I.9 are all crystalline substances that exhibit good thermal stability (except CN^6Az and CN^2Az^{CN}) and can be considered air-stable for practical purposes.

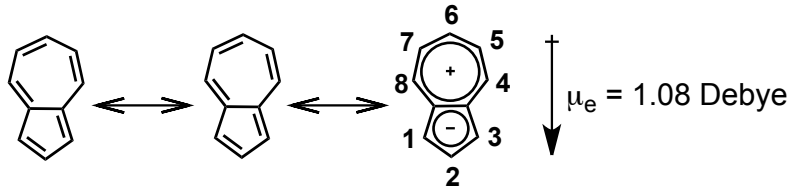

Figure I.8 - The resonance forms of azulene emphasizing the polar nature and numbering scheme of the azulenic scaffold. [24]

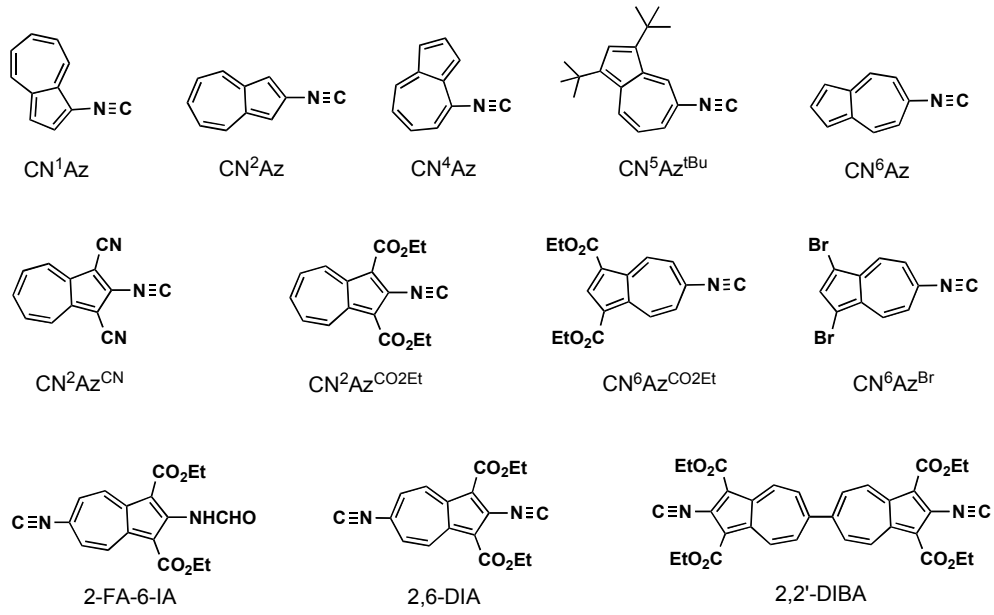

Figure I.9 - Structures and the corresponding abbreviations of the isocyanoazulene derivatives known to date. [30]

As shown in Figure I.10a, the frontier molecular orbitals of azulene have complementary density distributions, so the general reactivity profile of the azulenic scaffold is governed by the rules summarized in Figure I.10b. Notably, preparation of 2-substituted azulenes almost always requires having an appropriate substituent in place before closing the azulenic ring due to the quite unreactive nature of the C-H bond at the 2-position of the azulenic framework. The "parent" isocyanoazulenes $CN^{1}Az$, $CN^{4}Az$, $CN^{6}Az$, as well as the di-*t*-butyl derivative $CN^{5}Az^{tBu}$, can all be accessed regioselectively from azulene itself. [24, 26]

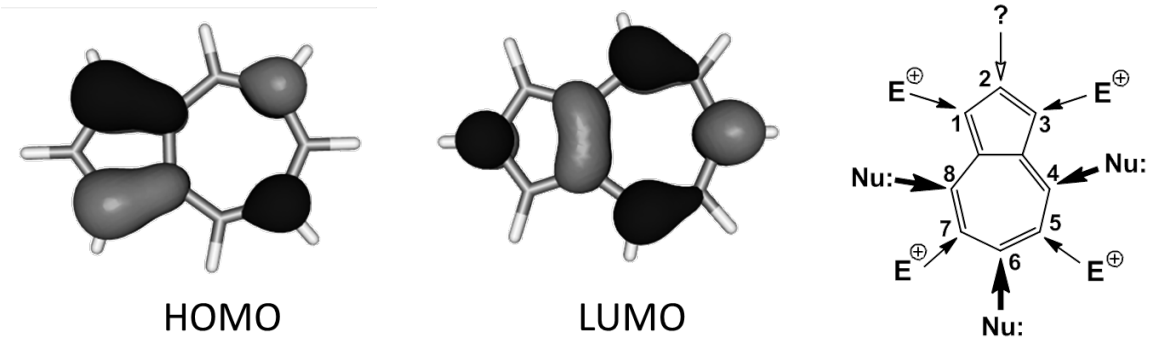

Figure I.10 - (a) Lowest unoccupied molecular orbital (LUMO) and highest occupied molecular orbital (HOMO) of azulene. (b) Sites of nucleophilic (Nu:) and electrophilic (E^{+}) attacks of the azulenic scaffold as general strategies for its functionalization. Adapted with permission from Ref. 24.

The isocyanoazulenes $CN^{2}Az$, $CN^{2}Az^{CN}$, $CN^{2}Az^{CO2Et}$, $CN^{6}Az$, $CN^{6}Az^{CO2Et}$, 2-FA-6-IA, 2,6-DIA, both isomers of $(OC)_5Cr(\eta^{1}$-2,6-DIA), and 2,2'-DIBA formed well-defined SAM films on the Au(111) surface. [11, 28, 29] These films were prepared without precautions to exclude air and ambient lighting. The grazing angle reflection absorption IR spectra of these films, along with ellipsometric film thickness measurements, suggest approximately terminal upright coordination of the molecules in all of these SAMs (Table I.1).

Table I.1 - Infrared vibrational data for selected isocyanoarenes before and after adsorption on gold surfaces

Molecule	**ν_{NC} of free isocyanoarene, cm^{-1}**	**ν_{NC} of surface bound isocyanide, cm^{-1}**	**ν_{XY} of ancillary reporter, cm^{-1}**	**Observed (Theoretical) thickness, Å**	**Reference**
DIB	2125	2181	2120 (isocyanide)	10 (10.3)	22
DIB	2127	2170	2122 (isocyanide)	Not reported	20
DIB	2129	2172	2121 (isocyanide)	12.7 (10.3)	12
DIBP	2126	2121	2191 (isocyanide)	14 (14.6)	22
DIBP	2127	2121	2190 (isocyanide)	13.9 (14.7)	12
TIMC	2119	2175	-	5.8±5 (6.4)	23
CN^2Az	2127	2174	-	Not reported	11
CN^6Az	2117	2176	-	Not reported	11
CN^6Az^{Br}	2115	2179	-	Not reported	11
2-FA-6-IA	2116	2170	-	Not reported	11
CN^2Az^{CO2Et}	2127	2169	-	8±1 (10.5)	11
CN^6Az^{CO2Et}	2115	2178	-	11±3 (12.5)	11
2,6-DIA	2116, 2125	2163	2117 (isocyanide)	14±1 (12.5)	11
2,2'-DIBA	2130	2170	2119 (isocyanide)	20.5±2.4 (19.1)	28
CN^2Az^{CN}	2114	2156	2214 (nitrile)	11.7±0.6 (10.7)	29
DIF	2118	2181	-	14.1 (8.8)	31, 32

See Figures 7, 9,11 for structures corresponding to the abbreviations. DIB = 1,4-diisocyanobenzene, DIBP = 4,4'-diisocyanobiphenyl.

The IR solution spectrum of the $(OC)_5Cr(\eta^1$-2,6-DIA) isomer shown in Figure I.11a features four IR-active bands in ν_{NC} and ν_{CO} stretching regions. [11, 24] The ν_{NC} bands at 2115 and 2135 cm^{-1} correspond to the free isocyanide terminus and the Cr-bound isocyanide group, respectively (Figure I.11b). The other two more intense bands at 2043 and 1962 cm^{-1} are due to $\nu_{CO}(A_1)$ and $\nu_{CO}(E)$ vibrations associated with the $[Cr(CO)_5]$ moiety. Upon SAM film formation on Au(111), the band at 2115 cm^{-1} moves to 2174 cm^{-1}, thereby indicating coordination of the free isocyanide group of $(OC)_5Cr(\eta^1$-2,6-DIA) to the gold surface (Figure 11c). In addition, the relative intensities of the $\nu_{CO}(A_1)$ and $\nu_{CO}(E)$ bands change dramatically compared to the solution spectrum, which suggests approximately parallel orientation of the equatorial carbonyl ligands to the metal surface and, thus, upright coordination of the entire molecule on the surface. The measured ellipsometric thickness of the SAM of this $(OC)_5Cr(\eta^1$-2,6-DIA) complex on Au(111) is 18(2) Å, which is practically identical to the expected thickness value of 17 Å for the perfectly upright orientation on the gold surface.

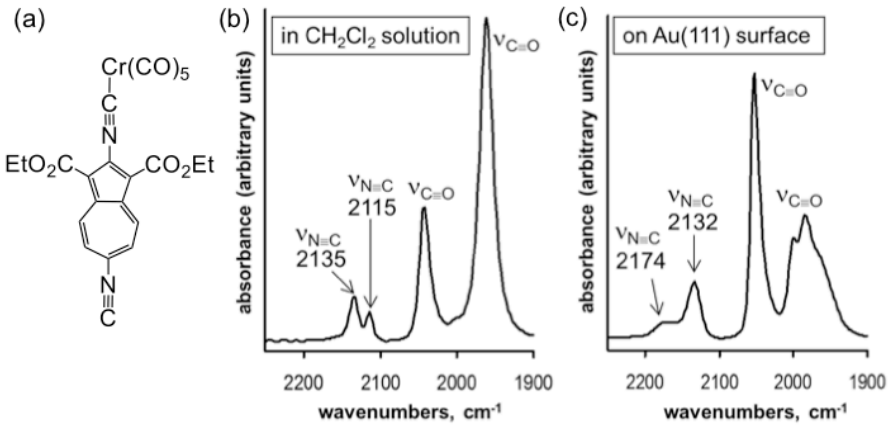

Figure I.11 – (a) IR spectrum of the mononuclear complex $[(OC)_5Cr]$(eta^1-2,6-DIA) in CH_2Cl_2 solution (the $[(OC)_5Cr]$ fragment is bound to the 2-isocyanide terminus of 2,6-DIA); (b) Reflection-absorption IR spectrum of $[(OC)_5Cr]$(eta^1-2,6-DIA) absorbed on Au(111).[24]

Comparison of the reflection-absorption IR spectra for the SAMs of 2,6-DIA with those for the SAMs of CN^2Az^{CO2Et} and CN^6Az^{CO2Et} on Au(111) suggests that the diisocyanoazulene 2,6-DIA preferentially binds to the gold surface via its 2-isocyano group, which is a slightly better electron donor than the 6-isocyano terminus (Table I.1) [11]. SAM films of the diisocyanobiazulene 2,2'-DIBA also feature terminal upright coordination of this nearly 2 nm long molecule [28] (please, see Chapter 2 for further discussion). These SAM films of 2,6-DIA and 2,2'-DIBA pave the way for the opportunity to probe the conductivity properties of linear molecular wires based on the 2,6-azulenic scaffold.

Finally, Siemeling *et al.* reported that DIF forms well-ordered SAM films on Au(111) and coordinates via both of its isocyanide groups to the metal surface. The ν_{NC} value of 2118 cm^{-1} blue shifts to 2181 cm^{-1} upon adsorption. In addition, the dipodal adsorption mode of DIF Au(111) was indicated by X-ray photoelectron spectroscopy measurements which showed single N(1s) emission [31, 32].

I.3 References

1 Azzam, R. M. *Ellipsometry and Polarized Light*, North Holland: New York, 1977; pp 153-268.

2 Tompkins, H. G. *Spectroscopic Ellipsometry and Reflectometry: A User's Guide*, Wiley: New York, 1999; pp 9-15, 42.

3 Rudolph Research. Auto EL-III Automatic Ellipsometer Instruction Manual; New Jersey, 1984; pp 1-4.

4 Tompkins, H. G. *A User's Guide to Ellipsometry*, Academic Press: Boston, 1993: pp 9.

5 Fukiwara, H. *Spectroscopic Ellipsometry: Principles and Applications*, Wiley & Sons: Chichester, England, 2007; pp 19, 82.

6 Aroca, R. *Surface-enhanced Vibrational Spectrscopy*, Wiley, Chichester, England, 2006; pp 64, 60, 65.

7 Harris, C. H.; Bertolucci, M. D. *Symmetry and Spectroscopy An Introduction to Vibrational and Electronic Spectroscopy*, Oxford University Press: New York, 1978; pp 151-159.

8 Cotton, F.A., Wilkinson, G. *Advanced Inorganic Chemistry, Fifth Edition*, John Wiley & Sons: New York, 1988; pp 938.

9 Attard, G., Barnes, C. Surfaces, Oxford University Press: New York, 1998; pp 18.

10 Stapleton, J.J., Daniel, T.A., Uppili, S., Cabarcos, O.M., Naciri, J., Shashidhar, R., Allara, D.L. Self-assembly, characterization, and chemical stability of isocyanide-bound molecular wire monolayers on gold and palladium surfaces. *Langmuir*, **2005**, *21* (24), 11061-11070.

11 DuBose, D.L., Robinson, R.E., Holovics, T.C., Moody, D.R., Weintrob, E.C., Berrie, C.L., Barybin, M.V. Interaction of mono- and diisocyanoazulenes with gold surfaces: First examples of self-assembled monolayer films involving azulenic scaffolds. *Langmuir*, **2006,** *22* (10), 4599-4606.

12 Swanson, S.A., McClain, R., Lovejoy, K.S., Alamdari, N.B., Hamilton, J.S., Scott, J.C. Self-assembled diisocyanide monolayer films on gold and palladium. *Langmuir*, **2005**, *21* (11), 5034-5039.

13 Hong, S., Reifenberger, R., Tian, W., Datta, S., Henderson, J., Kubiak, C.P. Molecular conductance spectroscopy of conjugated, phenyl-based molecules on Au(111): The effect of end groups on molecular conduction. *Superlattices and Microstructures* **2000,** *28*, 289-303.

14 Chen, J., Wang, W., Klemic, J., Reed, M.A., Axelrod, B.W., Kaschak, D.M., Rawlett, A.M., Price, D.W., Dirk, S.M., Tour, J.M., Grubisha, D.S., Bennett, D.W. Molecular wires, switches, and memories. *Annals of the New York Academy of Sciences* **2002,** *960*, 69-99.

15 McCreery, R. Molecular electronic junctions. *Chemistry of Materials*, **2004**, *16* (23), 4477-4496.

16 Choi, S.H., Kim, B., Frisbie, C.D. () Electrical resistance of long conjugated molecular wires. *Science*, **2008**, *320* (5882), 1482-1486.

17 Samori, P., Cacialli F.Eds. *Functional Supramolecular Architectures: For Organic Electronics and Nanotechnology*, Volume 1–2; Wiley-VCH: Weinheim, 2011.

18 Chu, C., Ayers, J.A., Stefanescu, D.M., Walker, B.R., Gorman, C.B., Parsons, G.N. Enhanced conduction through isocyanide terminal groups in alkane and biphenylene molecules measured in molecule/nanoparticle/molecule junctions. *Journal of Physical Chemistry C*, **2007**, ***111*** (22), 8080-8085.

19 Kim, B., Beebe, J.M., Jun, Y., Zhu, X.-Y., Frisbie, C. D. Correlation between HOMO

alignment and contact resistance in molecular junctions: aromatic thiols versus aromatic isocyanides. *Journal of the American Chemical Society*, **2006**, *128* (15), 4970-4971.

20 Murphy, K.L., Tysoe, W.T., Bennett, D.W. A comparative investigation of aryl isocyanides chemisorbed to palladium and gold: An ATR-IR spectroscopic study. *Langmuir*, **2004**, *20* (5), 1732–1738.

21 Lazar, M. and Angelici, R.J. Isocyanide binding modes on metal surfaces and in metal complexes, In *Modern Surface Organometallic Chemistry*; Basset, J.-M. Psaro, R., Roberto D., Ugo, R., Eds, Wiley-VCH, Weinheim, 2009 pp. 513–556.

22 Henderson, J.I., Feng, S., Bein, T., Kubiak, C.P. Adsorption of diisocyanides on gold. *Langmuir*, **2000**, *16* (15), 6183-6187.

23 Toriyama, M., Maher, T.R., Holovics, T.C., Vanka, K., Day, V.W., Berrie, C.L., Thompson, W.H., Barybin, M.V. Multipoint anchoring of the [2.2.2.2]metacyclophane motif to a gold surface via self-assembly: Coordination chemistry of a cyclic tetraisocyanide revisited. *Inorganic Chemistry*, **2008**, *47* (8), 3284-3291.

24 Barybin, M.V. Nonbenzenoid aromatic isocyanides: New coordination building blocks for organometallic and surface chemistry. *Coordination Chemistry Reviews*, **2010**, *254* (11-12), 1240-1252.

25 Robinson, R.E., Holovics, T.C., Deplazes, S.F., Lushington, G.H., Powell, D.R., Barybin, M.V. (2003) First isocyanoazulene and its homoleptic complexes. *Journal of the American Chemical Society*, **125** (15), 4432-4433.

26 Robinson, R.E., Holovics, T.C., Deplazes, S.F., Powell, D.R., Lushington, G.H., Thompson, W.H., Barybin, M.V. Five possible isocyanoazulenes and electron-rich complexes thereof: A quantitative organometallic approach for probing electronic inhomogeneity of the azulenic framework. *Organometallics*, **2005**, *24* (10), 2386-2397.

27 Holovics, T.C., Robinson, R.E., Weintrob, E., Toriyama, M., Lushington, G.H., Barybin, M.V. The 2,6-diisocyanoazulene motif: Synthesis and efficient mono- and heterobimetallic complexation with controlled orientation of the azulenic dipole. *Journal of the American Chemical Society*, **2006,** *128* (7), 2300-2309.

28 Maher, T.R., Spaeth, A.D., Neal, B.M., Berrie, C.L., Thompson, W.H., Day, V.W., Barybin, M.V. Linear 6,6'-biazulenyl framework featuring isocyanide termini: Synthesis, structure, redox behavior, complexation, and self-assembly on Au(111). *Journal of the American Chemical Society*, **2010**, *132* (45), 15924-15926.

29 Neal, B.M., Vorushilov, A.S., DeLaRosa, A.M., Robinson, R.E., Berrie, C.L., Barybin, M. V. Ancillary nitrile substituents as convenient IR spectroscopic reporters for self-assembly of mercapto- and isocyanoazulenes on Au(111). *Chemical Communications*, **2011**, *47* (38), 10803-10805.

30 Barybin, M. V.; Meyers, J. J., Jr.; Neal, B. M. Renaissance of Isocyanoarenes as Ligands in Low-Valent Organometallic Chemistry. In *Isocyanide Chemistry: Applications in Synthesis and Material Science*. Nenajdenko, V., Ed. Wiley-VCH: Weinheim, 2012, pp 493-529. (ISBN-10: 3-527-33043-7).

31 Siemeling, U., Rother, D., Bruhn, C., Fink, H., Weidner, T., Träger, F., Rothenberger, A., Fenske, D., Priebe, A., Maurer, J., Winter, R., The interaction of 1,1'-diisocyanoferrocene with gold: Formation of monolayers and supramolecular polymerization of an aurophilic ferrocenophane. *The Journal of the American Chemical Society,* **2005**, *127* (4), 1102-1103.

32 Weidner, T., Ballav, N., Zharnikov, M., Priebe, A., Long, N.J., Winter, R., Rothenberger, A., Fenske, D., Rother, D., Bruhn, C., Fink, H., Siemeling, U. Dipodal ferrocene-based adsorbate molecules for self-assembled monolayers on gold. *Chemistry – A European Journal*, **2008**, *14* (14), 4346-4360.

CHAPTER II

II. Self-assembled Monolayer Films of Biazulenyl Isocyanides

Portions of this work have been published in:

Maher, T.R., Spaeth, A.D., Neal, B.M., Berrie, C.L., Thompson, W.H., Day, V.W., Barybin, M.V. Linear 6,6'-biazulenyl framework featuring isocyanide termini: Synthesis, structure, redox behavior, complexation, and self-assembly on Au(111). *Journal of the American Chemical Society*, **2010**, *132* (45), 15924-15926.

II.1 Introduction

As the quest for miniaturizing electronics continues to gain momentum, new materials are critical for driving progress in this field. In 1974, Aviram and Ratner described the use of organic molecules as rectifiers. [1] Since then, there has been a considerable effort invested in the design of molecular wires, diodes, fuses, switches and resists, as will be discussed herein. In particular, conjugated organic linkers have been explored as molecular wires for bridging electron domains. Molecular systems include at least three parts as seen in Figure 1 below: 2 junction regions between the molecule and the contacts and the central region of the molecule itself. The nature of the junction group used to chemisorb organic molecules to a metal has a profound effect on the conductivity characteristics of the corresponding molecular films as will be illuminated *vide infra*. The thiolate group has been, by far, the most studied junction unit. While a number of excellent reviews on various aspects of the thiol chemistry in the context of molecular films available [2], the surface chemistry of organic isocyanides has been explored to lesser extent. For a discussion comparing the two junction groups, please see the Introduction section to Chapter 4. This Introduction will focus mainly on the chemistry of isocyanide molecules on surfaces.

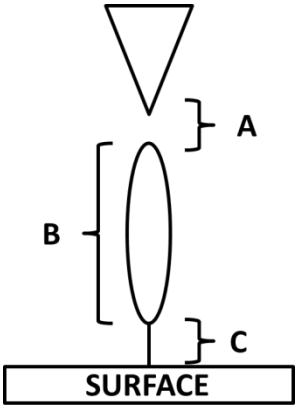

Figure II. 1 - Conductance of an electron through a molecular junction has many interfaces. A - Between the junction and the probe. B – Through the molecule. C – Between the junction group of the molecule and the surface.

Despite the fact that a reasonable consensus among researchers regarding binding modes of organic isocyanides on various metal surfaces has been achieved over the past 15 years, experimental differentiation between some of the suggested modes is, indeed, challenging. Figure 2 illustrates a few of the suggested interactions of isocyanides with metallic surfaces. A thorough review on this topic that systematically addresses isocyanide films on specific metal surfaces has been recently published by Angelici. [3] Additionally, self-assembly of organic isocyanides on metal surfaces, as well as physicochemical properties of the resulting thin films, has been subject of several reviews. [4-6]

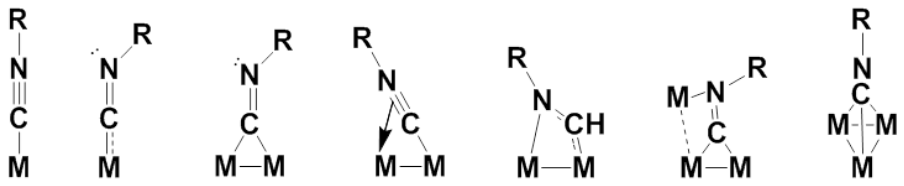

Figure II. 2 – Possible geometries for isocyanide coordination. Adapted from Ref. 3.

The following sections provide an overview of recent advances in the field with the primary focus on self-assembled monolayer (SAM) films of isocyanoarenes on gold relevant to potential applications in molecular electronics. First, packing and orientation of isocyanoarene molecules in the corresponding monolayers will be discussed. Second, several aspects of molecular conductance of isocyanoarenes, as determined by a variety of the state-of-the-art techniques, will be explored and compared. Last, first principle studies toward the applications and uses of isocyanoarenes in the molecular electronics will be discussed.

II.1.1. Packing and orientation

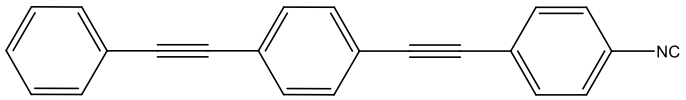

Figure II. 3 - OPE-NC

The packing and orientation of molecular films are of critical importance for use in electronics applications and these SAM characteristics have been subject of much research. Numerous examples of both alkyl and aryl isocyanide SAM films on gold surfaces have been described. For example, Allara and coworkers studied adsorption of 4,4′-di(phenylene-ethynylene)benzene (Figure II.3), a member of the family of OPE molecules, on Au(111) surfaces. [7] By monitoring the position of the NC stretching band in the infrared reflection spectra of the resulting SAM films under various conditions, the nature and stability of the gold-isocyanide bond was elucidated. A substantial blue shift of the N≡C stretching band upon coordination of the isocyanide molecules to the gold surface indicated primarily σ-donor function of the isocyanide junction group. Based on

the surface infrared spectroscopy selection rules and a quantitative analysis, an upright orientation of the isocyanoarene molecules with respect to the metal surface was suggested. X-ray photoelectron spectroscopic measurements, in conjunction with RAIR experiments, indicated oxidation of the bound isocyanide junction to isocyanate, N=C=O, upon exposure of the monolayer film to both ambient air atmosphere and to ozone. In another experiment involving OPE-NC adsorbed on Au(111), the initial measurable growth of the IR band signifying oxidation of the isocyanide junction to isocyanate took approximately one hour. [8] A complete oxidation occurred when the films were exposed to ambient laboratory atmosphere for six days.

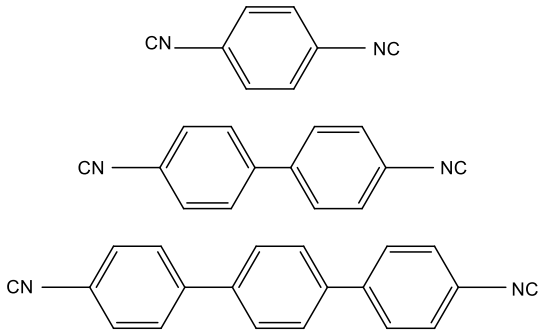

Figure II. 4. – From top to bottom: the structures of PDI, BPDI, and TPDI.

For the SAM films containing linear diisocyanoarenes, the oxidation process appears to involve the free, non-coordinating isocyanide group. Swanson *et al*. described monolayers of polyphenylene diisocyanides, shown in Figure 4, and their adsorption to Au(111) surfaces. Using reflection absorption infrared spectroscopy and grazing-angle attenuated total reflection IR, three signals in the region 2100 -2300 cm^{-1} were observed in that study. The lowest energy band at ca. 2120 cm^{-1} was attributed to a non-coordinating isocyanide group, the middle peak at ca. 2170 cm^{-1} was assigned to a

surface-bound isocyanide, and the highest energy band at ca. 2270 cm^{-1} was thought to arise due to oxidation of non-coordinating isocyanide groups.

The coordination of 4-methylphenyl isocyanide (MPI) to form its films on Au(111) and Cu(111) in ultra-high vacuum (UHV) conditions was studied and compared via temperature-programmed desorption (TPD), time-of-flight (TOF) mass spectroscopy, and X-ray and ultraviolet photoelectron spectroscopies (XPS and UPS). [9] TPD gave direct evidence of two different chemisorbed structures on the Au surface giving rise to peaks in the TPD spectrum at 305 and 375 K. As depicted in Figure II.5, two structures were proposed based on the TPD, XPS, and computational data: one with binding via an atop site (the 305 K peak), while the other featuring a slightly tilted binding to a 3-fold hollow site, seen in Figure II.5 (a). In contrast, the data for monolayer films on Cu(111) indicated the isocyanide nitrogen being sp^2-hybridized in nature and the molecule bonded via a bent atop or a bridge, as shown in (b) in Figure II.5

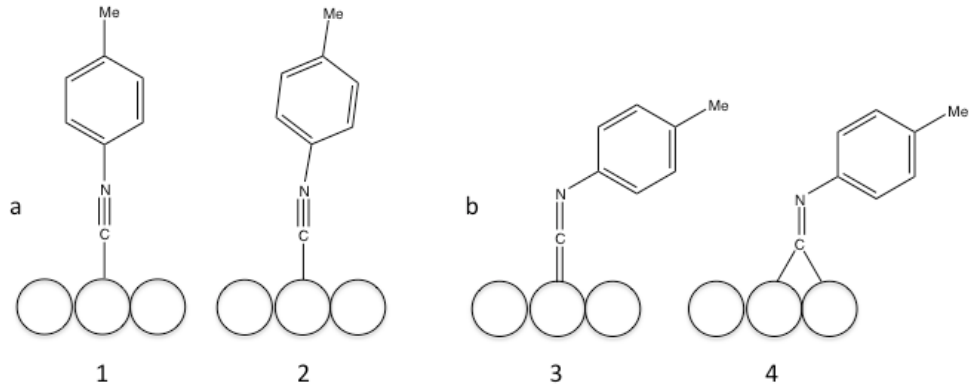

Figure II. 5 - Possible binding geometries of MPI: on (1) atop site on Au(111), (2) three-fold hollow site on Au(111), (3) double atop on Cu(111), and (4) double bridge on Cu(111).

At low coverages (~0.004 ML), the molecules of PDI were observed to orient approximately parallel to the Au(111) surface. At such low coverage, IR spectroscopy was not instructive as there are not enough molecules to observe the ν(CN) signal. Instead, scanning tunneling microscopy (STM) was employed to observe one-dimensional structures of the PDI films. Theoretical assessment of various possible arrangements of PDI on the gold surface indicated that the features observed by STM comprise chains consisting of alternating PDI-Au-PDI units. [10] In a subsequent work, Tysoe *et al*. deposited PDI onto a gold substrate and then heated the resulting sample to 400 K *in vacuo* to afford well-packed, one-dimensional Au-PDI oligomers similar to those in their previous findings, as imaged by STM. [11] A Density Functional Theory, DFT, analysis suggested the gold atoms of the oligomers were located in three-fold hollow sites, with the aromatic rings being parallel to and 3.6 Å above the gold surface with a isocyano-gold bond distance of 2.00 Å. Upon increasing coverage, RAIR spectra of the PDI monolayers were recorded to reveal a single νCN stretching band at 2137 cm^{-1}. These PDI-saturated surfaces were exposed to 10 L of carbon monoxide at 90 K. RAIRS of the resulting samples indicated that the CO molecules were bound to the surface in an upright coordination, a phenomenon that does not occur for Au(111) above 80 K. The adsorbed CO was stable on the surface up to 150 K and desorbed completely at 180 K. [11]

The packing of isocyanoarene films on Au(111) has been the subject of several theoretical investigations. DFT calculations suggested that the most energetically favorable packing of PDI on gold involves a 2√3Å x √3Å unit cell as opposed to a √3Å x √3Å unit cell, thereby minimizing intermolecular repulsion while retaining a strong NC-

Au bond. [12] Computational comparison of the energetics of various binding modes of isocyanide junction groups to gold surfaces indicated that the most favorable binding scenario would involve an adatom site, then, isoenergetic bridging and fcc sites, and, finally, an atop site. This finding implies that the LGA and GGA calculations overestimated the $d\pi \rightarrow p\pi^*$ backbonding contribution to the Au-CNR bonding as this is not the result seen experimentally. Additionally as the tilt angle of the isocyanide is increased from the surface normal, the νCN stretching frequency for the bound isocyanide was found to be very similar to the unbound isocyanide's νCN stretching frequency. Computational studies of CH_3NC adsorbed on Au(111) suggested that the atop site was the only viable adsorption position. [13]

Sum frequency generation (SFG) spectroscopy, computations, and vibrational spectroscopy provided insight into the nature of the metal-isocyanide bond as well as molecular orientation for PDI and MPI adsorbed on Au, Pt, Ag, and Pd surfaces. It was determined the isocyanides bind to the Au, Pt, and Ag at atop sites while adsorbing to bridging sites on Pd. The tilt angle of the adsorbed molecules on the metal surfaces was shown to increase in the order of Pt, Pd, Ag, and Au. [14]

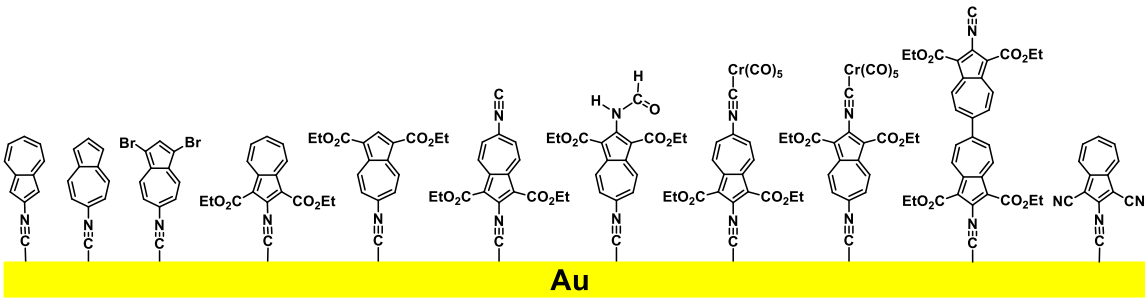

Figure II. 6 - Various isocyanoazulenes that have been shown to coordinate to the Au(111) surface. Adapted from Ref. 6.

In contrast to Tysoe's work, various derivatives of isocyanoazulenes and diisocyanoazulenes [15-17] have formed monolayers that orient in an upright fashion, akin to previously reported SAMs of PDI and OPE. In the case of 2,6-diisocyano-1,3-diethoxycarbonylazulene, only one isocyanide binds to the surface, likely the isocyanide group attached to the five-membered ring (the 2 position) of the azulenic framework, as seen in Figure II.7 (15).

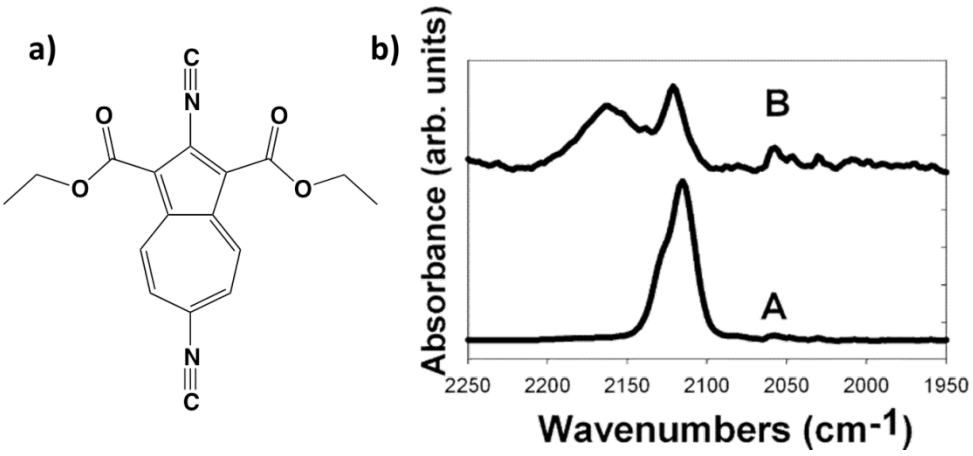

Figure II. 7 - a) Structure of 2,6-diisocyano-1,3-diethoxycarbonylazulene. b) IR spectra of (A) the azulene in solution and (B) when coordinated to the Au(111) surface. Adapted from Ref. 15.

Further proof of an upright orientation of the linear 2,6-diisocyanoazulene scaffold on the Au(111) surface was obtained through the formation of SAMs of the diisocyanoazulene motif having either of its isocyanide termini capped with a 16-electron [$Cr(CO)_5$] unit. The SAM films prepared from either of the two $(OC)_5Cr$(2,6-diisocyano-1,3-diethoxycarbonylazulene) isomers were conveniently characterized by RAIRS in νNC and νCO regions. Importantly, in addition to the NC infrared reporters, the relative intensities of the carbonyl stretching bands provided qualitative information regarding molecular orientation in the above organometallic SAM films. Unlike the previously described PDI or OPE films on gold, the 2,6-diisocyanoazulene-based monolayers remarkably proved to be reasonably air-stable with no signs of oxidation of either the bound or free isocyanide groups documented upon storage of the samples in ambient atmosphere for several days.

III.1.2. Molecular conductance

A number of important considerations need to be taken into account when investigating conductance through molecular systems. First, there are a variety of modes of electron transport from one electrode to another, which are dependent not only on the nature of the molecular backbone of the linker, but also the length of the molecule (*vide infra*). Second, the alignment of the Fermi level of the metal with the Frontier Molecular Orbitals (FMOs) of the linker is critical for establishing good conductivity. Third, differences in the analytical method(s) of measuring the conductance should be considered, especially before making direct comparisons of results obtained using different techniques. Several excellent reviews covering the analytical techniques

suitable for conductivity studies [19-21], as well as the current theory of molecular conductance [22-24] are available. These topics will be discussed herein briefly in the context of isocyanide chemistry.

Aspects of the conductance of aromatic isocyanides have been explored in a variety of ways, such as using nanoporous devices [25], scanning tunneling microscopy (STM) [4], metal-molecule-metal sandwich devices [26,27], STM break junction [28], and conductive probe atomic force microscopy (CP-AFM). [29] This section will summarize basic molecular conductance theory as well as the associated principles and techniques relevant to recent advances in the chemistry of isocyanoarenes adsorbed mainly on Au(111) surfaces.

An early scanning tunneling microscopy (STM) study of the SAM films on Au(111), that involved polyphenylene molecules terminated with thiol or isocyanide groups at one or both ends, compared the Fermi level to the HOMO energies of the corresponding molecules. [4] As the mechanism for charge transfer within thiol-based systems had been studied extensively at the time of publication, a model assuming the Fermi energy level being closer to the HOMO of the thiol and dithiol molecules was considered. The same assumption was used for the related isocyanide-containing systems. The observed trend for the Fermi-HOMO energy difference was as expected for the thiol systems. Indeed, as the number of aromatic rings increased, the offset between the two levels decreased. However, the offset rose in the case of the analogous isocyanide systems upon increasing the number of phenylene rings in their structure. This increase in offset was explained in terms of donation of electron charge of the

isocyanide into the metal surface. As the number of phenylene rings increases, the effective electronic donation increases thus creating a partial positive charge within the organic molecule, which in turn lowers its HOMO energy. This moves the HOMO level away from the Fermi energy level, thereby widening the offset. The ν(CN) of the coordinated isocyanide junction in the isocyano- and diisocyanoarene monolayers on metallic gold clearly increases upon insertion of additional phenylene rings (Table 2.1), thus supporting the above electron donation argument.

Table II.1 - Infrared stretching frequencies of isocyanide groups of free molecules (KBR pellet sample) and bound to Au surface. Adapted from Ref. 4.

Molecule	ν(CN) of free molecule	ν(CN) when bound to Au
PMI	2126 cm^{-1}	2140 cm^{-1}
BPMI	2127 cm^{-1}	2150 cm^{-1}
TPMI	2128 cm^{-1}	2155 cm^{-1}
PDI	2120 cm^{-1}	2181 cm^{-1}
BPDI	2121 cm^{-1}	2191 cm^{-1}
TPDI	2121 cm^{-1}	2194 cm^{-1}

In performing calculations for PDI on Au(111) surfaces using a combination of GW (G is Green's function, W is the screened Coulomb interaction), both quasi-particle corrections and surface screening were found to be important to obtain estimates of the energy level of the molecule and energy of the surface that were sensible. [32] The calculations found a large barrier for electron transport between the Fermi level and the LUMO of the PDI, which DFT did not predict. [33] As such, it was concluded that PDI SAMs may not be the most effective system for electron transport.

The electron transport properties of various isocyanide molecules between two metal junctions have been explored using a variety of techniques. Bennet *et al*. fabricated

a system with the PDI linking two metal (gold or platinum) contacts. [22] One of the isocyanide termini served as a chemisorbed contact. The other isocyanide junction was engaged with the metal evaporated onto the monolayer. This design provided a closed circuit for measured conductivity and assessing transport mechanism. Upon changing the direction of the bias, injecting electrons from the chemisorbed contact or from the evaporated contact, and changing the extent of bias (low or high), different conduction mechanisms were probed between the different metal contacts, as summarized in Table II.2.

Table II.2 - Barriers and conduction mechanisms from Ref. 22.

Metal contact	**Au**	**Pd**
Chemisorbed	0.35 eV, thermionic	0.22 eV, thermionic (0.19 eV, hopping at low bias)
Evaporated	0.38 eV, thermionic (0.3 eV, hopping at low bias)	0.21 eV, hopping

Simultaneously measuring the conductivity of PDI between two Au electrodes and using surface enhanced Raman spectroscopy (SERS) allowed recording current-voltage (I-V) curves while monitoring the isocyanide stretching frequency. [27] Notably, the device underwent damage if the applied voltage exceeded 0.5 V. The I-V curves obtained in this study were similar to those documented in previous reports [25, 26, 34] for PDI systems and featured symmetric, nonlinear shapes. According to the SERS data, the isocyanide stretching frequency did not change when the voltage was swept in the range of 0.5 V to -0.5 V.

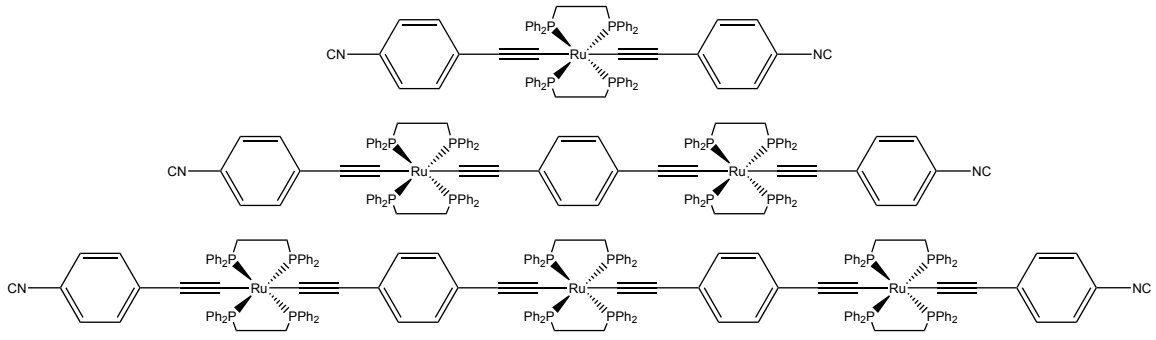

Figure II. 8 - Molecular wires

A series of redox-active conjugated molecular wires made of ruthenium(II) bis(sigma-arylacetylide) units, Figure 8, capped with isocyanides were analyzed for their conductivity properties. [39] The series ranged from having one to three ruthenium(II) centers and formed self-assembled monolayers on Au substrates. These films were characterized using ellipsometry, X-ray photoelectron spectroscopy, reflection-absorption infrared spectroscopy, and cyclic voltammetry. Using conductive probe atomic force microscopy, the resistance versus molecular length was calculated and found to be low compared to other conjugated organic molecular wires. When studied at low temperatures, the two shorter wires were shown to exhibit direct tunneling behavior, whereas the longer R3 wire was observed to exhibit Coulombic blockade behavior. The varying lengths of the molecule explained this difference in conductivity, where R3 (4.9 nm) was too long for direct tunneling.

II.2 Work Described in Chapter II

This chapter discusses the formation and studies of SAM films of all biazulenyl isocyanides developed in our laboratories to date. In addition to detailed physicochemical analysis of these monolayer films, their stability in various environments is addressed. Future directions of this research are outlined at the conclusion of the chapter.

II.3 Experimental Section

II.3.1. General Procedures and Starting Materials

The biazulenes used in these studies were prepared as described by various Barybin group researchers. Preparations of **1** may be found in Barybin, M.V., *et al., Journal of the American Chemical Society*, **2010**, *135*, 15924-15926 [18], **2** and **3** in Dr. David McGinnis' Thesis [40], and **4** in unpublished work Toshinori Nakakita, T., Meyers, J. J., Jr., Barybin, M.V. Unpublished work. The chemical structures of these compounds may be seen in Figure II.9.

Gold-coated mica substrates were either purchased from Platypus Technologies or were fabricated in the Berrie lab using an Edwards Auto 306 rotary evaporator. "House" Au(111) was deposited on freshly cleaved sheets of mica under a vacuum pressure of *ca.* 1.5 x10^{-7} torr with a deposition rate of about 1 Å/sec, as measured by a quartz crystal microbalance. Gold films were coated between 250 and 300 Å thick and were subsequently stored under high vacuum or inert atmosphere conditions until use. Commercial silicon wafers, coated with a 50 Å titanium adhesion layer and then with *ca.* 1000 Å of gold, were purchased from Platypus Technologies.

Unless otherwise stated, all substrates were soaked in distilled $CHCl_3$, acetone, and 200-proof ethyl alcohol for one to two hours in each solvent with no precautions against exposure to ambient air or lighting. Substrates were then removed and dried in a stream of N_2 gas. Physical constants of the substrates were measured using a Rudolph Research Auto El III fixed wavelength ellipsometer. Measurements were made with a 632.8 nm wavelength HeNe laser. The optical constants of each individual cleaned, bare

gold substrate were measured prior to its exposure to isocyanide solutions. These optical constants were used to determine the thickness of the organic film covering the substrate upon isocyanide exposure and subsequent workup of the sample. Typical values for n ranged from 0.161 to 0.181 and K values ranged from 3.52 to 3.55. A refractive index of 1.45 was assumed [41] for the SAMs described in this chapter. At least five separate spots on the substrate were analyzed to determine both the optical constants and the film thicknesses. The film thickness values reported herein constitute averages of these measurements with the corresponding standard deviations given in parentheses.

All surface IR experiments involved grazing angle reflection absorption Fourier transform infrared spectroscopy. These data for the SAMs films were obtained on a Thermo Nicolet 670 FTIR spectrometer with a VeeMax grazing angle accessory set up at an incident angle of 70°. Prior to acquiring an IR spectrum of each SAM sample, a background spectrum was recorded using a corresponding similarly treated bare Au substrate. Typically, 1000 scans from 600 to 4000 cm^{-1} at 4 cm^{-1} resolution were collected for both the background and sample spectra.

II.3.2. Preparation of SAM films of 2,2'-diisocyano-1,1',3,3'-tetraethoxycarbonyl-6,6'-biazulene (1) and 1,2-bis(2-isocyano-1,3-diethoxycarbonylazulen-6-yl)ethyne (2)

Gold-coated mica substrates from Platypus technologies, Agilent Technologies, and house-coated Au(111) were used to prepare these monolayers. Before use of the Platypus Technologies substrates, these commercial gold substrates were cleaned with Piranha solution (**Warning**: extreme care should be exercised in handling Piranha solution as this strong oxidant reacts violently with organic substances and poses an

explosion danger), then rinsed thoroughly with large volumes of Millipore water, dichloromethane, ethanol, and acetone. Agilent Technologies and house-coated Au(111) substrates were not treated using the above protocol because the Piranha solution would strip the gold coating from the mica surface. Instead, the Au-on-mica films were cleaned as outlined in the General Procedures section.

After drying with a stream of N_2 gas, ellipsometric physical constants of the bare gold substrates were taken. Monolayer films of respective isocyanides were formed by immersing a freshly cleaned gold substrate into a 2 mM solution of the isocyanides in distilled CH_2Cl_2 or - $CHCl_3$ for *ca*. 24 hrs. Then, the gold samples were removed, rinsed thoroughly with CH_2Cl_2 or $CHCl_3$, depending on the original solvent used to prepare the solution of the isocyanides, and dried in a flow of N_2 gas. No precautions to exclude air or ambient laboratory lighting were taken during this procedure.

II.3.3. Preparation of 6-isocyano-2,2'-biazulene (3) SAM films

Gold-coated mica substrates from Platypus technologies and house-coated Au(111) were used in the formation of monolayers of this biazulene derivative. Prior to their use, both kinds of substrate were cleaned as outlined in the General Procedures section.

After drying with a stream of N_2 gas, ellipsometric physical constants of the bare gold samples were taken. Monolayer films of **3** were formed by immersing a freshly cleaned gold substrate into a 2 mM solution of **3** in distilled $CHCl_3$ for *ca*. 24 hrs. Then, the gold sample was removed, rinsed thoroughly with distilled CH_2Cl_2 or $CHCl_3$, and

dried in a flow of N_2 gas. No precautions to exclude air or ambient laboratory lighting were taken during this procedure.

II.3.4. Preparation of 2-isocyano-2',6-biazulene (4) SAM films

Mica substrates featuring house-coated Au(111) were used in the formation of these biazulenic monolayers. The substrates were cleaned as outlined in the General Procedures section prior to their use.

After drying with a stream of N_2 gas, ellipsometric physical constants of the bare gold samples were taken. Monolayer films of **4** were formed by immersing a freshly cleaned gold substrate into an 8 mM solution of **4** in distilled $CHCl_3$ for *ca*. 24 hrs. Then, the gold sample was removed, rinsed thoroughly with distilled $CHCl_3$, and dried in a flow of N_2 gas. No precautions to exclude air or ambient laboratory lighting were taken during this procedure.

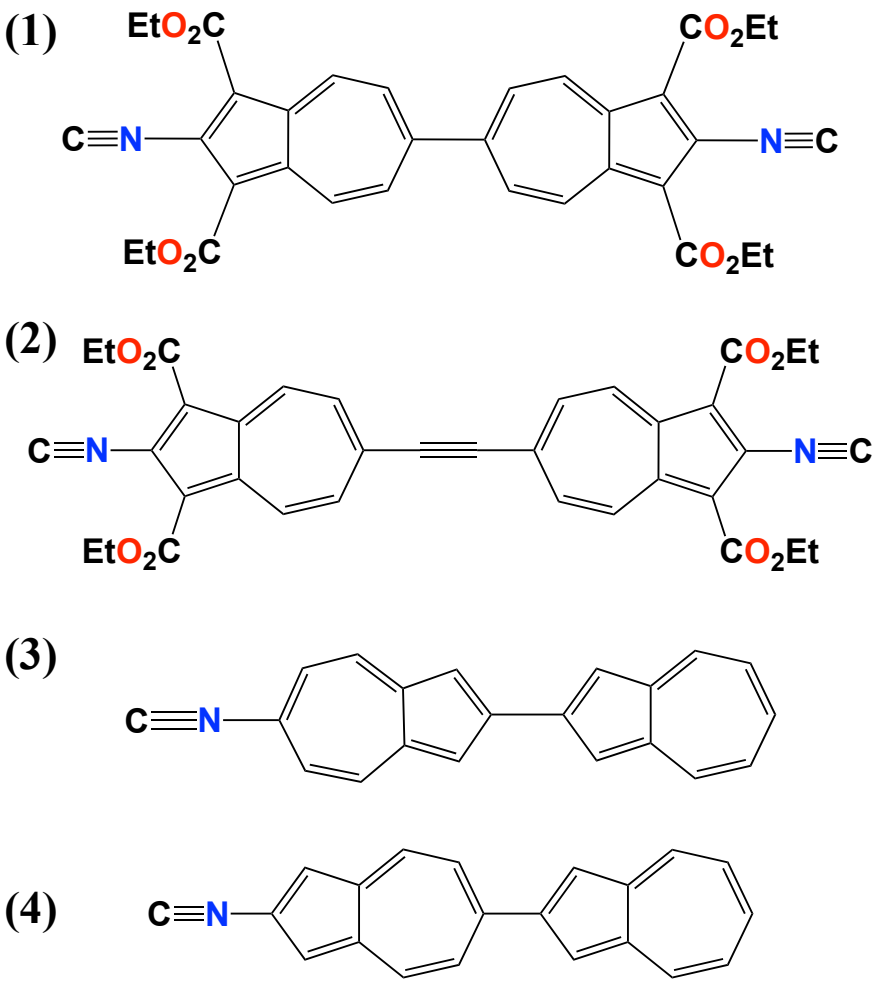

Figure II.9 – Structures of diisocyanobiazulenes **1**, **2**, **3**, and **4**

II.4 Results and Discussion

II.4.1 SAM films of 1

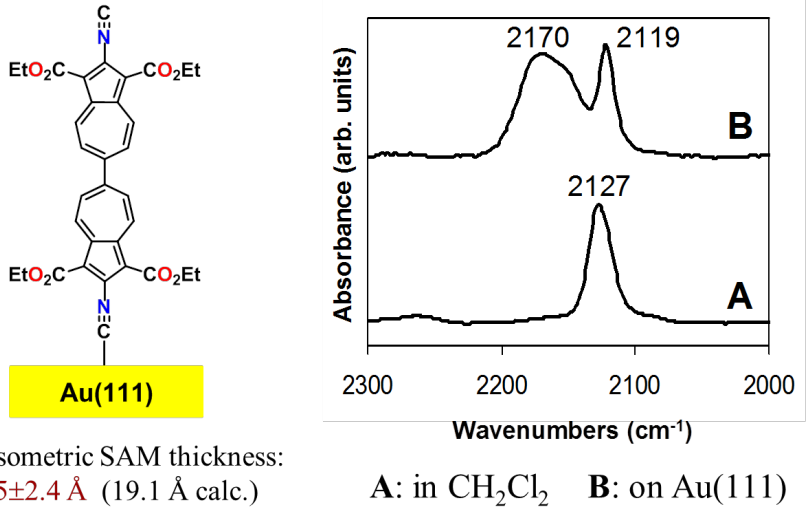

- Ellipsometric SAM thickness: 20.5±2.4 Å (19.1 Å calc.)

A: in CH_2Cl_2 **B**: on Au(111)

Figure II. 10 – Left:- Schematic illustration of an upright coordination of 1 to the Au(111) surface. Right: A - FTIR spectrum of 1 in $CHCl_3$ solution. B – RAIR spectrum of 1 adsorbed to the Au(111) surface

Formation of SAM films of the linear biazulenic derivative **1** was accomplished without any precautions taken against exposure of the materials to ambient air or lighting. A gold(111) substrate was immersed into a 2mM solution of **1** in distilled $CHCl_3$ for a period of about 24 hrs. After workup that included thorough rinsing and drying, ellipsometric and IR studies were performed on the resulting sample. The ellipsometric thickness of the film of **1** was measured to be 20.5 ± 2.4 Å. This experimentally determined thickness value strongly suggests a monolayer nature of the film with approximately upright orientation of the molecules of **1** with respect to the metal surface. Indeed, the expected film thickness for the perfectly upright η^1 coordination of **1** to the

Au surface should be about 19.1 Å. The latter theoretical estimate was obtained by adding 2.0 Å, which is a typical Au(0)-CNR bond length,[3] to the crystallographically determined 17.1 Å distance between the two isocyanide carbon atoms in **1**[18, 42]. Notably, the nearly parallel orientation of the long molecular axis of **1** with respect to the surface normal is consistent with similar observations documented for SAMs of a number of other isocyanoarenes and linear diisocyanoarenes on gold. [4,7,8,16]

The grazing incidence reflection absorption infrared (RAIR) spectrum of a freshly prepared film of **1** on Au(111) also suggests the end-on adsorption of **1** to the Au surface, as well as the monolayer rather than multilayer nature of the resulting film. Indeed, the spectrum exhibits two bands in the isocyanide stretching region (Figure II.10). The higher energy band at 2170 cm^{-1} corresponds to $\nu_{C\text{-}N}$ of the C≡N terminus of **1** bound to the gold surface. The broad nature of this band is typical for aryl isocyanide SAMs on gold [7, 8, 43, 44] and can be attributed to some inhomogeneity in the environment of the surface adsorption sites due to defects in the Au(111) film prepared via gold vapor deposition. [45] Notably, the $\nu_{C\text{-}N}$ stretch for SAMs of 2-isocyano-1,3-diethoxycarbonylazulene on Au(111) also occurs at 2170 cm^{-1}.[16] Since the isocyanide carbon's lone pair is antibonding with respect to the C≡N bond [6], donation of electron density from the –NC junction to gold upon chemisorption of **1** results in a pronounced (43 cm^{-1}) blue shift in ν_{CN} for the gold-bonded isocyanide terminus of **1** relative to that of the compound in solution. Concurrently, such coordination should induce a slight positive charge [4] within the π-system of **1**, which may lead to weakening of the C≡N bond of the unbound isocyanide group, provided there is a sufficient extent of conjugation between the two

azulenyl moieties. In accord with this argument, the sharp $\nu_{C\text{-}N}$ band at 2119 cm^{-1} in the RAIR spectrum in Figure 10 that corresponds to the uncoordinated -N≡C end of **1** is depressed by 8 cm^{-1} relative to $\nu_{C\text{-}N}$ observed for **1** in CH_2Cl_2 solution (or, by 11 cm^{-1} compared to $\nu_{C\text{-}N}$ for the bulk compound in Nujol mull). Interestingly, when adsorbed on metallic gold, linear benzenoid diisocyanoarenes featuring up to three linked arylene units also show 2 – 9 cm^{-1} red shifts in ν_{CN} for their free -N≡C end relative to ν_{CN} for the corresponding bulk substances, presumably for the same reason. [8, 44]

As mentioned in the introduction to this Chapter, oxidation of isocyanoarene SAMs has been observed for both mono- and diisocyanoarenes adsorbed on gold. [7,8] However, whether the coordinated or free (or both) isocyanide termini undergo oxidation is still a matter of debate. [7, 8] In 2006, Barybin and Berrie described several isocyanoazulenic films on Au(111) that were remarkably robust and did not undergo rapid deterioration on air as do most benzenoid isocyanoarene SAMs on gold. [16] In fact, one such isocyanoazulene film was shown to have little to no signs of degradation for nineteen days with no precautions taken against ambient laboratory lighting or atmosphere.

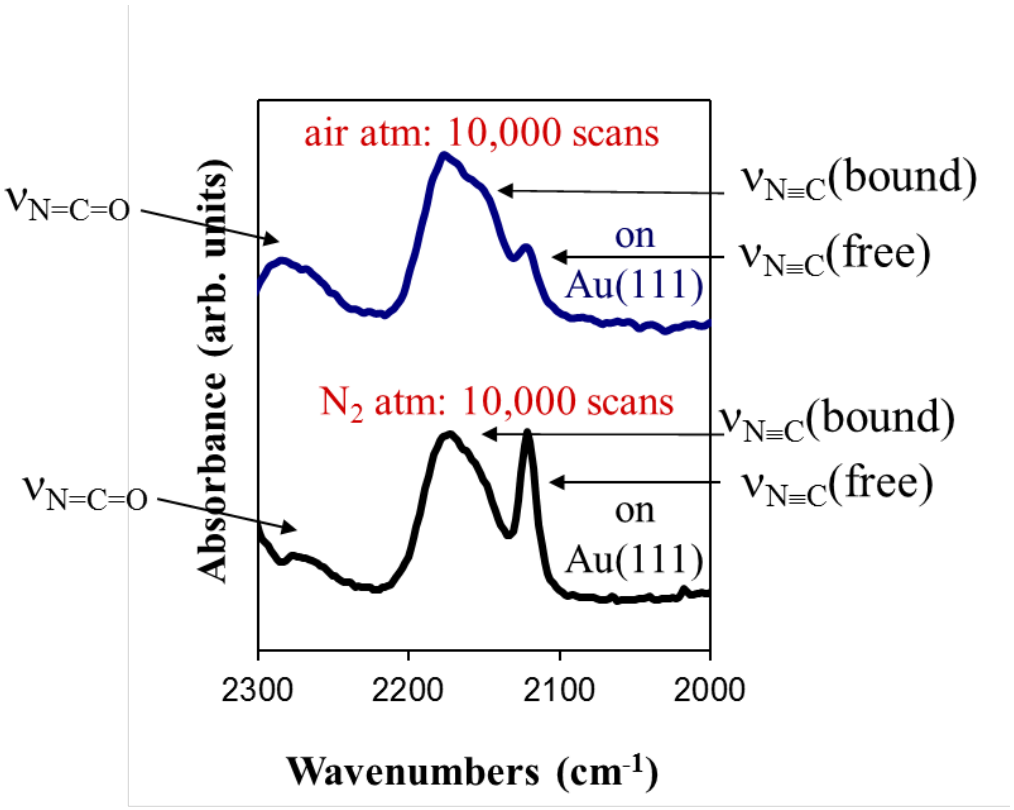

Figure II. 11 - Bottom: RAIR spectrum of a SAM of 1 in N2 atmosphere after 10,000 scans. Top: RAIR spectrum of 1 in ambient air atmosphere after 10,000 scans.

It is important to note that initial attempts to form a SAMs of **1** on Au(111) had resulted in the film thickness values being within what was expected for a perfect upright adsorption of **1:** 18±2 Å experimentally versus 19.1 Å theoretically, *vide supra*. No oxidation of either of the isocyanide groups of the adsorbed **1** to produce an isocyanate moiety, R-N=C=O, had been detectable in the RAIR spectra of these films. When the author of this Thesis repeated the adsorption experiments, film thicknesses and RAIR spectra reported above were obtained, in addition to the information concerning the stability issues with respect to the isocyanate formation. RAIR spectra were initially recorded by taking 10,000 scans in an ambient air environment that had been scrubbed to

remove both water and carbon dioxide. While monitoring the progress of the 10,000-scan protocol, which takes one hour and forty-three minutes, growth of a band at 2270 cm^{-1}, that had not been present at the beginning of the experiment, was noted (Figure 11). This peak is attributable to the formation of the isocyanate functionality. Conducting the same 10,000-scan experiment in the atmosphere of 98% nitrogen gas allowed to severely suppress, if not eliminate altogether, the buildup of the RAIR feature the at 2270 cm^{-1}. Notably, the RAIR spectrum of a SAM film of **1** on Au(111), acquired in the CO_2/H_2O-scrubbed air atmosphere using a 1,000-scan protocol (*ca.* 10 min acquisition time), suggested that minute amounts of the isocyanate species begin to accumulate even at very short exposures of the sample to air.

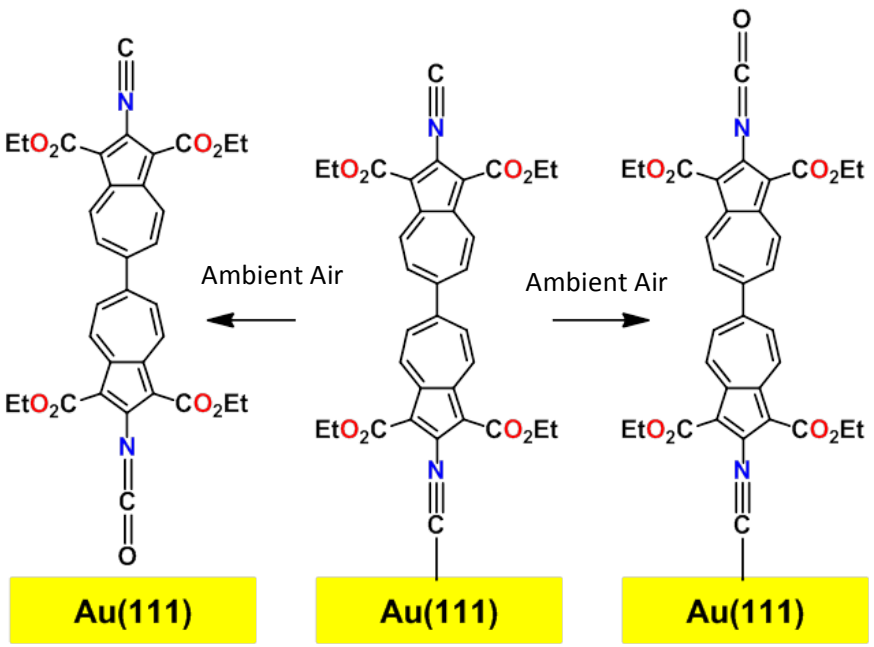

Figure II. 12 – Possible outcomes of the air-oxidation of 1 adsorbed on the Au(111) surface

Given the formation of the isocyanate functionality upon exposure of SAMs films of **1** on Au(111) to air, it is important to differentiate which isocyanide group of **1**, coordinated or "free", undergoes oxidation (Figure 12). The RAIR spectra of a SAM of **1** exposed to air atmosphere over different periods of time, indicate that the intensity of the free, uncoordinated isocyanide stretching band decreases while the peak corresponding to the isocyanate group grows over time. Moreover, the intensity of the band corresponding to the coordinated isocyanide junction remains relatively unchanged unlike both the free isocyanide and the isocyanate peaks. This lack of change in the bound isocyanide signal, coupled with decreasing intensity of the non-coordinated isocyanide and growth of the new isocyanate band, strongly suggests that it is the non-coordinated isocyanide terminus of **1** that undergoes oxidation to isocyanate. A similar conclusion was reached by

Swanson *et al.* in their studies of the oxidation of linear benzenoid diisocyanoarenes adsorbed on gold. [8]

II.4.2 SAM films of 2

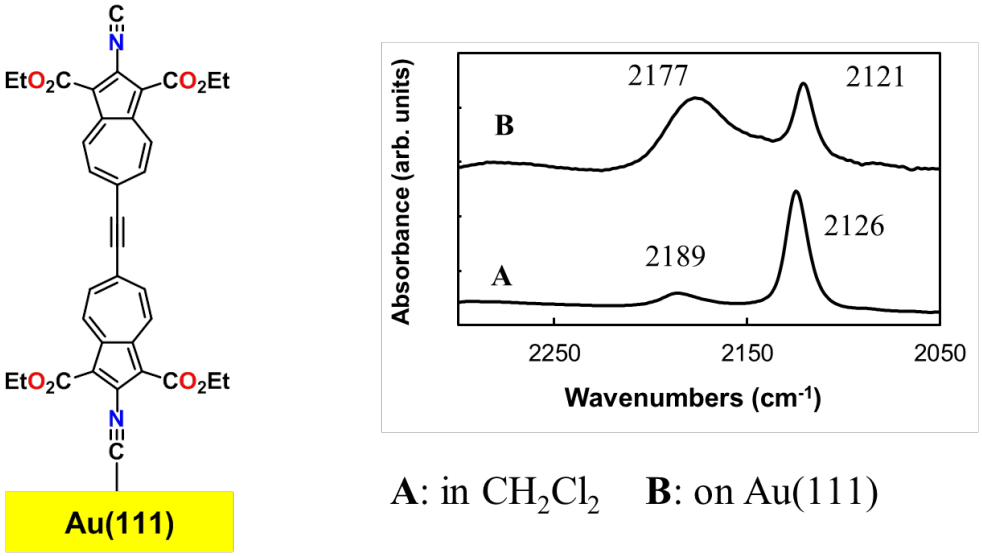

Figure II. 13 - Left: Schematic illustration of an upright coordination of 2 to the Au(111) surface. Right: A – FTIR spectrum of 2 in CH_2Cl_2 solution. B - RAIR spectrum of 2 adsorbed to the Au(111) surface.

The air-stable biazulene derivative **2**, synthesized by Dr. David McGinnis of the Barybin group [40], is a linear, symmetric molecule featuring two isocyanide termini available for coordination to metal atoms, ions and surfaces. Exposure of a Au(111) substrate to a dilute, 2mM solution of the diisocyanobiazulene **2** for 24 hours with no precautions to exclude ambient air and laboratory lighting afforded a thin organic film. Ellipsometric and RAIR analyses of this film suggested its monolayer nature. The molecular length of **2**, defined as the distance between its two isocyano carbon atoms, is about 21 Å, as determined by considering its MM2-optimized model in ChemBio3D

Ultra 12. Addition of 2.0 Å, a typical gold(0) - isocyanide carbon bond distance [3], to this value gives the overall expected thickness of 23 Å for a monolayer of **2** on gold that would feature an upright coordination on the organic molecules to the metal surface. This expected monolayer thickness value matches reasonably well the ellipsometrically measured film thickness of 26.9± 1.0 Å. Thus, the linear diisocyanide **2** forms *ca.* 2.5 nm-tall SAMs on Au(111) with approximately vertical orientation of its nonbenzenoid aromatic scaffold with respect to the metal surface.

The infrared spectrum of **2** in solution features a single characteristic isocyanide CN stretching band at 2119cm^{-1} (Figure 13). A very weak peak at 2189 cm^{-1}, corresponding to the C≡C stretching vibration, is also seen in this IR spectrum. This latter vibrational mode is IR-forbidden given the symmetry of **2** and, therefore, gives rise to a band of a very weak intensity. Upon adsorption to gold, the ν(CN) for coordinated isocyanide junction blue-shifts to 2177 cm^{-1}, whereas the ν(CN) band corresponding to the unbound isocyanide terminus of **2** undergoes a 5 cm^{-1} red shift compared to the ν(CN) value for **2** in solution. These observations nicely parallel those discussed above for the adsorption of diisocyanobiazulene **1**.

II.4.3 SAM films of 3

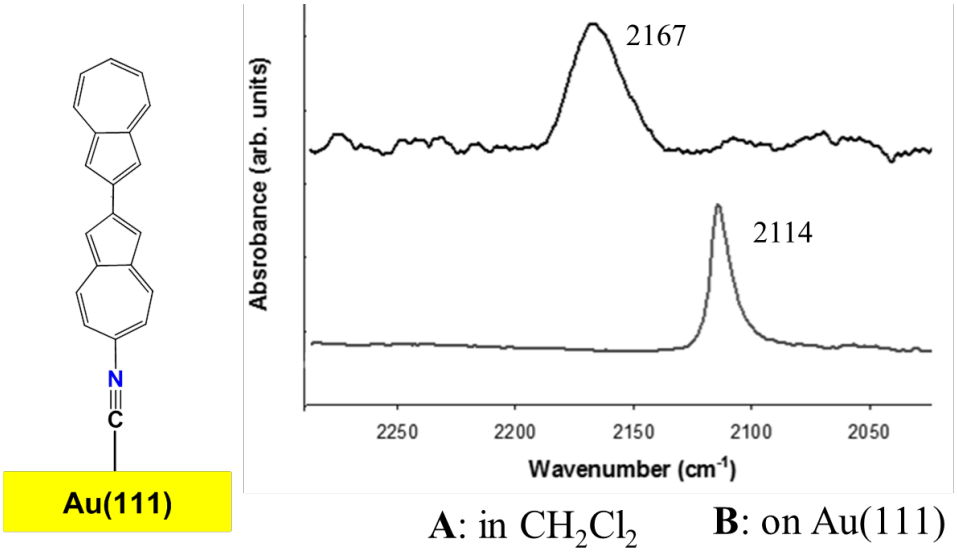

Figure II. 14 - Left: Schematic illustration of an upright coordination of 3 to the Au(111) surface. Right: A – FTIR spectrum of 3 in CH_2Cl_2. B - RAIR spectrum of 3 adsorbed to the Au(111) surface.

While the Barybin group has been successful in synthesizing the 6,6'-biazulene motif linearly equipped with two isocyanide termini (compound **1**), isolation of a complementary system featuring bonding of the azulenic fragments through the 5-membered rings (i.e., carbon atoms 2 and 2') is yet to be accomplished. Nevertheless, Drs. Maher and McGinnis succeeded in preparing the 2,2'-biazulenyl compound, namely 6-isocyano-2,2'-biazulene (**3**), that incorporates one isocyanide terminus. In solution, the isocyande group of **3** gives rise to a characteristic ν(CN) band at 2114 cm^{-1}. Upon exposing an Au(111) substrate to a dilute solution of **3**, adsorption of the compound on the gold surface occurs as evidenced by a blue shift of the ν(CN) band to 2167 cm^{-1} (Figure 14). Of note, there is no free isocyanide signal seen in the surface spectrum

shown in Figure 14. This suggests that the film is only one molecule-thick with the isocyanide group being coordinated to the metal surface. Moreover, the molecules of **3** are likely to be oriented parallel to the surface normal, as depicted in Figure 14, following the selection rules for surface enhanced spectra as discussed in Chapter 1 of this Thesis.

Ellipsometric determination of the thickness of the above film of **3** on gold yielded the value of 25±1.5 Å. For an upright coordination of this molecule, one would expect the SAM thickness to be around 17 Å, including the Au-C bond distance of 2.0 Å. The apparent significant discrepancy between the experimental and expected film thickness values does not necessarily rule out the formation of a monolayer. Previously, Dr. Tiffany Maher performed similar experiments attempting to form monolayers of **3** during her graduate work in the Barybin group. Dr. Maher documented preliminary evidence of monolayer formation with infrared spectra that were suggestive of a single molecule-thick film. However, her experimental thickness measurements resulted in the value of 27(2) Å. In her Ph.D. Thesis, Dr. Maher proposed that the visible light absorbance of the organic molecule affected the measurement. Compound **3** was, indeed, shown to have a slight absorbance at 632 nm, the wavelength of the HeNe laser used in our ellipsometric experiments. The model used in analyzing our ellipsometric data assumes no significant absorption of the incident laser radiation by the film. Therefore, absorption of the laser radiation by the biazulenic film may have skewed the calculations in determining the ellipsometric thickness for **3** on gold. With further detailed consideration of the model used, the author of this Thesis finds it doubtful that the absorbance of laser light would alter substantially the experimental film thickness value, especially given that the extinction coefficient of **3** at 632 nm is so low. It is more likely

that the films were contaminated with a hydrocarbon material when placed on the ellipsometer. Hydrocarbon particles floating in the air could physisorb to the surface and would not be immediately apparent in the RAIR spectrum but would certainly affect results of ellipsometric measurements. The use of spectroscopic ellipsometry would rule out any error caused by absorption of the incident laser radiation, thus possibly determining the cause of the thicker than expected measurements on the fixed wavelength instrument.

II.4.4 SAM films of 4

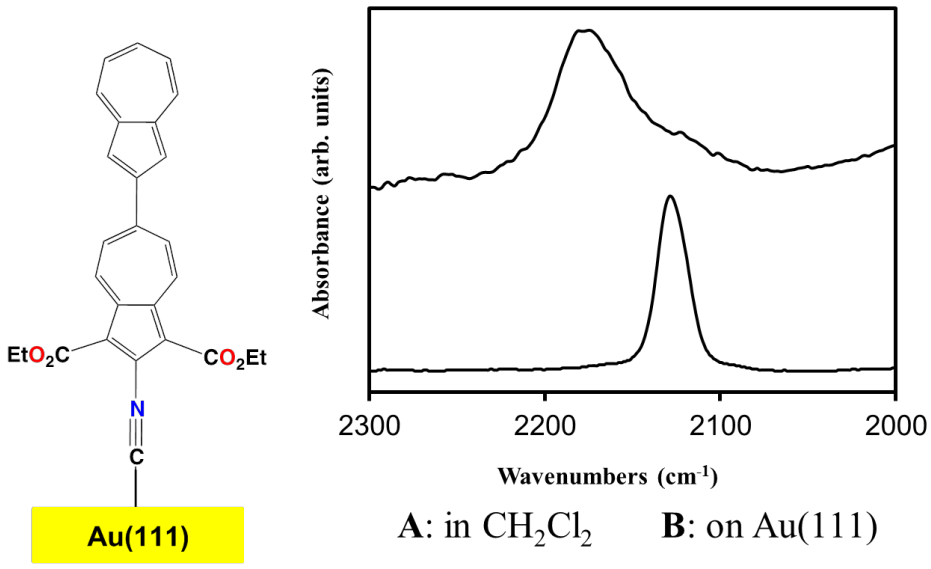

Figure II. 15 - Left: Schematic illustration of an upright coordination of 4 to the Au(111) surface. Right: A - FTIR spectrum of 4 in CH_2Cl_2. B - RAIR spectrum of 4 adsorbed to the Au(111) surface.

The most recent addition to the family of biazulenic SAMs on gold involves 2-isocyano-1,3-diethoxycarbonyl-2',6-biazulene (**4**), recently synthesized in the Barybin

group. This polar biazulenic compound features one isocyanide terminus, but, unlike **1** and **3**, contains the azulenic motifs with the dipoles aligned in the same direction. Synthesized by Toshinori Nakakita and John Meyers, the biazulenyl derivative **4** completes the series of three possible linear biazulenic frameworks, namely 2,2', 6,6', and 2,6'. Formation of thin films using compound **4** proved to be the most challenging of any isocyanoazulenic SAMs that the author of this Thesis has attempted to prepare to date. Our standard methodology of monolayer formation involving a 2mM solution of the organic compound in distilled $CHCl_3$, exposure of a gold substrate to the above solution for twenty-four hours, and no precautions against air or lighting was unsuccessful in obtaining SAMs of **4**. Conducting the monolayer formation experiments under a nitrogen gas atmosphere and precluding exposure to laboratory lighting did not result in any success either. Attempt to prevent aggregation on the surface and limit any undesirable side reactions, by lowering the solution concentration to 1 mM, 0.5 mM, and 0.25 mM, while excluding ambient air atmosphere and lighting, were not helpful. Finally, higher solution concentrations of **4** were tested and succeeded in monolayer formation. Using an 8 mM solution of **4** in chloroform, the first successful SAM of **4** on Au(111) was formed and characterized.

The ellipsometric film thickness for **4** adsorbed on metallic gold was determined to be 13 Å, averaged from the measurements at five spots on the same substrate. A Chem3D-optimized model of **4** suggests the molecular length of about 13 Å along its long axes. While the experimentally determined thickness is somewhat shorter than expected for a perfectly upright coordination of **4**, possibly because of a less dense packing structure than other isocyanobiazulenic films, the deviation is not large.

Certainly, no multilayer formation has occurred. The RAIR spectrum of **4** on gold supports this conclusion. The CN stretching band for **4** in solution occurs at 2120 cm^{-1}. Upon coordination of **4** to the gold surface, this peak shifts to higher energy to appear at 2169 cm^{-1}, as expected for an isocyanide film. The surface IR spectrum shows no features corresponding to free, uncoordinated isocyanide groups, which suggests that multilayer formation on the gold surface is unlikely

Since the initial formation of the SAM of **4** on Au(111) in an 8 mM solution, additional SAMs have been formed at the lower concentrations of 4 mM. In addition, one example of monolayer formation was observed when attempting to use the standard concentration of 2 mM. This later case provided reasonable ellipsometric and RAIR data. It is this Author's findings that the best method for monolayer formation of **4** is to use higher concentration solutions as done with the 8 mM solution experiments.

II.5. Conclusions and Outlook

In this chapter, the formation and characterization of the first self-assembled monolayer films involving three possible types of biazulenic scaffolds have been presented. The films feature terminal (η^1) coordination of the isocyanide junction groups and approximately upright orientation of the isocyanoarene frameworks with respect to the gold surface. These characteristics nicely parallel those documented for SAMs of isocyanoazulene derivatives containing one azulenic moiety [15] as well as SAMs of most benzenoid isocyanoarenes. [3] The accessibility of well-defined molecular films of **1** and **2** opens a previously unavailable intriguing opportunity to experimentally probe the conductivity characteristics of a molecular wire based on the symmetric nonbenzenoid aromatic 6,6'-biazulenyl framework. While incorporation of the second isocyanide terminus into the structures of 2,2'- and 2,6'-biazulenyl derivatives **3** and **4** is yet to be accomplished, the successfully formed SAMs of the monoisocyanide derivatives **3** and **4** on Au(111) will serve as an important proof-of-concept model in our future quest for 2,2'- and 2,6'-biazulenyl-based charge transport materials.

The next research steps capitalizing on the work described in this chapter will involve systematic evaluation of the charge transport characteristics of the new isocyanobiazulenic SAMs on gold and, perhaps, on other metal surfaces (*e.g.*, Pd). Specifically, the conductivity properties of these SAM films will be studied as a function of connectivity of the azulenic units within the biazulenic saffold (*i.e.*, 2,2', 6,6', or 2,6') and incorporation of –C≡C– spacers between azulenic moieties. Additional SAM stability and surface imaging studies should be considered as well.

II.6 References

1 Aviram, A.; Ratner, M. A. Molecular rectifiers. *Chemical Physics Letters* **1974**, *29*, 277-283.

2 (a) Love, J. C. Estroff, L. a; Kriebel, J. K. Nuzzo, R. G.; Whitesides, G. M. Self-assembled monolayers of thiolates on metals as a form of nanotechnology. *Chemical reviews* **2005**, *105*, 1103-69. (b) Maksymovych, P., Oleksandr, V., Dougherty, D.B., Sorescu, D.C., Yates, J.T. Jr. Gold adatom as a key structural component in self-assembled monolayers of organosulfur molecules on Au(111*) Progress in Surface Science*, **2010**, *85*, 206-240. (c) Chinwangso, P., Jamison, A.C., Lee, T.R., Multidentate Adsorbates for Self-Assembled Monolayer Films. *Accounts of Chemical Research*, **2011**, *44*, 511-519. (d) Vericat, C., Vela, M.E., Benitez, G., Carro, P., Salvarezza, R.C. Self-assembled monolayers of thiols and dithiols on gold: new challenges for a well-known system. *Chemical Society Reviews*, **2010**, *39*,1805-1834.(e) Gooding, J.J., Ciampi, S., The monolayer level modification of surfaces: from self-assembled monolayers to complex molecular assemblies. *Chemical Society Reviews*, **2011**, *40*, 2704-2718.

3 Lazar, M. and Angelici, R.J. Isocyanide binding modes on metal surfaces and in metal complexes, In *Modern Surface Organometallic Chemistry*; Basset, J.-M. Psaro, R., Roberto D., Ugo, R., Eds, Wiley-VCH, Weinheim, 2009 pp. 513–556.

4 Hong, S. Reifenberger, R. Tian, W. Datta, S. Henderson, J. I.; Kubiak, C. P. Molecular conductance spectroscopy of conjugated, phenyl-based molecules on Au(111): the effect of end groups on molecular conduction. *Superlattices and Microstructures* **2000**, *28*, 289-303.

5 Angelici, R. J. R. J.; Lazar, M. Isocyanide ligands adsorbed on metal surfaces: applications in catalysis, nanochemistry, and molecular electronics. *Inorganic chemistry* **2008**, *47*, 9155-65.

6 Barybin, M. V. Nonbenzenoid aromatic isocyanides: New coordination building blocks for organometallic and surface chemistry. *Coordination Chemistry Reviews* **2009**, *254*, 1240-1252.

7 Stapleton, J. J. Daniel, T. a; Uppili, S. Cabarcos, O. M. Naciri, J. Shashidhar, R.; Allara, D. L. Self-assembly, characterization, and chemical stability of isocyanide-bound molecular wire monolayers on gold and palladium surfaces. *Langmuir*, **2005**, *21*, 11061-11070.

8 Swanson, S.A., McClain, R., Lovejoy, K.S., Alamdari, N.B., Hamilton, J.S., Scott, J.C. Self-assembled diisocyanide monolayer films on gold and palladium. *Langmuir*, **2005**, *21*, 5034-5039.

9 Sohn, Y.; White, J. M. Solely sigma-Atop Site Bonding of Phenyl Isocyanide on Au (111)? Comparison with on Cu (111). *Journal of Physical Chemistry C* **2008**, *112*, 5006–5013.

10 Boscoboinik, J. a; Calaza, F. C. Habeeb, Z. Bennett, D. W. Stacchiola, D. J. Purino, M. a; Tysoe, W. T. One-dimensional supramolecular surface structures: 1,4-diisocyanobenzene on Au(111) surfaces. *Physical chemistry chemical physics* **2010**, *12*, 11624-11629.

11 Boscoboinik, J. Kestell, J. Garvey, M. Weinert, M.; Tysoe, W. T. Creation of Low-Coordination Gold Sites on Au(111) Surface by 1,4-phenylene Diisocyanide Adsorption. *Topics in Catalysis* **2011**, *54*, 20-25.

12 Li, Y. Lu, D. Swanson, S. a; Scott, J. C.; Galli, G. Microscopic Characterization of the Interface between Aromatic Isocyanides and Au(111): A First-Principles Investigation. *Journal of Physical Chemistry C* **2008**, *112*, 6413-6421.

13 Gilman, Y. Allen, P. B.; Hybertsen, M. S. Density-Functional Study of Adsorption of Isocyanides on a Gold (111) Surface. *Journal of Physical Chemistry B* **2008**, *112*, 3314-3320.

14 Ito, M. Noguchi, H. Ikeda, K.; Uosaki, K. Substrate dependent structure of adsorbed aryl isocyanides studied by sum frequency generation (SFG) spectroscopy. *Physical chemistry chemical physics*, **2010**, *12*, 3156-63.

15 DuBose, D. L. Robinson, R. E. Holovics, T. C. Moody, D. R. Weintrob, E. C. Berrie, C. L.; Barybin, M. V. Interaction of mono- and diisocyanoazulenes with gold surfaces: first examples of self-assembled monolayer films involving azulenic scaffolds. *Langmuir*, **2006**, *22*, 4599-606.

16 Neal, B. M. Vorushilov, A. S. Delarosa, A. M. Robinson, R. E. Berrie, C. L.; Barybin, M. V. Ancillary nitrile substituents as convenient IR spectroscopic reporters for self-assembly of mercapto- and isocyanoazulenes on Au(111). *Chemical Communications*, **2011**, *47*, 10803-10805.

17 Maher, T. R. Spaeth, A. D. Neal, B. M. Berrie, C. L. Thompson, W. H. Day, V. W.; Barybin, M. V. Linear 6,6'-Biazulenyl Framework Featuring Isocyanide Termini: Synthesis, Structure, Redox Behavior, Complexation, and Self-Assembly on Au(111). *Journal of the American Chemical Society* **2010**, *132*, 15924-15926.

18 Mishchenko, A. Zotti, L. a; Vonlanthen, D. Bürkle, M. Pauly, F. Cuevas, J. C. Mayor, M.; Wandlowski, T. Single-Molecule Junctions Based on Nitrile-Terminated Biphenyls: A Promising New Anchoring Group. *Journal of the American Chemical Society* **2011**, *133*, 184-187.

19 Luo, L. Choi, S. H.; Frisbie, C. D. Probing Hopping Conduction in Conjugated Molecular Wires Connected to Metal Electrodes . *Chemistry of Materials* **2011**, *23*, 631-645.

20 Bergren, A. J.; McCreery, R. L. Analytical Chemistry in Molecular Electronics. *Annual review of analytical chemistry*, **2010**, *4*, 173-195.

21 Chen, F. Hihath, J. Huang, Z. Li, X.; Tao, N. J. Measurement of single-molecule conductance. *Annual review of physical chemistry* **2007**, *58*, 535-564.

22 Jan van der Molen, S.; Liljeroth, P. Charge transport through molecular switches. Journal of physics. *Condensed matter*, **2010**, *22*, 133001.

23 McCreery, R. L. Molecular Electronic Junctions. *Chemistry of Materials* **2004**, *16*, 4477-4496.

24 Heimel, G. Rissner, F.; Zojer, E. Modeling the electronic properties of pi-conjugated self-assembled monolayers. *Advanced materials*, **2010**, *22*, 2494-2513.

25 Chen, J., Calvet, L.C., Reed., M.A., Carr, D.W., Grubisha, D.S., Bennent, D.W. Electronic transport through metal–1,4-phenylene diisocyanide–metal junctions. *Chemical Physics Letters* **1999**, *313*, 741-748.

26 Dupraz, C. J. Beierlein, U.; Kotthaus, J. P. Low temperature conductance measurements of self-assembled monolayers of 1,4-phenylene diisocyanide. *Chemphyschem*, **2003**, *4*, 1247-1252.

27 Jaiswal, A. Tavakoli, K. G.; Zou, S. Coupled surface-enhanced Raman spectroscopy and electrical conductivity measurements of 1,4-phenylene diisocyanide in molecular electronic junctions. *Analytical chemistry* **2006**, *78*, 120-124.

28 Kiguchi, M. Miura, S. Hara, K. Sawamura, M.; Murakoshi, K. Conductance of a single molecule anchored by an isocyanide substituent to gold electrodes. *Applied Physics Letters*, **2006**, *89*, 213104.

29 Kim, B. Beebe, J. M. Jun, Y. Zhu, X.-Y.; Frisbie, C. D. Correlation between HOMO alignment and contact resistance in molecular junctions: aromatic thiols versus aromatic isocyanides. *Journal of the American Chemical Society* **2006**, *128*, 4970-4971.

30 Beebe, J. M. Kim, B. S. Frisbie, C. D.; Kushmerick, J. G. Measuring Relative Barrier Heights in Molecular Electronic Junctions with Transition Voltage Spectroscopy. *ACS Nano* **2008**, *2*, 827–832.

31 Tan, A. Balachandran, J. Sadat, S. Gavini, V. Dunietz, B. D. Jang, S.-Y.; Reddy, P. Effect of Length and Contact Chemistry on the Electronic Structure and

Thermoelectric Properties of Molecular Junctions. *Journal of the American Chemical Society* **2011**, *133*, 8838-8841.

32 Li, Y. Lu, D.; Galli, G. Calculation of Quasi-Particle Energies of Aromatic Self-Assembled Monolayers on Au(111). *Journal of Chemical Theory and Computation* **2009**, *5*, 881-886.

33 Xue, Y.; Ratner, M. End group effect on electrical transport through individual molecules: A microscopic study. *Physical Review B* **2004**, *69*, 085403.1-085403.5.

34 Lee, J.-O. Lientschnig, G. Wiertz, F. Struijk, M. Janssen, R. a J. Egberink, R. Reinhoudt, D. N. Hadley, P.; Dekker, C. Absence of Strong Gate Effects in Electrical Measurements on Phenylene-Based Conjugated Molecules. *Nano Letters* **2003**, *3*, 113-117.

35 Kiguchi, M. Miura, S. Hara, K. Sawamura, M.; Murakoshi, K. Conductance of single 1,4-disubstituted benzene molecules anchored to Pt electrodes. *Applied Physics Letters* **2007**, *91*, 053110.

36 Lörtscher, E. Cho, C. J. Mayor, M. Tschudy, M. Rettner, C.; Riel, H. Influence of the Anchor Group on Charge Transport through Single-Molecule Junctions. *Chemphyschem* **2011**, *12*, 1677-1682.

37 Lee, Y. Carsten, B.; Yu, L. Understanding the anchoring group effect of molecular diodes on rectification. *Langmuir* **2009**, *25*, 1495-1499.

38 Rodríguez-Bolívar, S. Gómez-Campos, F. Álvarez de Cienfuegos, L. Fuentes, N. Cárdenas, D. Buñuel, E. Carceller, J. Parra, A.; Cuerva, J. Conductance and application of organic molecule pairs as nanofuses. *Physical Review B* **2011**, *83*, 1-11.

39 Kim, B. S. B.-S. B. Beebe, J. M. J. M. Olivier, C. Rigaut, S. Touchard, D. Kushmerick, J. G. Zhu, X.-Y. X. Y.; Frisbie, C. D. Temperature and length dependence of charge transport in redox-active molecular wires incorporating ruthenium (II) bis (sigma-arylacetylide) complexes. *Journal of Physical Chemistry C* **2007**, *111*, 7521–7526.

40 McGinnis, David M. Synthesis and Coordination of Azulene- and Ferrocene-Based Isoyanide Ligands University of Kansas, 2011. UMI, Ann Arbor MI

41 a) Clear, S.C., Nealey, P.F., *Langmuir*, **2001**, *17*, 720-732. b) Le Grange, J.D., Markham, J.L, Kurkjian, C.R., *Langmuir*, **1993,** *9*, 1749-1753. c) Wasserman, S.R., Whitesides, G.M., Tidswell, I.M., Ocko, B.M., Pershan, P.S., Axe, J.D. *Journal of the American Chemical Society*, **1989**, *111*, 5882-5861.

42 Maher, Tiffany R. Design of Novel Electron-rich Organometallic Frameworks Involving Metal-Isocyanide Junctions University of Kansas, 2009, UMI Ann Arbor MI, #3354892.

43 Toriyama, M., Maher, T.R., Holovics, T.C., Vanka, K., Day, V.W., Berrie, C.L., Thompson, W.H., Barybin, M.V., *Inorganic Chemistry*, **2008**, *47*, 3284-3291.

44 Henderson, J.I, Feng, S., Bein, T., Kubiak, C.P. Adsorption of Diisocyanides on Gold *Langmuir*, **2000**, *16*, 6183-6187.

45 Lazar, M., Angelici, R.J. *Journal of the American Chemical Society*, **2006**, *128*, 10613-10620.

CHAPTER III

III. First Self-assembled Monolayer Films of Mercaptoazulenes

Portions of this work have been published in

Neal, B. M.; Vorushiolov, A. S.; DeLaRosa, A. M.; Robinson, R. E.; Berrie, C. L.; Barybin, M. V. Ancillary nitrile substituents as convenient IR spectroscopic reporters for self-assembly of mercapto- and isocyanoazulenes on Au(111). *Chemical Communications*, **2011**, 47, 10803-10805.

III.1 Introduction

Organosulfur compounds of thiols ($HS(CH_2)_nX$), disulfides ($X(CH_2)_mS$-$S(CH_2)_mX$), and sulfides ($X(CH_2)_mS(CH_2)_mX$), where n and m are the number of methylene units and X is the terminal functional group, have been used to form SAMs on Au substrates since 1983. [1] Much of the earlier literature focused on the formation of such SAMs via adsorption from solution or vapor deposition to Au and Ag. [1-5] The initial studies explored many basic fundamentals, such as optimal conditions and procedures for film formation, as well as orientation of the adsorbed molecules with respect to the surface and relative to each other. Subsequent reports considered not only adsorption of new organosulfur compounds on Au, but also self-assembly and orientation of the previously known molecules on different substrates, such as Ag, Cu, Pd, Pt, Ni, and Fe. [6]

SAM films of straight chain aliphatic hydrocarbon thiols on Au(111) constitute one of the most studied systems. [1,6] As outlined by Whitesides, metallic gold surfaces are particularly attractive for SAM film formation for several reasons: 1) there are relatively straightforward methods of preparing high quality gold thin films, *e.g.*, by physical vapor deposition, *vide supra* 2) patterning on gold is relatively easy to accomplish 3) gold is an inert metal, 4) many analytical techniques have been developed to characterize changes to thin Au substrates, and 5) gold does not appear to be toxic to cells. [1] For the studies of mercaptoazulenes described here, reasons 1, 3, and 4 are the most pertinent.

Self-assembly of alkane thiolates on Au, as well as properties of the resulting molecular films, has been reviewed by Whitesides *et al*. and Salvarezza *et al.* [1,6] Given that mercaptoazulenes represent an unusual class of aromatic organothiols, SAMs of

these nonbenzenoid mercaptoarenes, reported in this Thesis, are best compared and contrasted with those of previously known benzenoid mercaptoarenes. Similar to SAMs of homologous aliphatic thiolates, the molecular tilt angle in benzenoid aromatic thiolate films is influenced by the number of elementary units (i.e., six-membered rings) in the organic chain. Table III.1 summarizes some characteristics of representative aromatic thiolates absorbed on metallic gold.

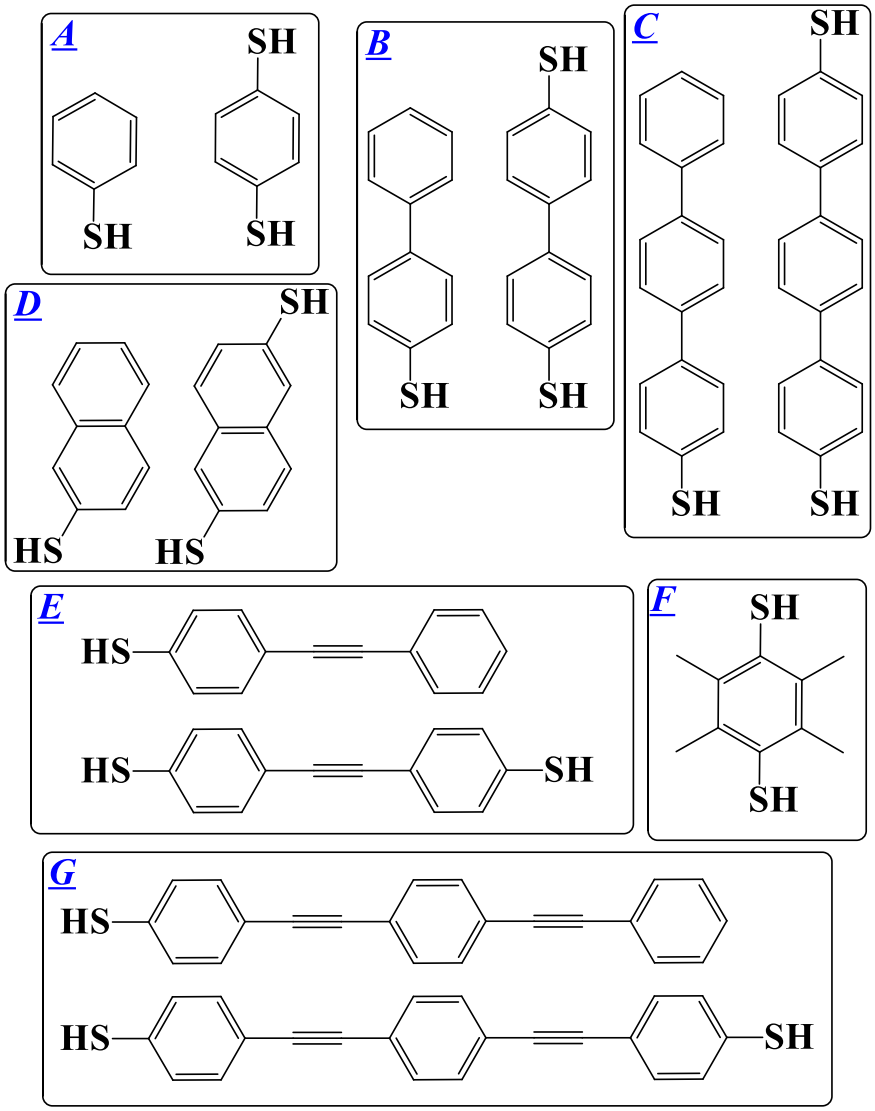

Figure III.1 - Structures of various benzenoid aromatic thiols and dithiols: (A) benzenethiol and benzene-1,4-dithiol, (B) biphenyl-4-thiol and biphenyl-4,4'-dithiol, (C) terphenyl-4-thiol and terphenyl-4,4''-dithiol, (D) naphthalene-2-thiol and naphthalene-2,6-dithiol, (E) OPE(2)-4-thiol and OPE(2)-4,4'-dithiol (F) α, α'-xylyldithiol (G) OPE(3)-4-thiol and OPE(3)-4,4''-dithiol.

Table III.1 – Various aromatic thiols and their properties when they are incorporated in SAM films on Au substrates. Structures of these are shown in Figure III.1

Molecule	Tilt Angle	Thickness characterization	Thickness obs. (Å)	Thickness calc. (Å)	Water contact angle (°)	Ref
Benzene thiol	-	XPS	6.0-8.3 Å	-	-	7
Biphenyl-4-thiol	-	ellipsometry	14 Å	-	73 (adv); 69 (red)	8
Biphenyl-4,4'dithiol	-	ellipsometry	13 Å	-	67 (adv); 62 (red)	8
Biphenyl-4,4'dithiol	-	ellipsometry	12.2 Å	13 Å	69° to 71°	9
α, α'-xylyldithiol	24°	ellipsometry	8.3 Å	-	69° to 71°	9
Biphenyl-4-thiol	-	ellipsometry	12±1 Å	-	-	10
Biphenyl-4,4'-dithiol	-	ellipsometry	16.5±1.25 Å	-	-	10
Naphthalene-2-thiol	44°	-	-	-	-	11
OPE(3)-4-thiol	30°	spectr. ellipsometry	18±0.1 Å	-	-	12
OPE(3)-4-thiol	25	spectroscopic ellipsometry	19 Å		74° ± 3°	13
OPE(3)-4-thiol	31	HRXPS	18 Å		74° ± 3°	13
OPE(1)-4thiol	30	NEXAFS	13 Å		74° ± 3°	13
Benzene thiol	-	ellipsometry	9±3 Å	5.6Å	58±3°	14
OPE(2)-4-thiol	-	ellipsometry	12±2Å	12.4Å	70±3°	14
OPE(3)-4-thiol	-	ellipsometry	19±2Å	19.2 Å	80±3°	14
Benzene thiol	-	ellipsometry	1±1 Å	-	80±2° (adv); 76±2° (rec)	15
Biphenyl-4,4'-thiol	-	ellipsometry	9±2 Å	-	85±1° (adv); 82±1° (rec)	15
Terphenyl-4-thiol	-	ellipsometry	11±1 Å	-	80±2° (adv); 79±2° (rec)	15
Benzene thiol	-	XPS	5.5	8.1	-	16
Benzene thiol	-	spectr. ellipsometry	6.1	8.1	-	16
Naphtalene-2-thiol	-	XPS	8.2	10.3	-	16
Naphtalene-2-thiol	-	spectr. ellipsometry	8.5	10.3	-	16
Benzene-1,4-dithiol	-	XPS	8.2	8.8	-	16
Benzene-1,4-dithiol	-	spectr. ellipsometry	8.6	8.8	-	16
Naphthalene-2,6-dithiol	-	XPS	10.2	11.0	-	16
Naphthalene-2,6-dithiol	-	spectr. ellipsometry	10.3	11.0	-	16

The packing arrangements of SAMs of several aromatic thiols were compared using cyclic voltammetry (CV), RAIR, STM, ellipsometry, and contact angle measurements. [17] Effectively, the molecules studied belong to one of two categories. The first, with molecules such as benzene thiols and biphenyl thiols having the thiol functional group directly linked to the aromatic ring, formed poorly packed monolayers. The second class, molecules with a methylene unit between the thiol and aromatic rings, formed much better packed monolayers with CV results being what was typically seen in monolayers of alkanethiols. The packing differences documented for these two groups of SAMs were attributed to the methylene unit. As illustrated in Figure III.2, for benzenethiol, the 180° Au-S-C bond angle would allow the molecule to be parallel to the surface normal while a ~104° Au-S-C bond angle would force the molecule to be tilted away from the surface normal causing poorer packing. The insertion of a methylene unit between the ring and the sulfur atom allows the sulfur to assume the ~104° bond angle and arrange the aromatic rings in a well-ordered packing.

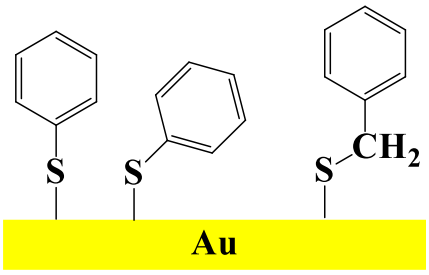

Figure III.2 - Benezenethiol (BT), left, and benzylthiol (phenylmethanethiol or PMT), right, coordinated to the Au surface showing the possible geometries of the Au-S-C bond angles and the resulting molecular orientation on the surface. Adapted from Ref. 17.

Studying films of benzenethiol and benzeneselenol on Au(111) surfaces via STM, contact angles and thermal desorption spectroscopy, Witte *et al.* observed similar low packing order as previously described for the benzenethiol on the surface that was attributed to pronounced molecular tilting. [18] STM measurements suggested the long-range ordering of these monolayers to be poor, especially when compared to the analogous benzeneselenol system. Additionally, NEXAFS analysis of the thiol film indicated a molecular tilt angle of 54° with respect to the surface normal.

The BT SAMs formed poorly ordered monolayers unlike their BMT counterparts as determined by STM. [19] The addition of the methylene-spacer is thought to provide enough flexibility to allow for better Van der Waals interactions between the aromatic rings thereby allowing for better packing to take place. XPS data showed that both systems had strongly bound species to the Au(111) surfaces, but the BT monolayers had somewhat weaker coordinating molecules than the BMT films. By introducing the methylene spacer as in BMT, the number of weaker coordinating sulfur-species was drastically reduced because of BMT's more ordered packing on the surface. Increasing the temperature of the BT solution during monolayer formation to 50 - 75 °C facilitated ordered two-dimensional packing as evidenced by STM analysis. [20]

Film formation of butanedithiol, hexanedithiol, and nonanedithiol on Au(111) was investigated using two different procedures. [21] The first procedure employed 50 μM solutions of the dithiols in ethanol while the second protocol involved 1 mM solutions in n-hexane degassed with N_2. Butanedithiol, in either procedure, chemisorbed to the metal surface via both sulfur atoms in a lying-down configuration. Formed via the first

procedure, the SAMs of hexanedithiol and nonanedithiol showed the majority of molecules in a standing-up orientation. However, some of the terminal mercapto groups had formed disulfides with either other chemisorbed dithiols or extra dithiol molecules from solution. Using the second procedure, the hexanedithiol and nonanedithiol predominately chemisorbed in a standing-up fashion with only one sulfur atom chemisorbing with no oxidation of the terminal sulfur observed by RAIRS, XPS, and time of flight direct recoil spectroscopy. These results demonstrate the importance of both relatively long chain length and lack of O_2 for retaining the terminal thiol groups.

Using synchrotron angle resolved ultraviolet photoelectron spectroscopy studies of benzenethiol adsorption on Au(111) to study the orientation of the molecules on the surface it was concluded that the phenyl ring of the molecule orients preferentially parallel to the gold surface, with little dependence on the extent of surface coverage. [22] XPS measurements confirmed that the sulfur atom formed a thiolate bond to the surface. In a separate experiment, high resolution electron energy loss spectroscopy, HREELS, was used to study films of benzenethiol on gold surfaces and indicated disappearance of the S-H stretching band, that was observed for free BT (2580 cm^{-1}), upon coordination to the Au(111) surface. [23] The weak Au-S stretching band expected at ~460 cm^{-1} was not detectable. However, in contrast to their previous work, based on the observation of a weak peak at 3010 cm^{-1} corresponding to a C-H bending mode that would be forbidden if the molecule were coordinated perfectly upright, a mostly upright orientation was assumed.

Mercaptobiphenyls have a more significant molecular dipole compared to alkanethiols due to the conjugation between the two rings. [24] Due to this increased molecular dipole and high surface free energies compared to alkanethiols, water contact angle measurements have not been as useful in characterization of terminally functionalized mercaptobiphenyl films as compared to analogous terminally functionalized alkanethiols films. Also, the interface between the wetting liquid and the top, exposed part of the molecule is not as well packed as alkanethiols thus allowing for the wetting liquid to interact with the phenyl rings, making contact angle measurements less instructive. That said, monolayers of assorted 4'-substituted-4-mercaptobiphenyls were studied via ellipsometry and external reflection FTIR to suggest that these systems have low tilt angles with respect to the surface normal on the order of 15° and 30°. [25]

Ellipsometric and XPS data acquired for SAMs of biphenyldithiols indicated possible formation of disulfide bonds through involvement of the terminal sulfur atoms, in addition to retention of the thiol functional group in some molecules. [26] Coordination via both thiol junctions of the same molecule to the surface was not observed in any appreciable quantity. Contact of the sample with air was likely responsible for the oxidation of the biphenyl dithiol species suggested by XPS.

Upon coordination of naphthalene-2-thiol to the Au surface, there are three possibilities for rotation around the C-S bond of the napthalenethiolate unit such that the molecule may orient in a variety of fashions, as shown in Figure III.3. [27] The standing and lying phases were detected by STM, indicating that the π-π interactions between the molecules are important for ideal packing orientation. Both rotomers coexist in the same

SAM and differ in their position on the Au(111) surface with the standing molecules in atop and 3-fold hollow sites and the lying phase occupying a bridging position.

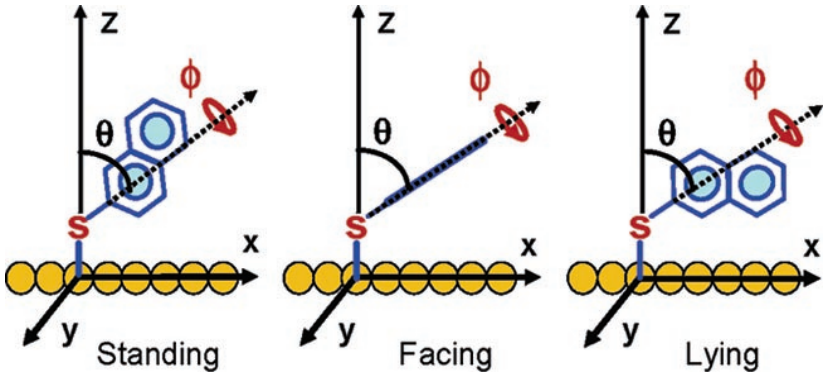

Figure III.3 - Three possible orientations of 2-napthalenethiol on the gold surface. In both the standing and lying orientations the angle of rotation of the molecule with respect to the S-C bond, ϕ, causes the molecule to be oriented perpendicularly to the surface. The tilt angle θ is the same for all orientations. From Ref 27.

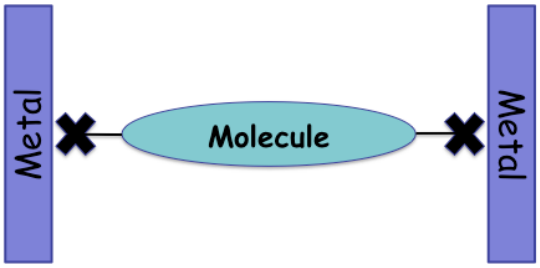

Figure III.4 - General model of the metal-molecule-metal framework where X denotes junction groups linking the metal surfaces to the molecule.

Similar to the isocyanoarenes discussed in Chapter 2, aromatic thiol and dithiol molecules have been of interest as conductors or diodes for use in molecular electronics.

Frisbie has recently probed the resistance to current of various oligoacene thiols, including mercapto- and dimercaptonaphthalene molecules. [28] The thicknesses of these films were determined using XPS and spectroscopic ellipsometry. The XPS data were also used to model adsorption of the dithiol molecules via both of their sulfur atoms. For the SAMs of 1,4-dimercaptobenzene on gold, roughly 25%±10% of the molecules were doubly bound to the Au surface, whereas 11%±10% of the 2,6-dimercaptonaphthalene molecules were doubly bound. The resistance of a molecular system, generally represented by Figure III.4 varies greatly depending on whether the organic linker was connected to both metals via chemical bonding, as in the case of a dithiol, or connected with one chemical junction and one physical, as in the case of a monothiol. [28] Frisbie's report is particularly interesting because it demonstrated not only decreased contact resistance, but also lower tunneling attenuation factor, (a measure of electronic decay as the charge moves across the molecule) for dimercapto- versus monomercapto-functionalized arenes. Additionally, computational work by Pati *et al.* had suggested the I-V curve for the 2,6-dimercaptonaphthalene molecule to be symmetric and Taniguchi *et al.*, experimentally confirmed this prediction later.

Figure III.5 - 2,6-Dimercaptoazulene and 2,6-dimercaptonapthalene considered in a theoretical study by Pati *et al.* in Ref. 29.

In their computational study, Pati *et al*. compared conductivity characteristics of isomeric 2,6-dimercaptonaphthalene and currently unknown 2,6-dimercaptoazulene

shown in Figure III.5. [29] Using non-equilibrium Green's function (NEGF) and Gaussian calculations, the I-V curve for 2,6-dimercaptonaphthalene was shown to be symmetric in both positive and negative bias regions, which was not true for 2,6-dimercaptoazulene. In the low-bias region, from 0.7 V to -0.7 V, both molecules were predicted to have nearly identical conductivities. However, markedly different currents were expected for these two systems at a higher bias. In the high positive bias region, the 2,6-dimercaptoazuleneframework was calculated to experience greater current than its isomeric naphthalene analogue. On the other hand, the 2,6-dimercaptonaphthalene scaffold was calculated to exhibit greater negative current compared to 2,6-dimercaptoazulene under high negative bias. Notably, for the azulenic system, electrons would flow from the seven-membered ring to the five-membered ring in the positive bias region and vice versa in the negative region, thereby signifying that the azulenic system would act as a molecular diode.

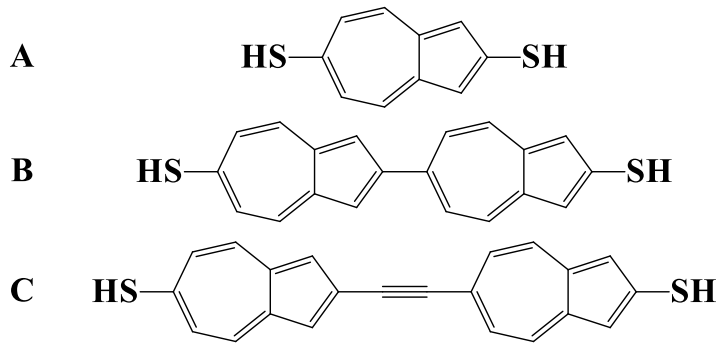

Figure III.6 – Hypothetical dimercaptoazulene and related polyazulene molecules considered in a theoretical study by Ref. 30.

A theoretical study by Zhang *et al*. on 2,6-dimercaptoazulene and other hypothetical azulene-like molecules shown in Figure III.6 provided conclusions similar to

those of Pati. [30] Zhang, using NEGF methods, calculated the I-V curves for these molecules and compared the ratios of current in a particular positive bias to the current at the corresponding negative bias. A ratio not equaling 1 would indicate that the molecule behaves as a rectifier, which was indeed the case for all azulenic and azulene-like molecules. While all of the molecules were predicted to rectify, the molecule A in Figure III.6 had the lowest ratio of current in the positive region compared to the negative region followed by the molecules B and then C. The predicted conductivities of the azulenic molecules considered by Zhang were greater than those of OPE derivatives. [31]

III.2 Work Described in Chapter III

This chapter addresses the formation, properties and stability of the SAM films of all mercaptoazulene derivatives developed in the Barybin lab to date. In addition, incorporation of ancillary nitrile substituents as infrared spectroscopic reporters for facile characterization of azulenic SAMs is discussed. Future directions of this research are outlined at the conclusion of the Chapter.

III.3 Experimental Section

III.3.1. General Procedures and Starting Materials

The mercaptoazulene derivatives involved in these studies were prepared as described elsewhere. Syntheses of **1**, **2**, and **4** are reported in Barybin *et al.*, *Chemical Communications*, **2011**, *47*, 10803-10805. [32] Preparation of **3** is documented in Dr. Alexander Vorushilov's Ph.D. Thesis. [33] Compounds **5**, **6**, and **7** will be reported in Scheetz, K. J., Vorushilov, A. S., Powell, D. R., Barybin, M. V., Manuscript in preparation.[34] The chemical structures of these molecules may be seen in Figure III.7.

Gold-coated mica substrates were either purchased from Platypus Technologies or fabricated in the Berrie lab using an Edwards Auto 306 rotary evaporator. "House" Au(111) was deposited on freshly cleaved sheets of mica under vacuum of *ca.* 1.5 $x10^{-7}$ torr with a deposition rate of about 1 Å/sec, as measured by a quartz crystal microbalance. Films were coated between 250 and 300 Å thick and were subsequently stored under high vacuum or in inert atmosphere conditions until use. Commercial silicon wafers, coated with a 50 Å titanium adhesion layer and then 1000 Å of gold, were purchased from Platypus Technologies.

Unless otherwise stated, all substrates were soaked in distilled $CHCl_3$, acetone, and 200-proof ethyl alcohol for one to two hours in each solvent with no precautions against exposure to ambient air or lighting. Substrates were then removed and dried in a stream of N_2 gas. Physical constants of the substrates were measured using a Rudolph Research Auto El III fixed wavelength ellipsometer. Measurements were made with a 632.8 nm wavelength HeNe laser. The optical constants of each cleaned, bare substrate

were measured prior to its exposure to thiol solutions. These optical constants were used to determine the thickness of the organic film on the substrate after exposure. Typical values of n ranged from 0.161 to 0.181 and K values from 3.52 to 3.55. A refractive index of 1.45 was assumed [35] for all SAMs described in this chapter. At least five separate spots on the substrate were analyzed to determine both the optical constants and the film thicknesses. The film thickness values reported herein constitute averages of these measurements with the corresponding standard deviations given in parentheses.

All surface IR experiments involved grazing angle reflection absorption Fourier transform infrared spectroscopy. These data for the SAMs were obtained on a Thermo Nicolet 670 FRIR spectrometer with a VeeMax grazing angle accessory set up at an incident angle of 70°. Prior to acquiring an IR spectrum of each SAM sample, a background spectrum was collected using a corresponding similarly treated bare substrate. Typically, 1000 scans from 600 to 4000 cm^{-1} at 4 cm^{-1} resolution were collected for both the background and sample spectra.

III.3.2. Preparation of 2-mercaptoazulene (1) SAM film

Both commercial gold-coated silicon (Platypus Technologies) and house-coated Au on mica substrates were soaked sequentially in distilled $CHCl_3$, acetone, and 200-proof ethanol for one to two hours in each solvent separately. After drying with a stream of N_2 gas, ellipsommetric physical constants of the bare gold substrates were measured. The SAM film was formed by soaking the freshly cleaned and characterized substrate in a 2mM solution of **1** in distilled $CHCl_3$ for approximately 24 hours. The substrate was then removed from the solution, rinsed thoroughly with distilled $CHCl_3$, and dried in a

stream of N_2 gas. No precautions to exclude air or ambient laboratory lighting were taken during this procedure.

III.3.3. Preparation of 1,3-diethoxycarbonyl-2-mercaptoazulene (2) SAM film

Both commercial gold-coated silicon (Platypus Technologies) and house-coated Au on mica substrates were soaked sequentially in distilled $CHCl_3$, acetone, and 200-proof ethanol for one to two hours in each solvent separately. After drying with a stream of N_2 gas, ellipsommetric physical constants of the bare gold substrate were measured. The SAM film was formed by soaking the freshly cleaned and characterized substrate in a 2mM solution of **2** in distilled $CHCl_3$ for approximately 24 hours. The substrate was then removed from the solution, rinsed thoroughly with distilled $CHCl_3$, and dried in a stream of N_2 gas. No precautions to exclude air or ambient laboratory lighting were taken during this procedure.

III.3.4. Preparation of 1,3-diethoxycarbonyl-6-mercaptoazulene (3) SAM film

Commercial gold-coated silicon (Platypus Technologies) and house-coated Au on mica substrates were soaked sequentially in distilled $CHCl_3$, acetone, and 200-proof ethanol for one to two hours in each solvent separately. After drying with a stream of N_2 gas, ellipsommetric physical constants of the bare gold substrates were measured. The SAM film was formed by soaking the freshly cleaned and characterized substrate in a 2mM solution of **3** in distilled $CHCl_3$ for approximately 24 hours. The substrate was then removed from the solution, rinsed thoroughly with distilled $CHCl_3$, and dried in a stream of N_2 gas. No precautions to exclude air or ambient laboratory lighting were taken during this procedure.

III.3.5. Preparation of 1,3-dicyano-2-mercaptoazulene (4) SAM film

Commercial gold-coated silicon (Platypus Technologies) and house-coated Au on mica substrates were soaked sequentially in distilled $CHCl_3$, acetone, and 200-proof ethanol for one to two hours in each solvent separately. After drying with a stream of N_2 gas, ellipsommetric physical constants of the bare gold substrate were measured. The SAM film was formed by soaking the freshly cleaned and characterized substrate in a 2mM solution of **4** in distilled THF for approximately 24 hours. The substrate was then removed from the solution, rinsed thoroughly with distilled $CHCl_3$ and ethanol, and dried in a stream of N_2 gas. No precautions to exclude air or ambient laboratory lighting were taken during this procedure.

III.3.6. Preparation of 1,3-diethoxycarbonyl-6-chloro-2-mercaptoazulene (5) SAM film

Commercial gold-coated silicon (Platypus Technologies) and house-coated Au on mica substrates were soaked sequentially in distilled $CHCl_3$, acetone, and 200-proof ethanol for one to two hours in each solvent separately. After drying with a stream of N_2 gas, ellipsommetric physical constants of the bare gold substrate were measured. The SAM film was formed by soaking the freshly cleaned and characterized substrate in making a 2mM solution of **5** in distilled $CHCl_3$ for approximately 24 hours. The substrate was then removed from the solution, rinsed thoroughly with distilled $CHCl_3$, and dried with a stream of N_2 gas. No precautions to exclude air or ambient laboratory lighting were taken during this procedure.

III.3.7. Preparation of 1,3-diethoxycarbonyl-2,6-dimercaptoazulene (6) SAM film

Commercial gold-coated silicon (Platypus Technologies) and house-coated Au on mica substrates were soaked sequentially in distilled $CHCl_3$, acetone, and 200-proof ethanol for one to two hours in each solvent separately. After drying with a stream of N_2 gas, ellipsommetric physical constants of the bare gold substrate was measured. SAM films were formed by soaking the freshly cleaned and characterized substrate in a 2mM solution of **6** in distilled $CHCl_3$ for approximately 24 hours. The substrate was removed from the solution, rinsed thoroughly with distilled $CHCl_3$, and dried with a stream of N_2 gas. No precautions to exclude air or ambient laboratory lighting were taken during this procedure.

III.3.8. Preparation of (1,3-diethoxycarbonyl-2-mercaptoazulen-6-yl)(triphenylphosphine)gold (7) SAM film

Commercial gold-coated silicon (Platypus Technologies) and house-coated Au on mica substrates were soaked sequentially in distilled $CHCl_3$, acetone, and 200-proof ethanol for one to two hours in each solvent separately. After drying with a stream of N_2 gas, ellipsommetric physical constants of the bare gold substrate were measured. The SAM film was formed by soaking a 2mM solution of **7** in distilled $CHCl_3$ for approximately 24 hours. The substrate was then removed from the solution, rinsed thoroughly with distilled $CHCl_3$, and dried in a stream of N_2 gas. No precautions to exclude air or ambient laboratory lighting were taken during this procedure.

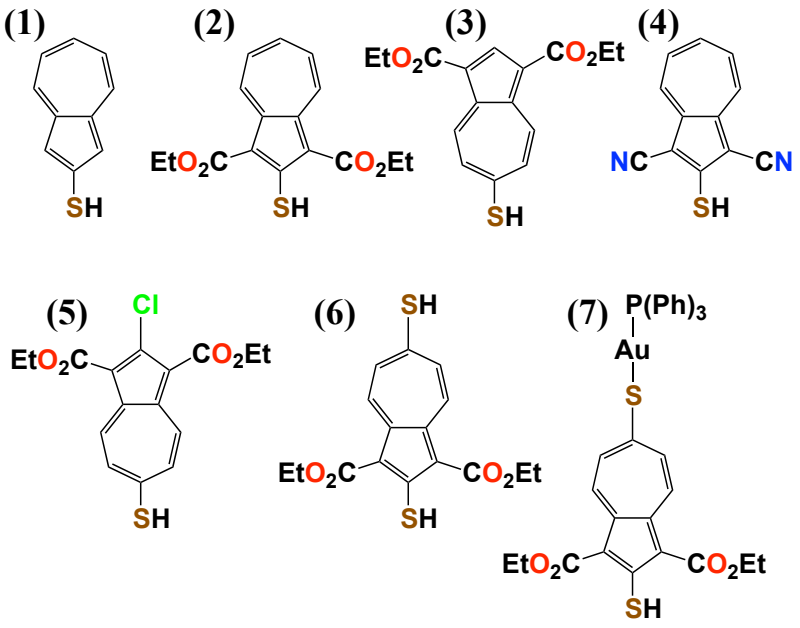

Figure III.7 – Structures of molecules **1**, **2**, **3**, **4**, **5**, **6**, and **7**

III.4 Results and Discussion

Studying mercaptoazulene SAMs presents some characterization challenges compared to SAMs of the related isocyanoazulenes. The isocyanide functional group serves not only as a good junction for coordinating an azulenic framework to the gold surface with controlled orientation, but also as a sensitive infrared spectroscopic reporter providing important information regarding coordination mode and molecular orientation with respect to the surface normal. Unfortunately, the SAM films of **1**, **2**, and **3** lack easily identifiable spectroscopic handles in the IR spectrum. As discussed previously, surface IR measurements had been proven instrumental for analyzing SAMs of aliphatic, straight chain alkanethiols by detecting the position of the ν(C-H) stretching bands corresponding to the methyl and methylene units of the hydrocarbon chain. However, this approach is of limited, if any, utility in the characterization of the SAM films of **1**, **2**, and **3** due to background subtraction issues, as well as the relatively smaller number of C-H bonds in the mercaptoazulene molecules compared to those in long, straight chain aliphatic hydrocarbons.

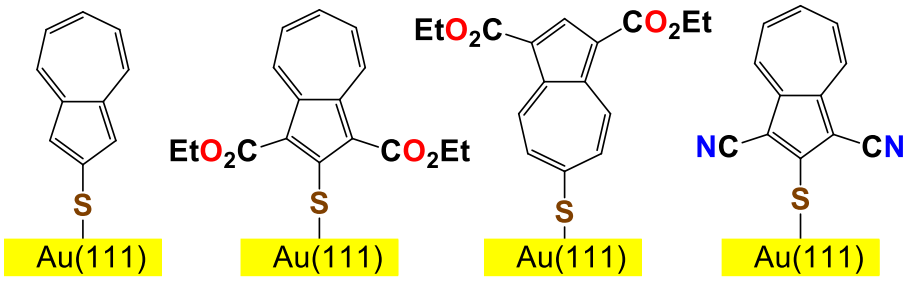

Figure III.7 - Proposed upright coordination of **1**, **2**, **3**, and **4,** respectively, on Au(111) surfaces

Table III.2 Observed ellipsometric (D_{obs}) and calculated for upright coordination (D_{calc}) thicknesses of SAMs of **1**, **2**, **3**, and **4** on Au(111)

	1	**2**	**3**	**4**
D_{obs} (Å)	10.9±0.6	12.3±2.0	12.9±1.9	11.7±1.9
D_{calc} (Å)	10.4	10.4	13.3	10.4

Ellipsometrically determined thicknesses of several novel mercaptoazulenic SAM films, as well as the corresponding theoretically estimated values for the upright molecular adsorption are provided in Table III.2. In the case of the crystallographically characterized **1** and **3** [32, 33], the X-ray data were used to obtain the D_{calc} values, which include the typical Au-S bond distance of 2.45 Å. [36] This assumes the molecules are oriented parallel to the surface normal as shown in Figure III.7 and feature a straight Au-S-C bond angle. It is also expected that the dimension of **2** along its molecular axis should be identical to that of **1** upon adsorption. Comparing the experimental and calculated data for the mercaptoazulene films in Table III.2, it is reasonable to conclude that all of these films constitute monolayers, even though the ellipsometric evidence should be regarded as circumstantial.

Table III.3 – Observed ellipsometric thicknesses of SAMs **1**, **2**, and **3** over time

Compound	**Day**	**Thickness (Å)**
1	1	15.9±0.7
	20	15.7±2.6
2	1	12.3±2.0
	15	13.4±3.4
3	1	12.8±1.9
	4	10.7±1.7

The stabilities of SAMs of 1, 2, and 3 on gold substrates were studied via ellipsometry over time. These films appear to be stable for a minimum of several days before film quality degrades. No precautions against lighting or air were taken during these experiments.

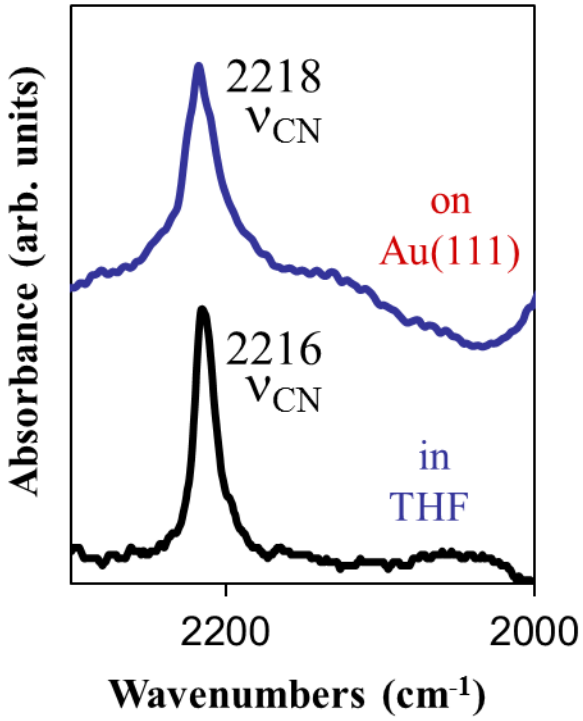

Figure III.8 IR spectrum of **4** in THF solution and on Au(111) surface

In order to obtain direct spectroscopic evidence for the formation of mercaptoazulenic SAM films, adsorption of compound **4**, that has nitrile substituents at positions 1 and 3 of the azulenic scaffold, on gold was then considered. This compound features the same 2-mercaptoazulene framework as **1** and **2**. Organic nitriles usually absorb IR radiation in the range of 2200 – 2230 cm^{-1}, which is not obscured by signals from other functional groups. Thus, they may serve as convenient spectroscopic reporters in the analysis of adsorption of **4** on metallic gold. The IR spectra collected for **4** in THF solution and coordinated to an Au(111) substrate are presented in Figure III.8. Only one ν(CN) band at essentially the same energy is observed for both **4** in solution and **4** adsorbed on Au(111).

The above finding is important for two reasons. First, because there is a strong ν(CN) signal in the surface IR spectrum, the molecules of **4** must be present on the surface and their nitrile oscillators cannot be oriented parallel to the surface due to the surface IR selection rules discussed in Chapter 1 of this Thesis. Second, the molecules of **4** are not coordinating to the surface via either nitrile group otherwise the position of the ν(NC) peak would likely shift to reflect changes in the electronic environment around theseis substituents, akin to what was documented for organic isocyanides chemisorbed to a metal surface. Combining the above IR evidence with the ellipsometrically determined film thickness of 11.7±1.9Å, it is clear that the molecules of **4** adsorb in an approximately upright fashion on Au(111). The value of D_{obs} documented for the SAM film of **4** correlates nicely with those obtained for the SAMs of mercaptoazulenes **1** and **2**, thereby giving further credence to the upright orientation of the molecules in the SAMs of **1**and **2** on gold.

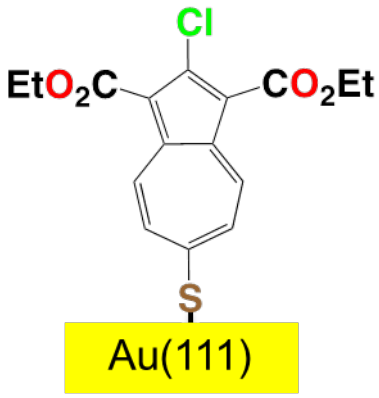

Figure III.9 Proposed orientation of **5** on Au surface

In addition to the 6-mercaptoazulene derivative **3**, originally synthesized by Dr. Alexander Vorushilov of the Barybin group, another 6-mercaptoazulene derivative,

namely 1,3-diethoxycarbonyl-2-chloro-6-mercaptoazulene, **5**, has recently become available through synthetic efforts of Kolbe Scheetz (Figure III.9). A thin film of **5** on Au(111) was formed and characterized in a manner similar to how it was done for other mercaptoazulene SAMs described above. The ellipsometrically determined thickness of the film of **5** on gold was 14.6±1.9 Å. This value compares well with the theoretically estimated film thickness, D_{calc}, of 13.5 Å, which assumes a perfectly upright coordination of the corresponding thiolate, a straight Au-S-C bond angle, and a typical Au-S bond length of 2.45 Å.

In the quest for the hitherto elusive 2,6-dimercaptoazulene moiety, Kolbe Scheetz of the Barybin group recently succeeded in synthesizing and isolating the first 2,6-dimercaptoazulene derivative, namely 1,3-diethoxycarbonyl-2,6-dimercaptoazulene, **6**, shown in Figure III.10.

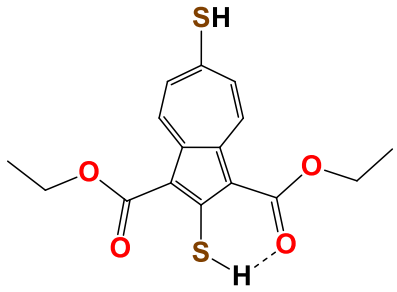

Figure III.10 – Structure of 1,3-diethoxycarboyl-2,6-dimercaptoazulene, **6**, showing intramolecular H-bonding interaction between the 2-mercapto group and an ester carbonyl.

A gold(111) substrate was immersed into a solution of **6** in $CHCl_3$ to form a thin film which was characterized by optical ellipsometry and RAIR spectroscopy. Because

the two mercapto groups of **4** are in significantly dissimilar chemical environments - one being attached to the seven-membered ring while the other being attached to the five-membered ring and also being engaged in a hydrogen bonding interaction with an ester carbonyl - the ν(SH) stretching bands for these mercapto substituents are markedly different in their energy and width. The IR spectrum of **6** in KBr features a sharp ν(S-H) peak at 2540 cm^{-1} corresponding to the 6-SH substituent and a much broader band at 2450 cm^{-1} due to the 2-SH functionality. The lower energy and substantially greater width of the latter ν(S-H) band is almost certainly a consequence of the hydrogen bonding interaction mentioned above. Thus, it might be reasonable to consider the ν(S-H) data in attempting to differentiate which mercapto terminus of **6** is engaged in forming the Au-S bond upon adsorption of **6** on gold, if such discrimination, happens at all. Preliminary IR spectroscopic results, that are illustrated in Figure III.11, turned out to be inconclusive at this point as there is no discernible ν(S-H) signal in the surface IR spectrum of the film of **6** on gold.

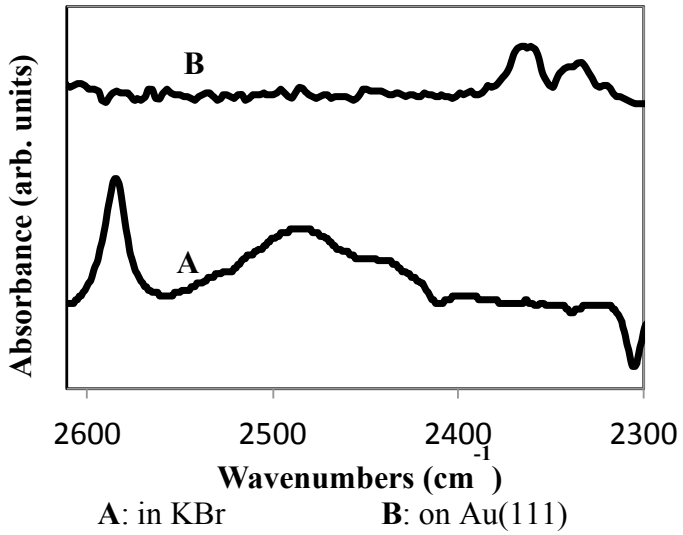

Figure III.11.(A) FTIR spectrum of **6** in KBr. (B) RAIR spectrum of **6** on Au(111)

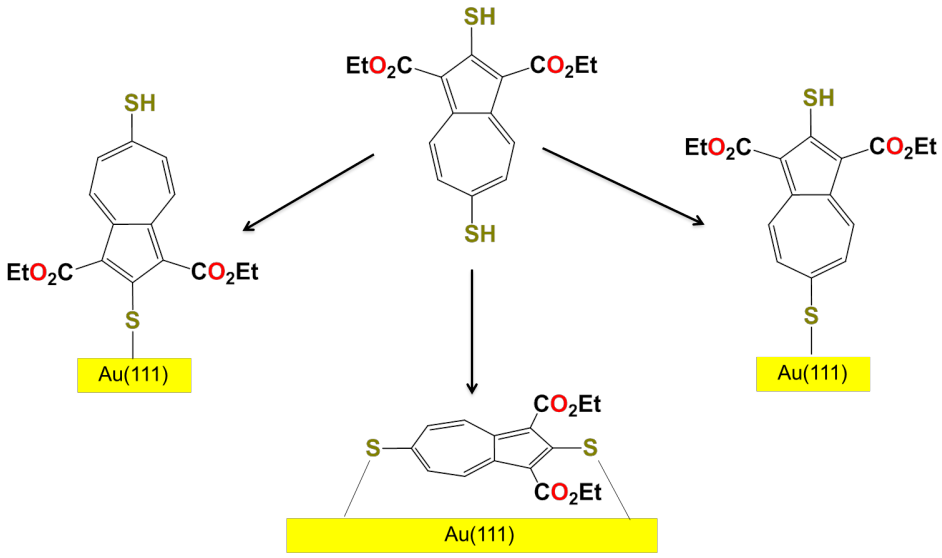

Figure III.12. Possible binding outcomes upon adsorption of **6** on Au(111).

In principle, **6** can coordinate to the Au(111) surface in at least three distinct ways, as shown in Figure III.12. Indeed, either of the mercapto termini or even both of

them may be envisioned to bind to the gold surface. Although the 6-mercapto oscillator gives a ν(S-H) band of a relatively weak intensity compared to various other IR-active functional groups, it does show up quite definitively in solution, Nujol mull, and KBr samples of **6**. Thus, if the 2-mercapto terminus of **6** is engaged in adsorption to the gold surface, the ν(S-H) signal for the uncoordinated 6-mercapto group might be detectable in the RAIR spectrum of the corresponding film. However, no such signal was observed. This result does not necessarily imply that **6** adsorbes to Au(111) via the 6-mercapto end or via both mercapto termini as the intensity of this expected ν(SH) peak could certainly be greatly affected by the orientation of the uncoordinated S-H bond with respect to the metal surface (see surface IR selection rules in Chapter 1). The ellipsometric thickness of the film of **6** on Au(111) was measured to be 11.6±3.1 Å, which is reasonably in line with the calculated thickness of *ca.* 11.8 Å expected for an upright adsorption of the molecule via either of its mercapto termini. The above film thickness value suggests that few, if any, molecules of **6** are chemisorbed to the gold surface via both mercapto junctions, although formation of a multi-layer cannot be completely ruled out. Nevertheless, given the lack of a definitive ν(SH) band corresponding to the 6-SH substituent, supports a tentative argument that **6** might be tethered to the surface through its less sterically encumbered mercapto substituent attached to the seven-membered ring of the azulenic moiety. Again, this tentative conclusion is circumstantial at best as there is currently no absolutely definitive IR-spectroscopic evidence available to support the claim.

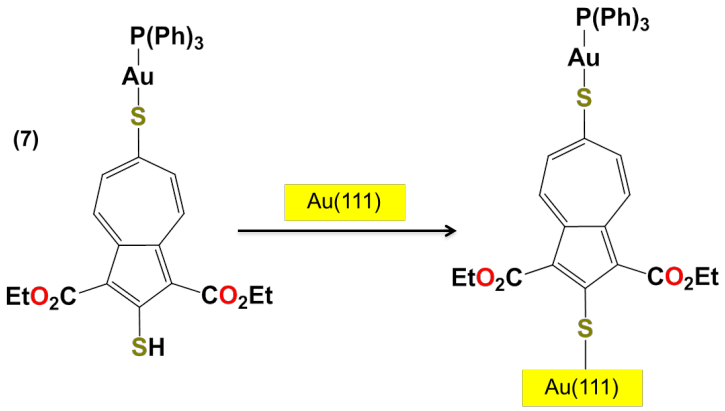

Figure III.13. – Proposed adsorption of complex **7** on an Au(111) surface.

Interestingly, Kolbe Scheetz has very recently demonstrated that the dimercaptoazulene **6** can be metallated in a perfectly regioselective and quantitative manner upon treatment with one equivalent of Ph_3PAuCl under basic conditions to afford the monometallic complex **7** shown in Figure III.13. X-ray structural characterization of **7** revealed metallation of the 6-SH terminus of **6.**[34] Formation of SAM films of **7** on Au(111) was attempted in this Thesis work. The molecular structure of **7** is certainly significantly larger than any of the other mercaptoazulenes studied by the Barybin group to date and also has the greatest potential for forming a disordered SAM due to the bulky nature of the gold-triphenylphosphine unit. Similar to all other mercaptoazulenes with the exception of **4**, compound **7** lacks useful IR spectroscopic reporters in its structure. Ellipsometric data collected for the films of **7** on Au(111) gave an average film thickness of 20.8±6.4 Å, which is 4% taller from the expected thickness of the film calculated by examining the crystal structure of **7** and including the Au-S bond distance of 2.45 Å (*vide supra*).

III.4 Conclusions and Outlook

Self-assembled monolayer (SAM) films of mercaptoarenes on metal surfaces are of substantial multidisciplinary interest as platforms for developing new advanced materials relevant to nanotechnological applications, including organic electronics. Until the work reported herein, most mercaptoarene SAMs incorporated benzenoid aromatic π-systems. In this Chapter, the first SAM films of mercaptoazulenes have been described. Our fixed-wavelength ellipsometric measurements suggest a monolayer nature of most of these films in which the adsorbed molecules orient approximately upright (i.e., linear Au-S-C units) with respect to the Au surface. Notably, the tilt of the aromatic rings in benzenoid aryl thiolate SAMs has been shown to vary widely from being vertical to almost parallel to the gold surface. Compound **4** is an especially interesting molecule, for it contains two spectroscopic reporters, nitrile groups, which greatly facilitated the surface IR studies. The SAM of **4** on Au(111) reported herein represents the first organothiolate film to be observed with the help of ancillary nitrile functional groups, to the best of the author's knowledge. The IR and ellipsometric evidence presented here excludes any significant nitrile-gold interactions in addition to the Au-SR (R = 1,3-dicyano-2-azulenyl) bonding for the SAM of **4** on Au(111). Thus, the cyano substituents in the SAMs of **4** do indeed serve as *ancillary* spectroscopic handles. By considering the coordination of **4** on the Au(111) surface, the nature of the analogous SAMs of mercaptoazulenes **1** and **2** can be better understood as well.

Preliminary studies of the adsorption of the linear dimercaptoazulene derivative **6** on gold indicate that the molecule appears to bind to the metal surface via its less-

hindered 6-mercapto terminus, although this tentative claim should be taken "with a grain of salt". The availability of the monometallic complex **7**, in which the 6-mercapto end is selectively metallated, provides a path for future work to orient the azulenic dipole of the 2,6-dimercaptoazulene moiety in one direction upon adsorption of this monometallated species on the gold surface.

In general, the accessibility of the novel mercaptoazulene SAMs on metallic gold surfaces presents a hitherto unavailable intriguing opportunity to experimentally probe the conductivity characteristics of the azulenic framework along its molecular axis. In addition, future work should include studies of mercaptoazulenic films by XPS to gain a deeper insight into the nature of the coordination of these molecules to the Au(111) surface. These XPS studies might be especially interesting in assessing the adsorption of dimercaptoazulene **6** to the gold surface to elucidate our understanding of which sulfur is binding to the Au(111) surface.

III.5 References

1 Love, J.C., Estroff, L.A., Kriebel, J.K., Nuzzo, R.G., Whitesides, G.M. Self-assembled monolayers of thiolates on metals as a form of nanotechnology. *Chemical Reviews*, **2005**, *105*, 1103-1169.

2 Nuzzo, R.G., Allara, D.L. Adsorption of bifunctional organic disulfides on gold surfaces *J. Am. Chem. Soc.*, **1983**, *105*, 4481-4483.

3 Porter, M.D., Bright, T.B., Allara, D.L, Chidsey, C.E.D. Spontaneously organized molecular assemblies. 4. Structrual characterization of n-alkyl thiol monolayers on gold by optical ellipsometry, infrared spectroscopy, and electrochemistry *J. Am. Chem. Soc.*, **1987**, 109, 3559- 3568.

4 Fenter, P., Eisenberger, P., Li, F., Camillone, N., III, , Bernasek, S., Scoles, G., Ramanarayanan, T.A., Liang, K.S. Structure of octadecyl thiol self-assembled on silver (111) surfaces: an incommensurate monolayer *Langmuir*, **1991**, *7*, 2013-2016.

5 Troughton, E.B., Bain, C.D., Whitesides, G.M., Nuzzo, R.G., Allara, D.L., Porter, M.D. Monolayer films prepared by spontaneous self-assembly of symmetrical and unsymmetrical dialkyl sulfides from solution onto gold substrates: structure, properties, and reactivities of constituent functional groups *Langmuir*, **1988**, *4*, 365-385.

6 Vericat, C., Vela, M.E., Benitez, G., Carro, P., Salvarezza, R.C. Self-assembled monolayers of thiols and dithiols on gold: new challenges for a well-known system. *Chemical Society Reviews*, **2010**, *39,* 1805-1834.

7 Whelan, C.M., Smyth, M.R., Barnes, C.J. HREELS, XPS, and Electrochemical study of benzenethiol adsorption on Au(111) *Langmuir*, **1999**, *15*, 116-126.

8 Kang, J.F., Ulman, A., Liao, S., Jordan, R., Yang, G., Liu, G. Self-assembled rigid Monolayers of 4'-substituted-4-mercaptobiphenyls on gold and silver surfaces *Langmuir*, **2001**, *17*, 95-106.

9 Andres, R.P., Bein, T., Dorogi, M., Feng, S., Henderson, J.I., Kubiak, C.P., Mahoney, W., Osifchin, R. G., Reifenberger, R. "Coulomb staircase" at room temperature in self-assembled molecular nanostructure. *Science*, **1996**, *272***,** 1323-1325.

10 Azzam, W., Wehner, B.I., Fischer, R.A., Terfort, A., Wöll, C. Bonding and orientation in self-assembled monolayers of oligophenyldithiols on Au substrates *Langmuir*, **2002**, *18*, 7766-7769.

11 Jiang, P., Nion, A., Marchenko, A., Piot, L., Fichou, D. Rotational polymorphism in 2-napthalenethiol SAMs on Au(111) *Journal of the American Chemical Society*, **2006**, *128*, 12390-12391.

12 Richter, L.J., Yang, C. S.-C., Wilson, P.T., Hacker, C.A., van Zee, R.D., Stapleton, J.J., Allara, D.L., Yao, Y., Tour, J.M. Optical characterization of oligo(phenylene-ethylene) self-assembled monolayers on gold *Journal of Physical Chemistry B*, **2004**, *108*, 12547-12559.

13 Nilsson, D., Watcharinyanon, S., Eng, M., Li, L., Moons, E., Johansson, L.S.O., Zharnikov, M., Shaporenko, A., Albinsson, B., Mårtensson, J. Characterization of self-assembled monolayers of oligo(phenyleethynylene) derivatives of varying shapes on gold: effect of laterally extended π-systems *Langmuir*, **2007**, *23*, 6170-6181.

14 Dhirani, A., Zehner, R.W., Hsung, R.P., Guyot-Sionnest, P., Sita, L.R. Self-assembly of conjugated molecular rods: a high-resolution STM study *Journal of the American Chemical Society*, **1996**, *118*, 3319-3320.

15 Sabatani, E., Cohen-Boulakia, J., Bruening, M., Rubinstein, I. Thioaromatic monolayers on gold: a new family of self-assembling monolayers. *Langmuir*, **1993**, *9*, 2974-2981.

16 Kim, B., Choi, S.H., Zhu,X.-Y.,Frisbie, C.D. Molecular tunnel junctions based on π-conjugated oligoacene thiols and dithiols between Ag, Au, and Pt contacts: effect of surface linking group and metal work function. *J. Am. Chem. Soc.*, **2011**, *133*, 19864-19877.

17 Tao, Y., Wu, C., Eu, J., Lin, W. Structure of Aromatic-derivatized thiol monolayers on evaporated gold. *Langmuir* **1997**, *13*, 4018-4023.

18 Käfer, D., Bashir, A., Witte, G. Interplay of anchoring and ordering in aromatic self-assembled monolayers. *J. Phys. Chem. C.*, **2007**, *111*, 10546-10551.

19 Noh, J., Ito, E., Hara, M. Self-assembled monolayers of benzenethiol and benzenemethanethiol on Au(111): Infulence of an alkyl spacer on the structure and thermal desorption behavior *Journal of Colloid and Interface Science*, **2010**, *342*, 513-517.

20 Kang, H., Park, T., Choi, I., Lee, Y., Ito, E., Hara, M., Noh, J. Formation of large ordered domains in benzenethiol self-assembled monolayers on Au(111) observed by scanning tunneling microscopy. *Ultramicroscopy*, **2009**, *109*, 1011-1014.

21 Millone, M.A.D., Hamoudi, H., Rodriguez, L., Rubert, A., Benitez, G.A., Vela, M.E., Salvarezza, R.C., Gayone, J.E., Sanchez, E.A., Grizzi, O., Dablemont, C., Esaulov, V.A. Self-assembly of alkanedithiols on Au(111) from solution: effect of chain length and self-assembly conditions. *Langmuir*, **2009**, *25*, 12945-12953.

22 Whelan, C.M., Barnes, C.J., Walker, C.G.H., Brown, N.M.D. Benzenethiol adsorption on Au(111) studied by synchrotron ARUPS, HREELS, and XPS. *Surface Science*, **1999**, *425*, 195-211.

23 Whelan, C.M., Smyth, M.R., Barnes, C.J. HREELS, XPS, and Electrochemical study of benzenethiol adsorption on Au(111) *Langmuir*, **1999**, *15*, 116-126.

24 Ulman, A. Self-assembled monolayers of 4-mercatobiphenyls. *Accounts of Chemical Research*, **2001**, *34*, 855-863.

25 Kang, J.F., Ulman, A., Liao, S., Jordan, R., Yang, G., Liu, G. Self-assembled rigid Monolayers of 4'-substituted-4-mercaptobiphenyls on gold and silver surfaces *Langmuir*, **2001**, *17*, 95-106.

26 Azzam, W., Wehner, B.I., Fischer, R.A., Terfort, A., Wöll, C. Bonding and orientation in self-assembled monolayers of oligophenyldithiols on Au substrates *Langmuir*, **2002**, *18*, 7766-7769.

27 Jiang, P., Nion, A., Marchenko, A., Piot, L., Fichou, D. Rotational polymorphism in 2-napthalenethiol SAMs on Au(111) *Journal of the American Chemical Society*, **2006**, *128*, 12390-12391.

28 Kim, B., Choi, S.H., Zhu,X.-Y.,Frisbie, C.D. Molecular tunnel junctions based on π-conjugated oligoacene thiols and dithiols between Ag, Au, and Pt contacts: effect of surface linking group and metal work function. *J. Am. Chem. Soc.*, **2011**, *133*, 19864-19877.

29 Dutta, S., Lakshmi, S., Pati, S.K. Comparative study of electron conduction in azulene and naphthalene. *Bull. Mater. Sci.*, **2008**, *31*, 353-358.

30 Zhou, K-G., Zhang, Y-H., Wang, L.-J., Xie, K.-F., Xiong, Y.-Q., Zhang, H.-L., Wang, C.-W. Can azulene-like molecules function as substitution-free molecular rectifiers? *Phys. Chem. Chem. Phys.*, **2011**, *13*, 15882-15890.

31 Xing, Y, Hongmei, L., Jianwei, Z., *J. Chem. Phys.*, **2006**, *125*, 094711/1-094711/6.

32 Neal, B. M.; Vorushiolov, A. S.; DeLaRosa, A. M.; Robinson, R. E.; Berrie, C. L.; Barybin, M. V. Ancillary nitrile substituents as convenient IR spectroscopic reporters of mercapto- and isocyanoazulenes on Au(111) *Chemical Communications*, **2011**, *47*, 10803-10805.

33 Vorushilov, A.S. Regioselective acylation of 2-methoxynaphthalene catalyzed by a C-H superacid and chemistry of mercaptoazulenes University of Kansas, 2010. UMI, Ann Arbor, MI.

34 Scheetz, K.J., Vorushilov, A.S., Spaeth, A.D., Barybin, M.V. Manuscript in preparation.

35 (a) S.C. Clear and P.F. Nealey, *Langmuir*, 2001, **17**, 720-732; (b) J.D. Le Grange, J. L. Markham, and C.R. Kurkjian, *Langmuir*, 1993, **9**, 1749-1753; (c) S. R. Wasserman, G. M. Whitesides, I. M. Tidswell, B.M. Ocko, P. S. Pershan, and J. D. Axe, *J. Am. Chem. Soc.*, 1989, **111**, 5882-5861.

36 Cossaro, A., Mazzarello, R., Rousseau, R., Casalis, L., Verdini, A., Kohlmeyer, A., Floreano, L., Scandolo, S., Morgante, A., Klein, M.L., Scoles, G., *Science*, **2008**, *321*, 943-946.

CHAPTER IV

IV. SAM Displacement Studies Involving Isocyanoazulenes and Mercaptoazulenes Adsorbed on Au(111)

Portions of this work have been published in:

Neal, B. M.; Vorushiolov, A. S.; DeLaRosa, A. M.; Robinson, R. E.; Berrie, C. L.; Barybin, M. V. Ancillary nitrile substituents as convenient IR spectroscopic reporters for self-assembly of mercapto- and isocyanoazulenes on Au(111) *Chemical Communications*, **2011**, 47, 10803-10805.

IV.1 Introduction

Before the field of molecular electronics can mature and become viable for application, a better understanding of the properties of molecular junctions is necessary. [1-3] Many of the molecular systems discussed in the previous Chapters are of interest for their potential abilities to act as charge transport materials. Figure 1 shows the basic diagram of a molecular junction on a surface.

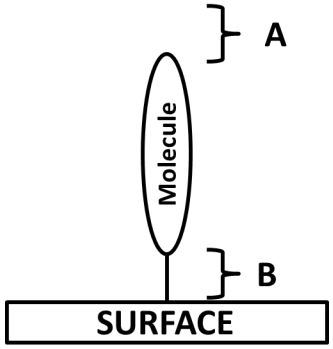

Figure IV.1 - Illustration of a molecule bound to a surface that emphases the various components of the molecular junction. A) the interface between the molecule and outside environment B) the molecule – surface junction.

Usually, the junction that tethers the molecule to the surface is a functional group; *e.g.*,a thiolate (see Chapter 3 of this Thesis for examples and discussion) or an isocyanide (see Chapter 2 of this Thesis for examples and discussion). In studies of isocyanides bound to Au(111), RAIRS evidence shows an increase in the CN bond strength upon coordination of the isocyanides to the metal surface, see Table I.1 in Chapter 1, signifying donation of the terminal isocyanide carbon atom's lone pair, which is somewhat antibonding with respect to the C≡N bond. The blue shift in ν(NC) also indicates that there is little to no π backbonding taking place

between coordinated isocyanide molecules and the Au atoms of the metallic gold. [4] The two complementary components of the η^1 coordination of an isocyanide to a transition metal atom, σ bonding and π back-bonding, are illustrated in Figure IV.2.

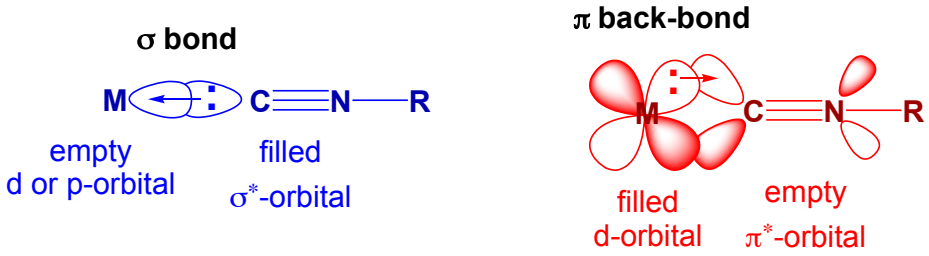

Figure IV.2 - Two complementary components of interaction of an organic isocyanide with a transition metal atom/ion. Left: σ-bonding involving isocyanide's lone pair and a metal's vacant valence orbital. Right: π-backbonding involving a virtual π* orbital of the isocyanide unit and a filled d-orbital of π-symmetry of the metal atom/ion. Reproduced with permission from Ref. 5.

There are many different known sulfur containing junction groups that are capable of forming SAMs on gold, such as thiolates, R-S^-, sulfides, R-S-R, disulfides, and R-S-S-R, where R is the tail group of the molecule. [6, 7] In the case of thiolate film formation from the corresponding thiols, while the exact mechanism is unknown, it is generally agreed that the process involves generation of dihydrogen [6, 7] or possibly, if oxygen is present, water. [6] Regardless of the pathway, the resulting S-Au bond is a strong bond worth of 44 [8] to 50 kcal/mol. [9] Reports have shown that the C-Au bond is a weaker bond compared to the S-Au bond at roughly half the worth. [10] In contrast, via STM break junctions, the Au-C bond in aryl isocyanide systems has been found to be comparable in strength to the Au-S bond in benzenethiol and both bonds stronger than Au-Au bonds. [11] Additionally, while isocyanide SAMs on Au(111) coordinate to the surface on atop sites, it has been shown that aliphatic

thiolate monolayers form with the sulfur atoms sitting in three-fold hollows on the surface [6-8, 12] as shown in Figure IV.3.

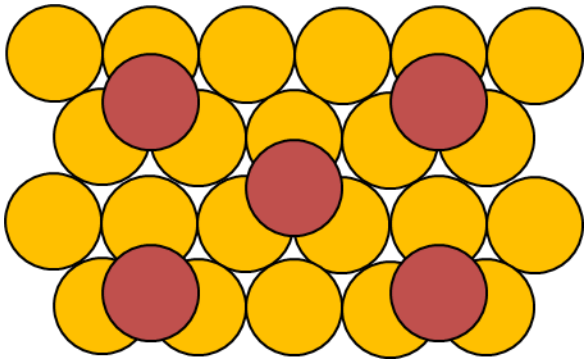

Figure IV.3 - A representation of the packing structure of an alkanethiol SAM on the Au(111) surface. The gold circles represent the Au atoms and the red circles represent the sulfur atoms occupying a three-fold hollow site.

For use in practical molecular electronic devices, the materials used must have well defined characteristics such as their stabilities and conductivities. As discussed in Chapter 2, many isocyanoarenes and diisocyanoarenes molecules have been proven to exhibit oxidation of isocyanide to form isocyanate, -C=N=O. There are reported cases, such as in the case of many azulenic moieties [13-15], of isocyanide molecules that have not undergone such oxidation. Indeed, while oxidation of many isocyanoarenes was seen within minutes spectroscopically [16, 17], no oxidation was observed in films of 1,3-diethoxycarbonyl-2,6-diisocyanoazulene for weeks. [13]

Conductance characteristics of single molecule bridges involving 1,4-diisocyanobenzene, 1,4-benzenedithiol, and 1,4-dicyanobenzene have been reported. [11] Using a STM break junction set up, the conductance of the 1,4-diisocyanobenzene was found to be similar, albeit slightly

lower, than that determined for the 1,4-benzenedithiol molecules. The 1,4-dicyanobenzene turned out to be an appreciably poorer conductor than the other two molecules attributed to a smaller electron attenuation factor, β, in part because of a weaker Au-NC bond strength compared to the similarly strong Au-S and Au-CN bonds. In addition using the shape of the conductance trace information collected, it was determined that the Au-S and Au-C bonds were stronger than the Au-Au bond on the Au(111) surface indicating that when the junction was broken, failure was due to removal of gold atoms from either the tip or the surface and not a breaking of the molecules themselves. Using the same experimental setup with platinum electrodes, the authors showed that the conductance characteristics of 1,4-diisocyanobenzene and 1,4-benzenedithiol were comparable to one another. In both cases, these conductivity values were an order of magnitude greater than those documented for the corresponding Au systems. [18]

Using a mechanically controllable break-junction (MCBJ) to analyze the charge transport properties of 1,4-benzene-dithiol and PDI, it was determined that, under UHV conditions, the isocyanide junction was superior compared to the thiol. [19] This conclusion was reached by comparing the plotted low-bias conductance histograms and variable-bias I-V characteristics. The observed peak width was related to variations of configurations of the molecules.

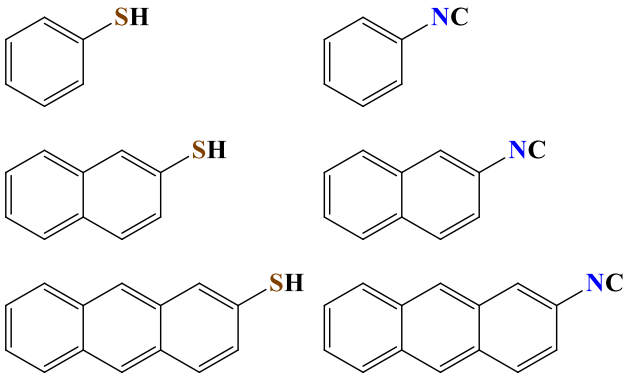

Figure IV.4 - Thiol and isocyanide oligioacenes used to form SAMs studied in Ref. 20.

In comparing SAM films of oligoacenes with either thiol or isocyanide junctions, shown in Figure IV.4, the barrier between the HOMO level of the molecules and the Fermi level of Au(111) was observed. [20] The ultraviolet photoemission spectroscopy (UPS) measurements determined the barrier was smaller for the thiol films compared to the corresponding isocyanide films. From CP-AFM measurements, the effective contact resistance of the isocyanide molecules was shown to be roughly three times greater than that of the thiol molecules. Because of the nature of the experiment, this difference was attributed to the contact resistances of the Au-CN-molecule and Au-S-molecule systems.

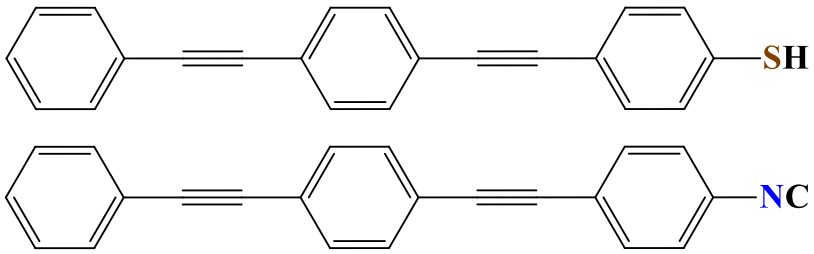

Figure IV.5 - Isocyanide and mercaptan OPE molecules studied in Ref. 21.

Determination of the alignment of the Fermi level of metal substrates with the HOMO and LUMO levels of the attached molecules is important for gaining insight into the mode of conduction of molecular systems, namely electron tunneling versus hole conduction. Electron tunneling will occur when the Fermi level is energetically closer in alignment to the LUMO while hole conduction will occur when the Fermi level is closer in energy to the HOMO. [21] By measuring the voltage at which the charge transport mechanism of π-conjugated molecules changes from direct tunneling to field emission and plotting this against the work function of various metals, Frisbie, *et al.* probed the Fermi level – molecular orbital alignment for OPE systems of isocyanide and thiol on Ag, Pd, Au, Pt. [21] The thiol OPE turned out to conduct via

hole conduction while the isocyanide OPE was found to conduct via electron tunneling. Based on their results, the authors concluded that the Ag-CN junction would provide the smallest barrier and therefore the least resistance in the metal-isocyanide systems probed.

Investigating the effect of changing the junction group with the same OPE molecules on gold substrates shown in Figure IV.5 above showed that both junctions caused changes in the Fermi level alignment of the metal to the HOMO level of the molecule, [22] as discussed above. [20] UPS experiments indicated that the thiolate junction leads to a closer alignment of the barrier between the Fermi level and the HOMO as compared to the isocyanide. The key factors behind this difference are thought to be the nature of bonding between the metal substrate and the junctions ,*i.e.,* the bonding between the Au and the sulfur atom allows for a charge transfer from the Au to the sulfur creating a dipole moment which shifts the Fermi level toward the HOMO of the molecule while a charge transfer occurs from the carbon's lone pair to the Au for the isocyanide leading to widening of the Fermi level-HOMO gap.

Reddy *et al.* used thermoelectric measurements obtained by AFM at known temperature differentials to gain insight into the alignment of the Fermi level and the frontier molecular orbitals of aromatic thiols and the aromatic isocyanide 4-isocyano-1,1':4',1''-terphenyl. [1] By calculating the thermopower parameters for various junctions and noting the sign of their values, it was determined from the positive thermopower obtained for the thiol systems that their electrical transport is hole dominated, which is consistent with the HOMO levels being closest to the Fermi level. In contrast, the transport through the isocyanide was electron tunneling as the isocyanide thermopower value was negative, thereby suggesting, along with calculations, that the Fermi level is closest to the LUMO.

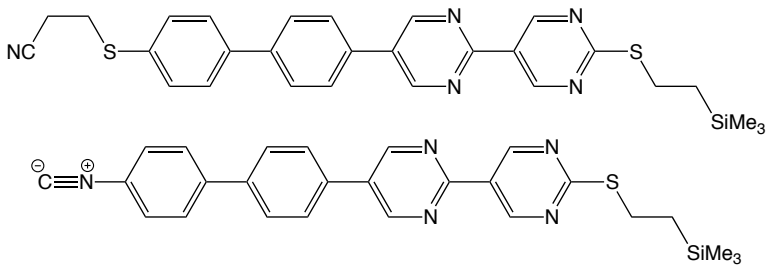

Figure IV.6 – Molecular diodes used to form SAMs in Ref. 23.

Molecular diodes, shown in Figure IV.6 were used to study the effect of the thiol and isocyanide junction groups on rectification. [23] Monolayers of dodecanethiol were exposed to these molecules to form mixed monolayer systems to which Au nanoparticles were attached to the free thiol junction on the diodes and were subsequently analyzed using scanning tunneling spectroscopy. The current vs. voltage curves showed the two molecules rectified current opposite of one with the thiol coordinated diode showing almost four times the rectification ratio compared to the isocyanide coordinated diode. Rectification current was defined as dividing the observed current at +1.5V by the current observed at -1.5V. Using calculations and control experiments, differences in the induced bond dipole at the surface were indicated to cause the opposite observations in rectification for otherwise structurally similar molecules.

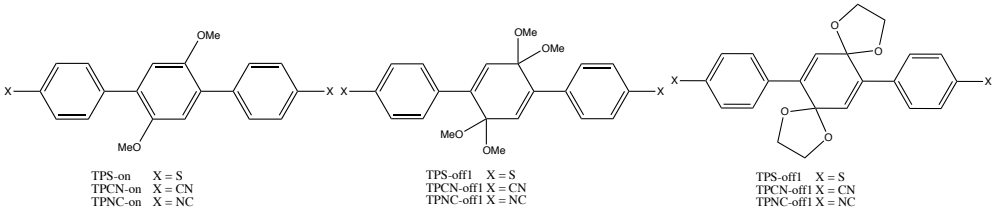

Figure IV.7 - Molecular diodes from Ref. 24.

Molecular nanofuses based on the p-tertphenyl moiety, Figure IV.7 were theorized and compared computationally. [24] Calculations on dithiol, dicyano-, and diisocyano- derivatives

bridging gold surfaces indicate that the dithiol species have a greater ratio of current comparing the "on" form of the molecule, seen in Figure IV.7 to the "off" structure at the same calculated bias voltages running through each molecule. This was rationalized by comparing the HOMO of both the "on" and "off" dithiol species and the LUMO of both the "on" and "off" diisocyanide species. It was calculated that the HOMO of the "on" dithiol species covers the entire molecule while the HOMO of the "off" species is localized on one half of the molecule and not the other. In the case of the diisocyanide, the LUMO covers the length of both the "on" and "off" species. The same argument made for the diisocyanide "on"/ "off" ratio is made to justify the lower on/off ratio of a dicyano substituted system. Additionally, it was calculated that a bias voltage of up to six volts would be required to cause the switch from "on" to "off" for the isocyano species.

While there are many comparisons of the electronic properties of structurally similar isocyanide and mercaptan molecules as discussed above, there are fewer studies comparing how these molecules compete for binding to surfaces. One of the earliest comparisons was performed by Kubiak, *et al*, when studying the displacement of octadecanethiol from an Au(111) surface by diisocyanides[25] exhibited in Figure IV.8.

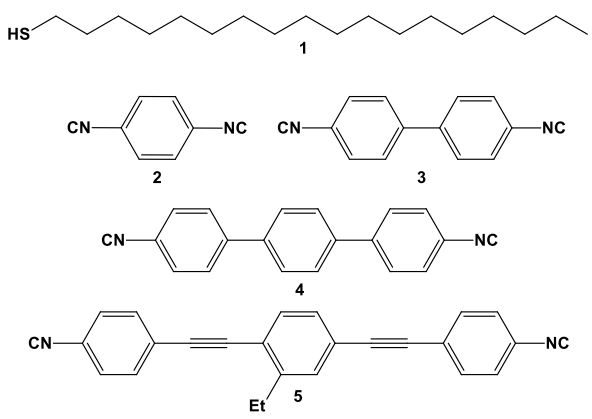

Figure IV.8 - Octadecanethiol (1) and various diisocyanides studied by Kubiak on Au(111) in Ref. 25.

Films of the diisocyanides were proven to form good monolayers on the surface by characterization of ellipsometry and RAIR. The work found several interesting results. First, it is possible to displace SAMs of octadecanethiol with the diisocyanides if the solvent used in the competition experiment was both aprotic and anhydrous. Conversely, if the solvent used for the competition portion of the experiment was protic or wet, no displacement of the original octadecanethiol SAM occurred. The differences in behavior were attributed to the ability of the solvent to solvate the existing octadecanethiol's alkyl chain with greater solvation, caused by less polar solvents, resulting in displacement by the various isocyanide moieties shown in Figure IV.8. [25] As with studying the formation of the films *sans* displacement, the displacement studies were characterized using the same ellipsometric and RAIR techniques.

As noted previously, studying the properties and self assembly of various functionalized molecules on Au(111) has not only advantages with respect to relatively easier working conditions but also in that various different functional groups and molecular chains have been studied extensively. Pranger, *et al*. have studied Cu surfaces and the relative binding affinity of

various functional groups to these substrates using displacement studies. [26] In their work, they directly compared para-disubstituted benzene moieties with diisocyano, dithiol, dicarboxylic acid, dinitrile, and diisothicyanate functional groups for their affinity to freshly prepared Cu substrates. Studying the XPS spectra and polarization modulation infrared reflection absorption spectroscopy (PM-IRRAS) of films formed from these competition experiments determined that the α,ω-dithiol and diisocyanide alkyl moieties had similar adhesion to the surface, based on the fact that the were present in roughly equal concentrations.

Pranger has noted that when the disubstituted alphatic dithiols and diisocyanides were competed against one another, not only did the two both absorb to the surface, but that both isocyanide junctions coordinated while only one of the thiol junctions absorbed leaving the other uncoordinated. While comparing 1,4-benzenedithiol to other difunctionalized benzenes besides 1,4-diisocyanopehenylene, they found both sulfur atoms coordinated to the surface but with the 1,4-diisocyanophenylene only one isocyanide coordinated to the copper. Competition experiments between the analogous dithiol and diisocyano benzene were attempted, but the two chemicals reacted with one another in solution leading to less definitive results compared with the aliphatic molecule's comparison.

IV.2 Work Described in Chapter IV

This Chapter discusses competitive displacement studies performed between various isocyanoazulene and mercaptoazulene species on Au(111) surfaces to determine if preferential binding of one of the species is observed. Additionally, the formation and study of the SAM films of two new isocyanoazulene moieties is detailed. The experimental methodologies of these studies will be discussed culminating with possible future directions at the end of this Chapter.

IV.3 Experimental Section

IV.3.1. General Procedures, starting materials and equipment.

The mercarptoazulenes used in these studies were prepared as published elsewhere[15] and properties of their films on gold are discussed in Chapter III of this Thesis. 2-Isocyano-1,3-dimethylazulene was synthesized by John J. Meyers, Jr. of the Barybin group. [27] 2-Amino-1,3-dicyanoazulene[28] and acetic-formic anhydride[29] were synthesized according to published procedures. All other reagents were obtained from commercial sources and used as received. Davisil (200-425 mesh, type 60A) silica gel was used for chromatographic purifications.

Unless specified otherwise, all operations were performed under an atmosphere of 99.5% argon further purified by passage through columns of activated BASF catalyst and molecular sieves. All connections involving the gas purification systems were made of glass, metal, or other materials impermeable to air. Solutions were transferred via stainless steel needles (cannulas) whenever possible. Standard Schlenk techniques were employed with a double manifold vacuum line. Dichloromethane and triethylamine were distilled over CaH_2. Chloroform was distilled over P_2O_5. Following purification, all distilled solvents were stored under argon. All solvents employed in chromatographic procedures were used as received from commercial sources. Solution infrared spectra were recorded on a PerkinElmer Spectrum 100 FTIR spectrometer with samples sealed in 0.1 mm gas-tight NaCl cells. NMR samples were analyzed using a Bruker DRX-400 spectrometer. ^{1}H and ^{13}C chemical shifts are given with reference to residual ^{1}H and ^{13}C solvent resonances relative to Me_4Si.

Gold-coated mica substrates were either purchased from Platypus Technologies or were fabricated in the Berrie lab using an Edwards Auto 306 rotary evaporator. “House” Au(111) was

deposited on freshly cleaved sheets of mica under a vacuum pressure of *ca.* 1.5 x10^{-7} torr with a deposition rate of about 1 Å/sec, as measured by a quartz crystal microbalance. Gold films were coated between 250 and 300 Å thick and were subsequently stored under high vacuum or inert atmosphere conditions until use. Commercial silicon wafers, coated with a 50 Å titanium adhesion layer and then with *ca.* 1000 Å of gold, were purchased from Platypus Technologies.

Unless otherwise stated, all substrates were soaked in distilled $CHCl_3$, acetone, and 200-proof ethyl alcohol for one to two hours in each solvent with no precautions against exposure to ambient air or lighting. Substrates were then removed and dried in a stream of N_2 gas. Physical constants of the substrates were measured using a Rudolph Research Auto El III fixed wavelength ellipsometer. Measurements were made with a 632.8 nm wavelength HeNe laser. The optical constants of each individual cleaned, bare gold substrate were measured prior to its exposure to isocyanide or thiol solutions. These optical constants were used to determine the thickness of the organic film covering the substrate upon isocyanide or thiol exposure and subsequent workup of the sample. Typical values of n ranged from 0.161 to 0.181 and K values from 3.52 to 3.55. A refractive index of 1.45 was assumed[30] for the SAMs described in this chapter. At least five separate spots on the substrate were analyzed to determine both the optical constants and the film thicknesses. The film thickness values reported herein constitute averages of these measurements with the corresponding standard deviations given in parentheses.

All surface IR experiments involved grazing angle reflection absorption Fourier transform infrared spectroscopy. These data for the SAMs films were obtained on a Thermo Nicolet 670 FTIR spectrometer with a VeeMax grazing angle accessory set up at an incident angle of 70°. Prior to acquiring an IR spectrum of each SAM sample, a background spectrum

was recorded using a corresponding similarly treated bare Au substrate. Typically, 1000 scans from 600 to 4000 cm^{-1} at 4 cm^{-1} resolution were collected for both the background and sample spectra.

IV.3.3. Preparation of 2-isocyano-1,3-dimethylazulene (1) SAM films

Gold-coated mica substrates from Platypus technologies and house-coated Au(111) were used in the formation of monolayers of this azulene derivative. Prior to their use, both kinds of substrates were cleaned as outlined in the General Procedures section.

After drying with a stream of N_2 gas, ellipsometric physical constants of the bare gold samples were taken. Monolayer films of **1** were formed by immersing a freshly cleaned gold substrate into a 2 mM solution of **1** in distilled $CHCl_3$ for *ca*. 24 hrs. Then, the gold sample was removed, rinsed thoroughly with either distilled CH_2Cl_2 or $CHCl_3$, and dried in a flow of N_2 gas. No precautions to exclude air or ambient laboratory lighting were taken during this procedure.

IV.3.4. Synthesis of 1,3-dicyano-2-isocyanoazulene (2)

An orange slurry of 2-amino-1,3-dicyanoazulene (1.02g, 5.28 mmol) in 50mL of neat acetic-formic anhydride was stirred for 15 hrs with gentle heating. The reaction mixture was then brought to room temperature and a pink flamingo solid was filtered off, washed extensively with CH_2Cl_2, and dried under vacuum to afford the crude product (1.058 g, 4.78 mmol), presumably 2-formamido-1,3-dicyanoazulene. Without further purification, a portion of this product (0.2337g, 1.056 mmol) was combined with triethylamine (0.5 mL, 3.6 mmol) and phosphorous oxychloride (0.14 mL, 1.5 mmol) in 25 mL of anhydrous CH_2Cl_2 under argon atmosphere. The resulting solution/slurry was stirred for 15 min at room temperature and then

quenched with 100 mL of 10% $KHCO_3$. The organic layer was separated and the aqueous layer was washed with 30 mL of CH_2Cl_2. The combined organic fractions were washed with water (4×30 mL) and dried over anhydrous Na_2SO_4. The drying agent was filtered off. The filtrate was concentrated under vacuum and subjected to chromatography on a short silica gel column (ca. 10 cm length × 5 cm OD) using neat CH_2Cl_2 to elute a purple band. All solvent was removed under vacuum and the residue was dried at 10^{-2} torr to afford **2** (0.1215g, 0.5985 mmol) as somewhat air-sensitive, raspberry-colored microcrystals in a 52% yield based on 2-amino-1,3-dicyanoazulene. HRMS (m/z, ES^-, 2 nM solution in CH_3CN/NH_4OAc): found for $[M-H]^-$ 202.0401; calcd for $C_{13}H_4N_3$ 202.0405. MS (m/z, ES^+): 203.1 ($[M^+]$). FTIR ($CHCl_3$): ν(CN) 2224 vs, 2114 s cm^{-1}. ^1H NMR (400 MHz, $CDCl_3$, 25 °C): δ 8.05 (t, $^3J_{HH}$ = 10 Hz, 2H, $H^{5,7}$), 8.31 (t, $^3J_{HH}$ = 10 Hz, 1H, H^6), 8.87 (d, $^3J_{HH}$=10 Hz, 2H, $H^{4,8}$) ppm. ^{13}C NMR (100.6 MHz, $CDCl_3$, 25 °C): δ 95.8, 112.1, 133.2, 141.1, 142.1, 144.8, 180.5 (isocyano -NC) ppm.

IV.3.5. Preparation of SAM films of 2

Gold-coated substrates from Platypus technologies were used in the formation of monolayers of this biazulene derivative. Prior to their use, both kinds of substrate were cleaned as outlined in the General Procedures section.

After drying with a stream of N_2 gas, ellipsometric physical constants of the bare gold samples were taken. Monolayer films of **2** were formed by immersing a freshly cleaned gold substrate into a 2 mM solution of **2** in distilled $CHCl_3$ for *ca*. 24 hrs. Then, the gold sample was removed, rinsed thoroughly with distilled CH_2Cl_2 or $CHCl_3$, and dried in a flow of N_2 gas. No precautions to exclude air or ambient laboratory lighting were taken during this procedure.

IV.3.6. General procedure for SAM displacement experiments

Displacement studies involved first forming and characterizing a SAM film of either an isocyanide or a mercaptan. Then, the film on the gold substrate was soaked in a solution of the different compound of interest considered for the SAM displacement. After 24 h, the substrate was removed, rinsed thoroughly with distilled CH_2Cl_2 or $CHCl_3$, and dried in a flow of N_2 gas, and the resulting film was characterized by ellipsometry and RAIRS.

IV.4 Results and Discussion

Commercially available 2,6-Xylyl isocyanide (CNXyl, Xyl = 2,6-dimethylphenyl) has been the most widely used aryl isocyanide in coordination chemistry[31] because of its reasonable thermal stability as well as satisfactory stability toward air. Recently, John Meyers of the Barybin group has synthesized and crystallographically characterized 2-isocyano-1,3-dimethylazulene (**1**). [27] The latter new nonbenzenoid isocyanoarene is remarkably air- and thermally stable and may be regarded as a direct structural analogue of benzenoid CNXyl. In this work, SAM films of **1** were formed on Platypus Au and "house" Au on mica substrates by soaking them in 2mM "KU blue" colored solutions of **1** in distilled $CHCl_3$ for 24h. The films, on both kinds of the gold substrates were invariably of high quality, as judged by ellipsometric thickness measurements and a well-defined ν(NC) band at 2167 cm^{-1} in the RAIRS spectra of the monolayers, shown in Figure IV.9. Remarkably, these SAMs appeared to be unchanged for days when stored in in an ambient laboratory environment.

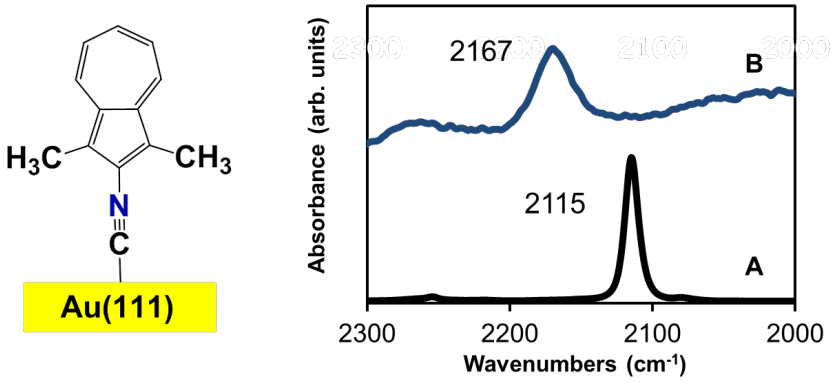

Ellipsometric SAM thickness
10.5±0.6 Å (10.7 Å calc.)

A: in CH_2Cl_2 **B**: on Au(111)

Figure IV.9 - IR spectra of 2-isocyano-1,3-dimethylazulene (**1**) in (A) a solution of $CHCl_3$ and (B) adsorbed to a Au(111) substrate.

The ellipsometric film thickness measurements were consistently 10.5±0.6 Å. These values compare nicely with the theoretically estimated thickness of 10.7 Å expected for the perfectly upright η^1 coordination of **1** on the gold surface. [15] In addition, the surface IR spectra of the SAMs of **1** clearly show one ν(NC) band at higher energy compared to ν(NC) observed for the solution spectrum of the compound and lack any features attributable to uncoordinated molecules of **1** or oxidation of **1** to the corresponding isocyanate. In comparison, Swanson, *et al.*, found small amounts of oxidation of 1,4-diisocyano-2,3,5,6-tetramethylbenzene when adsorbed onto gold surfaces using polarization-modulation infrared reflection-absorption spectroscopy. [17] The exceptional thermal and air stability of the films of **1** that provide a strong ν(NC) signal has led to our use of such SAMs for periodic calibration of our Nicolet FTIR instrument.

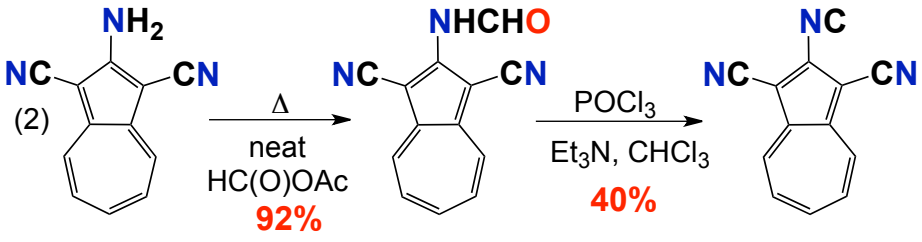

Scheme IV.1 - Synthesis of 2-isocyano-1,3-dicyanoazulene (**2**) from the corresponding amine precursor.

The synthesis of **2** was greatly facilitated by the pioneering work of Dr. Randall Robinson, whom first made and reported preliminary characterization of the compound in the Barybin group. It was from his initial work that the synthetic process was then improved upon. Starting from the yellow-orange 2-amino-1,3-dicyanoazulene, the flamingo pink 2-formamido-1,3-dicyanoazulene was presumptively able to be produced in reasonable yields. While the

amine was reasonably soluble, the formamide was sparingly soluble in organic solvents. This lack of solubility made characterization incredibly difficult. Of note, the best yields of the formamide were obtained when the formulation was carried out using neat acetic formic anhydride and proceeded poorly using in-situ generated acetic formic anhydride, which has worked well with other systems. [5, 32]

After the presumed formamide was dried, it was reacted with triethylamine and phosphorous oxychloride to perform a dehydration reaction to produce **2** as the product. The raspberry colored **2** could be purified by using column chromatography and proved much more soluble than the formamide. It was found that **2** is somewhat air-sensitive and a microcrystalline material. Of significance, the reaction should be performed under an argon environment and requires a significant amount of solvent to mostly dissolve the formamide for best results and highest yields. The overall yield from the amine to **2** was found to be a respectable 52%. Long term storage of **2** is possible inside of a refrigerator inside an inert, glove box environment. Interestingly, **2** and 1,3-dicyano-2-mercaptoazulene, SAMs of which are discussed in Chapter 3, are both obtainable from the same starting amino precursor.

The formation of SAMs of **2** were done without taking any precautions against ambient air nor lighting by soaking Platypus Au(111) substrates for twenty four hours in 2 mM solutions of (2) in distilled $CHCl_3$. The substrates were then removed and rinsed with distilled $CHCl_3$ and dried using N_2 gas and then analyzed via ellipsometry and surface IR techniques. Ellipsometric measurements revealed the film thickness was 11.7±0.6 Å. Considering previous research exploring structurally similar systems[13], the calculated thickness was determined to be 10.7 Å. As the two numbers are very close to one another, this is indeed indicative of a single molecular

film forming on the surface in an upright orientation previously observed for isocyanide SAMs (please see *vide supra* and Chapter 2 of this Thesis for examples and discussion).

The FTIR spectrum of **2** in $CHCl_3$ exhibits two characteristic $\nu_{C\equiv N}$ bands at 2114 and 2224 cm^{-1} that correspond to the isocyano and cyano oscillators, respectively. Upon chemisorption of **2** on Au(111), the isocyano $\nu_{C\equiv N}$ band broadens and undergoes a 42 cm^{-1} shift to higher energy while the cyano $\nu_{C\equiv N}$ band red-shifts by 10 cm^{-1} compared to the solution spectrum of **2** , seen in Figure IV.10.

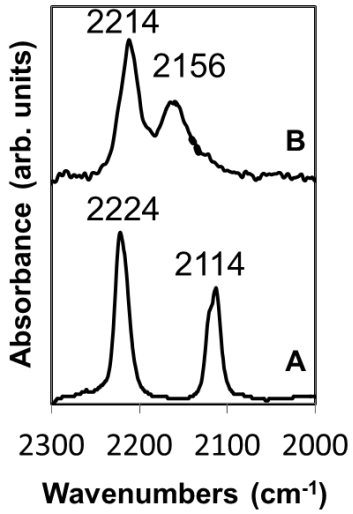

Figure IV.10 - (A) FTIR spectrum of **2** in $CHCl_3$. (B) RAIRS spectrum of **2** on Au(111) surface. From Ref. 15.

These changes, along with the ellipsometric film thickness measurements of 11.7 ± 0.Å, are consistent with coordination of **2** to the gold surface via the isocyano group in the terminal upright (or, "end-on") fashion compared to the calculated thickness of 10.7 Å using X-ray data for other 2-isocyanoazulene derivatives [33] and assuming the Au-C bond length to be 2.0 Å. [3] The broadening of the isocyano $\nu_{C\equiv N}$ band for **2** adsorbed on gold is likely caused by some

inhomogeneity in the adsorption sites, which is quite common for the Au(111) surfaces obtained through gold vapor deposition. [3] Donation of the isocyano carbon lone pair, which is antibonding with respect to the C NR interaction, to Au leads to strengthening of the isocyano C N bond and, hence, the blue shift in the corresponding $\nu_{C\equiv N}$ band upon coordination of **2**. However, this Au–CNR interaction slightly depletes the 1,3-dicyano-2-azulenyl moiety of its π-electron density, which may explain the small red shift for the cyano $\nu_{C\equiv N}$ band for **2** adsorbed on gold versus **2** in solution. This finding nicely parallels the up to 10 cm^{-1} depression in $\nu_{C\equiv N}$ frequencies documented for the "free" –NC ends of diisocyanoarenes chemisorbed on Au(111) compared to the $\nu_{C\equiv N}$ values for the corresponding compounds in solution. [3, 14]

Direct comparison of the relative affinity of various mercaptoazulenes and their analogous isocyanoazulenes has been performed. In these experiments, a SAM of either a mercapto- or isocyanoazulene is formed and characterized on the Au(111) surface as outlined previously. Once the monolayer's integrity has been characterized, the substrate is placed into a solution of a corresponding analogous molecule. Figure IV.11 illustrates the process.

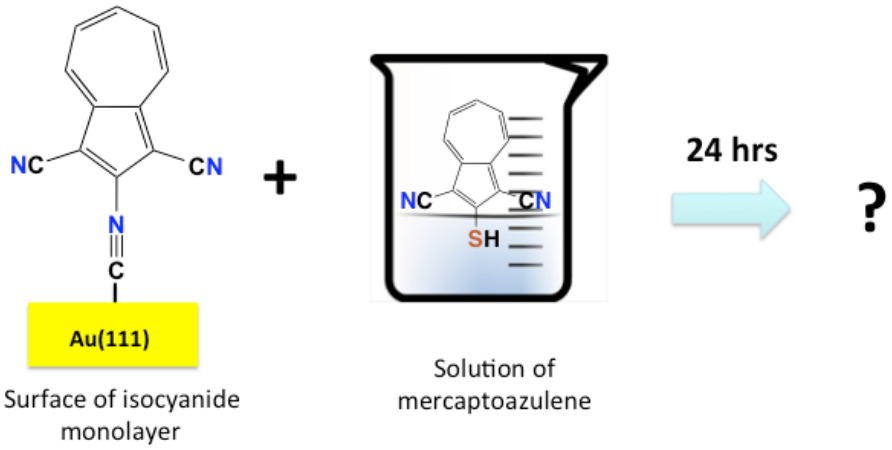

Figure IV.11 - An illustration of the process of the displacement studies

In the example in Figure IV.11 a monolayer of an isocyanide has been formed and characterized. The substrate with the isocyanide film is then placed in a solution of the mercaptan and exposed for ca. twenty four hours before the substrate is removed and characterized again to monitor for any changes.

One of the most obvious experiments done was testing the displacement of **1** by 2-mercaptoazulene and vice versa. As seen in Figure IV.12 when analyzing a film of 2-mercaptoazulene being exposed to the structurally very similar **1**, the changes in the surface IR spectra are negligible.

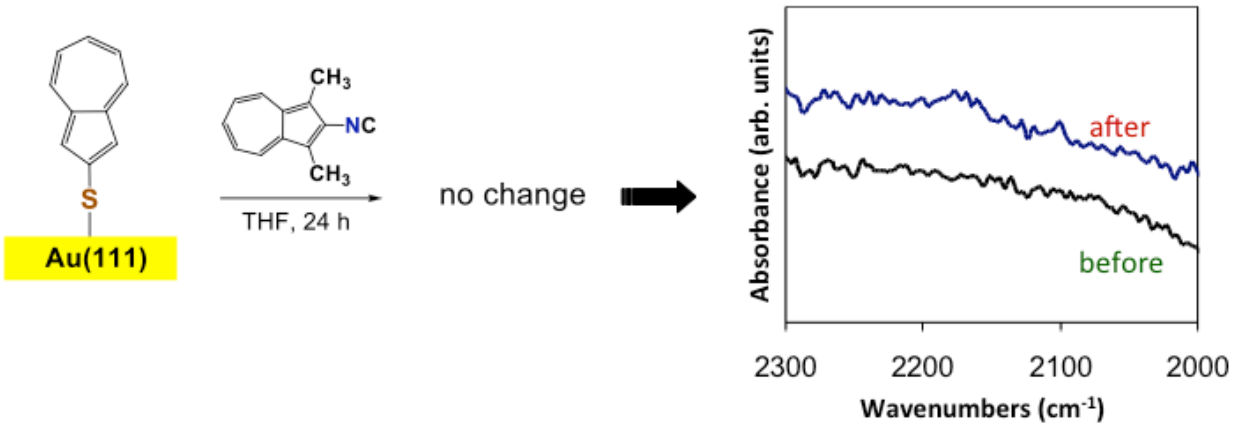

Figure IV.12 - Displacement experiment testing **1**'s ability to displace an existing SAM of 2-mercaptoazulene on Au(111).

As expected, there is no ν_{NC} signal seen in the spectrum of the 2-mercaptoazulene SAM in the IR. After 24 hours of exposure to **1** in $CHCl_3$, there is no definitive ν_{NC} stretching peak observed. However, in the opposite experiment where a SAM of **1** is formed and characterized before being exposed to the mercaptan, very obvious changes can been noticed, as seen in Figure IV.13.

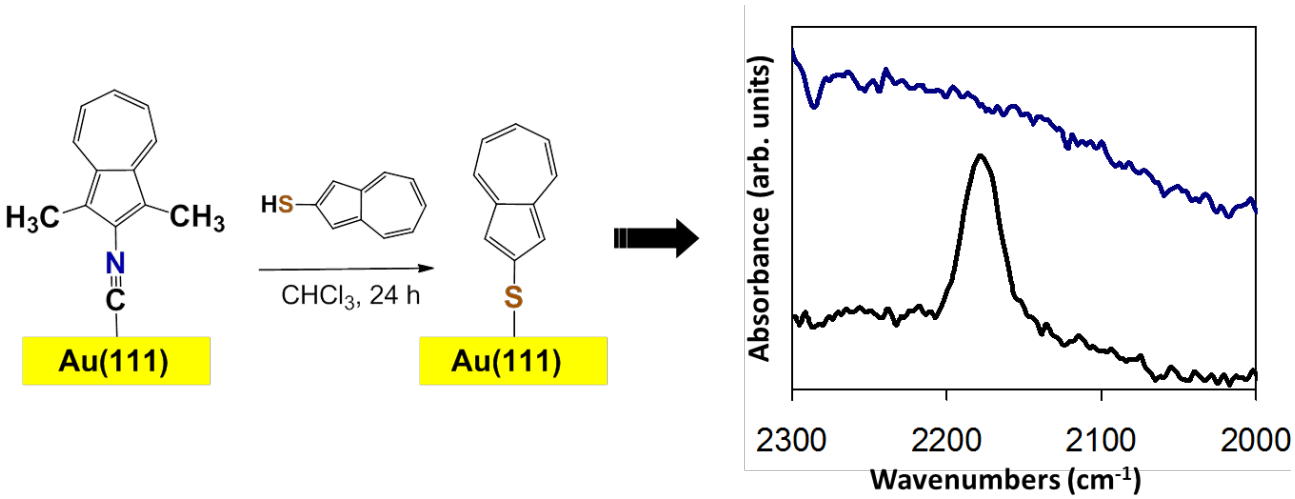

Figure IV.13 - Displacement experiment testing 2-mercaptoazulene's ability to displace an existing SAM of (1) on Au(111).

Here in Figure IV.13, it is seen that the SAM of **1** has its hallmark ν_{NC} peak at 2168 cm^{-1} corresponding to the formation of a well-packed monolayer). After exposure to the mercaptan, however, the ν_{NC} peak is not observed in the new spectrum indicative that the 2-mercaptoazulene is capable of displacing existing films of on Au(111) surfaces. This result is not definitive as to exactly what is happening because of the lack of an unambiguous spectroscopic reporter on the mercaptan.

This ambiguity is resolved when comparing the films of **2** and 1,3-dicyano-2-mercaptoazulene. As discussed in Chapter 3, 1,3-dicyano-2-mercaptoazulene is a significant molecule for its incorporation of ancillary spectroscopic reporters, the nitriles, to aid in surface IR characterization of its SAMs. Work done has shown that the molecule does not coordinate to the Au(111) surface via the nitrile groups, but rather through the sulfur and that the molecule forms monolayers well. When compared to **2**, this mercaptan may be considered the direct analogous structurally and electronically moiety, ruling both structure and electronics out as

possible reasons that the two molecules would coordinate differently for a reason other than the thiol or isocyanide junction groups affinity to the Au(111) surface.

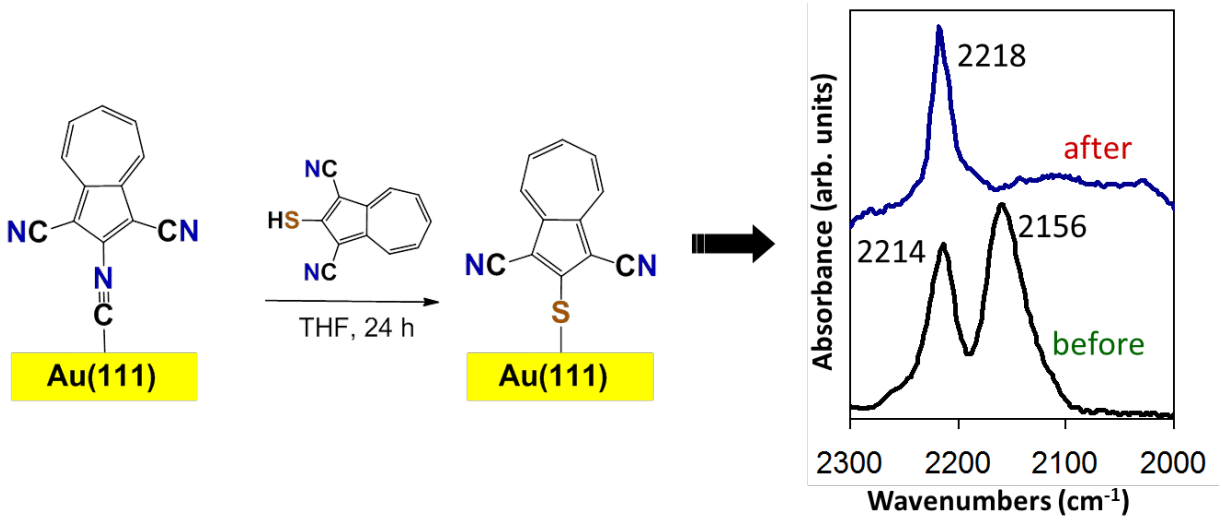

Figure IV.14 - Displacement experiment testing 1,3-dicyano-2-mercaptoazulene's ability to displace an existing SAM of **2** on Au(111).

Soaking a SAM of isocyanide **2** on gold in a 2 mM solution of 1,3-dicyano-2-mercaptoazulene in dry THF for 24 h, followed by thorough rinsing of the sample with anhydrous solvents , led to displacement of the original monolayer and formation of the new film identified as that of 1,3-dicyano-2-mercaptoazulene. Indeed, the RAIR spectrum of the sample indicated complete disappearance of the band at 2156 cm^{-1} corresponding to $\nu_{C\equiv N}$ of the Au-bound isocyanide junction, Figure IV.14. In addition, the $\nu_{C\equiv N}$ peak due to the cyano groups moved from 2114 to 2118 cm^{-1}. In fact, the resulting RAIR pattern was very similar to that of the SAM prepared from a solution of 1,3-dicyano-2-mercaptoazulene and "bare" gold (please see Chapter 3 of this Thesis).

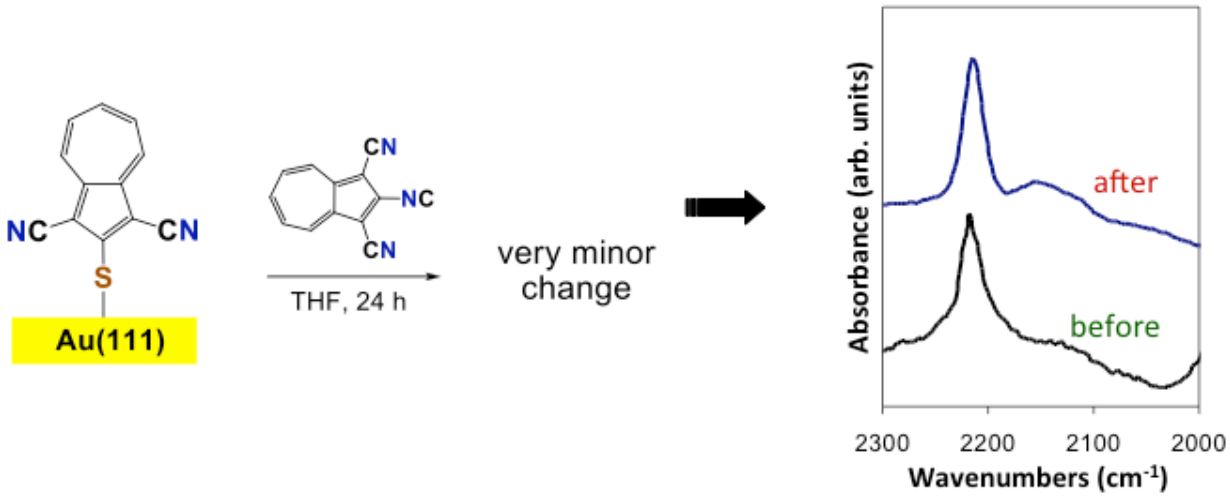

Figure IV.15 - Displacement experiment testing **2**'s ability to displace an existing SAM of 1,3-dicyano-2-mercaptoazulene on Au(111).

The reverse experiment, *i.e.*, exposing a pre-formed SAM of 1,3-dicyano-2-mercaptoazulene to a solution of **2**, produced minor RAIR changes at the baseline with no clear features assignable to $\nu_{C\equiv N}$ of a gold-bound isocyanide as seen in Figure IV.15 above. Importantly, this is the first monolayer film displacement study involving the RSH and RNC species with identical substituents R. In contrast, Kubiak *et. al.* previously demonstrated that octadecanethiol SAMs on Au(111) can be displaced by diisocyanoarenes, such as $CN(C_6H_4)_nNC$ (n = 1 – 3), in aprotic anhydrous solvents. [25] In the latter case, despite stronger Au-S than Au-CNR interactions, disruption of interchain packing *via* solvation of the adsorbed octadecanethiol molecules was thought to allow access to the surface by the isocyanide to effect disulfide reductive elimination. [25]

IV.5 Conclusions

This Chapter has described the synthesis of a new isocyanoazulene, **2**, and characterized films of **1** and **2** on Au(111) surfaces. Films of **1** have proven to be robust and survive in air for many days without any precautions taken against air. The synthesis of **2** is convenient as it comes from readily accessed azulenic derivatives. It was shown that incorporation of the nitrile ancillary spectroscopic reporters enhanced characterization of films of **2** on the surface. Use of spectroscopic reporters on mercaptan 1,3-dicyano-2-mercaptoazulene greatly facilitated the probing of displacement studies of isocyano- and mercaptoazulene films on gold. The displacement of the isocyano moieties exemplifies the higher affinity of the thiolate junction compared to the isocyano junction toward a gold surface.

Further competition experiments would provide insight into the role of electronics of the molecules in preferential binding of azulenic thiols versus isocyanides. Synthetic incorporation of nitrile reporters into the structures of other mercaptoazulenes will facilitate characterization of the corresponding novel molecular film materials.

IV.6 References

1 Tan, A., Balachandran, J., Sadat, S., Gavini, V., Dunietz, B.D., Jang, S., Reddy, P. Effect of length and contact chemistry on electronic structure and thermoelectric properties of molecular junctions. *Journal of the American Chemical Society*, **2011**, *133*, 8838-8841.

2 Mishchenko, A., Zotti, L.A., Vonlanthen, D., Bürkle, M., Pauly, F., Cuevas, J.C., Mayor, M., Wandlowski, T. Single-molecule junctions based on nitrile-terminated biphenyls: A promising new anchoring group. *Journal of the American Chemical Society*, **2011**, *133*, 184-187.

3 Faramarzi, V., Raimondo, C., Reinders, F., Mayor, M., Samori, P., Doudin, B. Optically switchable molecular device using microsphere based junctions. *Applied Physical. Letters*, **2011**, *99*, 233104/1-233104/3.

4 Lazar, M. and Angelici, R.J. Isocyanide binding modes on metal surfaces and in metal complexes, In *Modern Surface Organometallic Chemistry*; Basset, J.-M. Psaro, R., Roberto D., Ugo, R., Eds, Wiley-VCH, Weinheim, 2009 pp. 513–556.

5 McGinnis, David M. Synthesis and Coordination of Azulene- and Ferrocene-Based Isoyanide Ligands University of Kansas, 2011. UMI, Ann Arbor MI

6 Love, J.C., Estroff, L.A., Kriebel, J.K., Nuzzo, R.G., Whitesides, G.M. Self-assembled monolayers of thiolates on metals as a form of nanotechnology. *Chemical Reviews*, **2005**, *105*, 1103-1169.

7 Vericat, C., Vela, M.E., Benitez, G., Carro, P., Salvarezza, R.C. Self-assembled monolayers of thiols and dithiols on gold: new challenges for a well-known system. *Chemical Society Reviews*, **2010**, *39*, 1805-1834.

8 Dubois, L.H., Nuzzo, R.G. Synthesis, structure, and properties of model organic surfaces. *Ann. Rev. Phys. Chem.*, **1992**, *43*, 437-463.

9 Nuzzo, R.G., Zegarski, B.R., Dubois, L.H. Fundamental studies of the chemisorption of organosulfur compounds on gold(111) Implications for molecular self-assembly on gold surfaces. *J. Am. Chem. Soc.,* **1987**, *109*, 733-740.

10 Lazar, M. and Angelici, R.J. Isocyanide binding modes on metal surfaces and in metal complexes, In *Modern Surface Organometallic Chemistry*; Basset, J.-M. Psaro, R., Roberto D., Ugo, R., Eds, Wiley-VCH, Weinheim, 2009 pp. 513–556.

11 Kiguchi, M., Miura, S., Hara, K., Sawamura, M., Murakoshi, K. Conductance of a single molecule anchored by an isocyanide substituent to gold electrodes. *Applied Physics Letters*, **2006**, *89*, 213104.

12 Chinwangso, P., Jamison, A.C., Lee, T.R. Multidentate adsorbates for self-assembled monolayer films. *Accounts of Chemical Research*, **2011**, *44*, 511-519.

13 DuBose, D. L. Robinson, R. E. Holovics, T. C. Moody, D. R. Weintrob, E. C. Berrie, C. L.; Barybin, M. V. Interaction of mono- and diisocyanoazulenes with gold surfaces: first examples of self-assembled monolayer films involving azulenic scaffolds. *Langmuir*, **2006**, *22*, 4599-606.

14 Maher, T. R. Spaeth, A. D. Neal, B. M. Berrie, C. L. Thompson, W. H. Day, V. W.; Barybin, M. V. Linear 6,6'-Biazulenyl Framework Featuring Isocyanide Termini: Synthesis, Structure, Redox Behavior, Complexation, and Self-Assembly on Au(111). *Journal of the American Chemical Society* **2010**, *132*, 15924-15926.

15 Neal, B. M. Vorushilov, A. S. Delarosa, A. M. Robinson, R. E. Berrie, C. L.; Barybin, M. V. Ancillary nitrile substituents as convenient IR spectroscopic reporters for

self-assembly of mercapto- and isocyanoazulenes on Au(111). *Chemical Communications*, **2011**, *47*, 10803-10805.

16 Stapleton, J. J. Daniel, T. a; Uppili, S. Cabarcos, O. M. Naciri, J. Shashidhar, R.; Allara, D. L. Self-assembly, characterization, and chemical stability of isocyanide-bound molecular wire monolayers on gold and palladium surfaces. *Langmuir*, **2005**, *21*, 11061-11070.

17 Swanson, S.A., McClain, R., Lovejoy, K.S., Alamdari, N.B., Hamilton, J.S., Scott, J.C. Self-assembled diisocyanide monolayer films on gold and palladium. *Langmuir*, **2005**, *21*, 5034-5039.

18 Kiguchi, M., Miura, S., Hara, K., Sawamura, M., Murakoshi, K. Conductance of single 1,4-disubstitued benzene molecules anchored to Pt electrodes *Applied Physics Letters*, **2007**, *91*, 053110/1-053110/3.

19 Lörtscher, E., Cho, C.J., Mayor, M., Tschudy, M., Rettner, C., Riel, H. Influence of the Anchor Group on Charge Transport through single-molecule junctions *ChemPhysChem*, **2011**, *12*, 1677-1682.

20 Kim, B., Beebe, J.M., Jun, Y., Zhu, X.-Y., Frisbie, C.D. Correlation between HOMO alignment and contact resistance in molecular junctions: Aromatic thiols versus aromatic isocyanides *Journal of the American Chemical Society*, **2006**, *128*, 4970-4971.

21 Beebe, J.M., Kim, B., Frisbie, C.D., Kushmerick, J.G. Measuring relative barrier heights in molecular electronic junctions with transition voltage spectroscopy *ACS Nano*, **2008**, *2*, 827-832.

22 Zangmeister, C.D., Robey, S.W., van Zee, R.D., Kushmerick, J.G., Naciri, J., Yao, Y., Tour, J.M., Varughese, B., Xu, B., Reutt-Robey, J.E. Fermi level alignment in

self-assembled monolayer layers: the effect of coupling chemistry. *Journal of Physical Chemistry B*, **2006**, *110*, 17138-17144.

23 Lee, Y., Carsten, B., Yu, L. Understanding the anchoring group effect of molecular diodes on rectification. *Langmuir*, **2009**, *25*, 1495-1499.

24 Rodríguez-Bolívar, S. Gómez-Campos, F., Álvarez de Cienfuegos, L., Fuentes, N., Cárdenas, D., Buñuel, E., Carceller, J., Parra, A., Cuerva, J. Comductance and application of organic molecule pairs as nanofuses. *Physical Review, B*, **2011**, *83*, 125424/1-125424/11.

25 Henderson, J.I., Feng, S., Bein, T., Kubiak, C.P. Adsoprtion of diisocyanides on gold. *Langmuir*, **2000**, *16*, 6183-6187.

26 Pranger, L., Goldstein, A., Tannenbaum, R. Competitive self-assembly of symmetrical, difunctional molecules on ambient copper surfaces *Langmuir*, **2005**, *21*, 5396-5404.

27 Meyers, J.J., Jr., Barybin, M.V. Unpublished work.

28 Nozee, T., Set, S., Matsumura, S., Murase, Y. The synthesis of Azulene derivatives fromm troponoids. *Bulletin of the Chemical Society of Japan*, **1962**, *35*, 1179-1188.

29 Krimen, L.I. Acetic Formic Anhydride. *Organic Syntheses*, **1970**, *50*, 1-3.

30 (a) Clear, S.C., Nealey, P.F., *Langmuir*, **2001**, *17*, 720-732. b) Le Grange, J.D., Markham, J.L, Kurkjian, C.R., *Langmuir*, **1993,** *9*, 1749-1753. c) Wasserman, S.R., Whitesides, G.M., Tidswell, I.M., Ocko, B.M., Pershan, P.S., Axe, J.D. *Journal of the American Chemical Society*, **1989**, *111*, 5882-5861.

31 Barybin, M. V.; Meyers, J. J., Jr.; Neal, B. M. Renaissance of Isocyanoarenes as Ligands in Low-Valent Organometallic Chemistry. In *Isocyanide Chemistry: Applications in Synthesis and Material Science*. Nenajdenko, V., Ed. Wiley-VCH: Weinheim, 2012, pp 493-529. (ISBN-10: 3-527-33043-7).

32 Ditri, T.B., Fox, B.J., Moore, C.E., Rheingold, A.L, Figueroa, J.S. Effective control of ligation and geometric isomerism: Direct comparison of steric properties associated with bis-mesityl and bis-diisopropylphenyl *m*-terphenyl isocyanides. *Inorganic Chemistry*, **2009**, *48*, 8362-8375.

33 Holvics, T.C., Robinson, R.E., Weintrob, E.C., Toriyama, M., Lushington, G.H., Barybin, M.V. The 2,6-diisocyanoazulene motif: Synthesis and efficient mono- and heterobimetallic complexation with controlled orientation of the azulenic dipole. *Journal of the American Chemical Society*, **2006**, *128*, 2300-2309.

CHAPTER V

V. Overall Conclusions and Outlook

V. Overall Conclusions and Outlook

This dissertation's work has focused on the design of new azulenic materials and learning about their nature at the molecular level. Whereas the majority of azulene derivatives used in materials applications feature 1,3-substitution at the azulenic nucleus, this work has considered the electronically complementary systems based on the *linear* 2,6-azulenic scaffold that are attractive as organic electronics components. Compared to linear benzenoid aromatic molecular linkers, the 2,6-azulenic motif offers several unique advantages such as a remarkably small HOMO-LUMO gap and significant intrinsic dipole (*ca.* 1.0 Debye) associated with the aromatic framework. The latter phenomenon essentially makes the 2,6-azulenic scaffold being a potential molecular rectifier without the need of introducing chemically different substituents at the opposite ends of the aromatic moiety

Detailed understanding of the physicochemical characteristics of azulenic molecular films is critical before beginning to study their charge transport properties on bulk metal substrates. This Thesis has presented the chemistry of the first self-assembled monolayer films featuring linear biazulenic motifs with three different connectivities of the azulene units, as well as and several derivatives of mercaptoazulenes. The isocyanobiazulenic films were shown to adopt an approximately upright orientation of the molecules with respect to the Au(111) surfaces, as reported in Chapter 2. This work has allowed understanding of the chemical environment of the isocyanide junction groups and the molecular arrangement on the surface, which should facilitate further studies aimed at addressing charge transport across the biazulenic molecular bridges.

In Chapter 3, the films of several mercaptoazulenes were shown to have orientation of the molecules on the gold surface similar to that suggested for the analogous isocyanoazulene systems, i.e., approximately upright coordination of the molecules with respect to the surface. Study of the interactions of mercaptoazulenes and the Au(111) surface were greatly facilitated by incorporation of ancillary spectroscopic reporters, cyano functional groups, on the azulenic framework. These reporters observed in RAIRS spectra indicate that the 1,3-dicyano-2-mercaptoazulene films adopt upright orientations. As we have proven that air-stable films of these mercaptoazulenes on Au(111) are now obtainable, future work into investigating the differences in the charge transport properties between isocyanoazulenes and mercaptoazulenes is possible. The alignment of the Fermi level of the Au(111) surfaces and the molecular frontier orbitals of these mercaptoazulene units will be different compared to benzenoid systems, in part due to the fundamental difference in the aromatic delocalization energies of benzenoid and azulenic moieties. Also, the complementary mechanism of charge transport for thiol and isocyanide junctions may prove critical for future nanoelectronic applications and can now be explored with respect to these isocyano- and mercaptoazulenes.

Displacement studies directly comparing the affinity of the thiol and isocyanide junctions toward Au(111) were performed. By changing only the junction group in otherwise analogues molecules, the different affinities of each junction toward Au(111) was directly observed. The displacement of isocyanoazulenes by the mercaptoazulenes reaffirms the higher affinity of thiol linkers toward Au(111) compared to that of isocyanide linkers toward Au(111). These studies were greatly facilitated by incorporation of spectroscopic reporter units on the mercaptoazulene framework. The

synthesis of a structurally similar isocyanide with cyano spectroscopic reporters facilitated these displacement experiments. In the future, direct comparisons of the charge transport properties of isocyanide and thiol linkers will now be possible by understanding how to properly design mixed monolayer experiments such that both isocyano- and mercaptoazulene species are on the same Au(111) substrate. The use of mixed monolayer materials will facilitate conductive probe atomic force microscopy experiments, affording greater insight into differences in conductivities of isocyano- and mercaptoazulenes.

Appendix

Preliminary Synthesis of 1,3-Diisocyanoazulene

While this Thesis is focused on novel materials based on the 2,6-functionalized azulenic scaffold, preliminary synthetic studies were also conducted to address the feasibility of accessing hitherto unknown 1,3-diisocyanoazulene. This non-linear aromatic diisocyanide would be topologically complementary to the linear 2,6-diisocyanoazulene scaffold from the charge transport standpoint. Indeed, the former linker may be expected to primarily engage its HOMO to facilitate charge (hole) transfer between the metal termini, whereas the latter linear bridge has already been demonstrated to involve its LUMO in supporting charge (electron) delocalization.[3,4] Changing the connectivity positions of the junction groups on the azulenic framework should result in markedly different conductivity profiles of diisocyanoazulene linkers due to altering the alignment of the linker's frontier molecular orbitals with respect to the Fermi level of the metal surfaces.

A1. General procedures and starting materials for the synthesis of 1,3-Diisocyanoazulene

The syntheses of 1-nitroazulene and 1,3-dinitroazulene were performed according to Anderson, A.G., Jr., Scotoni, R., Jr., Cowles, E.J., Fritz, C.G., *Journal of Organic Chemistry,* **1957**, *22*, 1193-1196. Acetic-formic anhydride was prepared as reported elsewhere.[1] All other reagents were obtained from commercial sources and used as received.

Unless otherwise specified, all operations were performed in air. Chloroform was distilled over P_2O_5. Solution infrared spectra were recorded on a PerkinElmer Spectrum 100 FTIR spectrometer with samples sealed in 0.1 mm gas-tight NaCl cells. ^{1}H NMR samples were analyzed using a Bruker DRX-400 spectrometer. ^{1}H chemical shifts are given with reference to internal Me_4Si.

A.1.1 Synthesis of 1,3-diformamidoazulene (1)

To a solution of 1,3-dinitroazulene (0.079 g, 0.362 mmol) in 90 mL of toluene, 3 mL of *in situ* generated acetic formic anhydride was added, along with 1.27 g (10.7 mmol) of tin powder. The resulting mixture was then heated at 100 °C for 10 hours with stirring. Subsequently, the reaction was quenched by adding 200 mL of H_2O and transferred into a separatory funnel. The organic layer was separated and the aqueous layer was extracted with CH_2Cl_2 and ethyl acetate until this aqueous fraction turned nearly colorless. All organic extracts were combined, filtered through a medium porosity frit, washed with 100 mL of 10% K_2CO_3 , and dried with Na_2SO_4. The resulting mixture was filtered and the blue filtrate was then rotary evaporated to afford a hunter green powder of **1** (0.074 g, 0.345 mmol) in a 95 % crude yield. The product was used in the next step without further purification.

A.1.2 Synthesis of 1,3-diisocyanoazulene (2)

A solution/slurry of **1** (0.04 g, 0.19 mmol) in 25 mL of distilled CH_2Cl_2 was treated with neat diisopropylethylamine (0.06 mL, 3.5 mmol) via syringe immediately followed by phosphorous oxychloride (0.4 mL, 4.37 mmol) at room temperature. The color of the mixture changed from dark green to blue. After 1 hour of stirring, the reaction mixture turned purple-blue. The reaction was quenched with 10% K_2CO_3, transferred into a separatory funnel, and the organic and aqueous layers were separated. The aqueous fraction was extracted with 50 mL of CH_2Cl_2 twice. The organic fractions were combined and dried over Na_2SO_4. The drying agent was filtered off, and all solvent was removed from the filtrate under vacuum to afford compound **2** (0.015 g, 0.084 mmol) in a 45% yield as a black powder. FTIR (CH_2Cl_2): $\nu_{(C\equiv N)}$ 2118 cm^{-1}. ^1H

NMR (400 MHz, $CDCl_3$, 25 °C): δ 7.50 (t, $^3J_{HH}$ = 8.0 Hz, 2H, $H^{5,7}$), 7.73 (s, 1H, H^2), 7.90 (t, $^3J_{HH}$ = 8.0 Hz, 1H, H^6), 8.52 (d, $^3J_{HH}$ = 8.0 Hz, 2H, $H^{4,8}$).

A.2 Results and Discussion

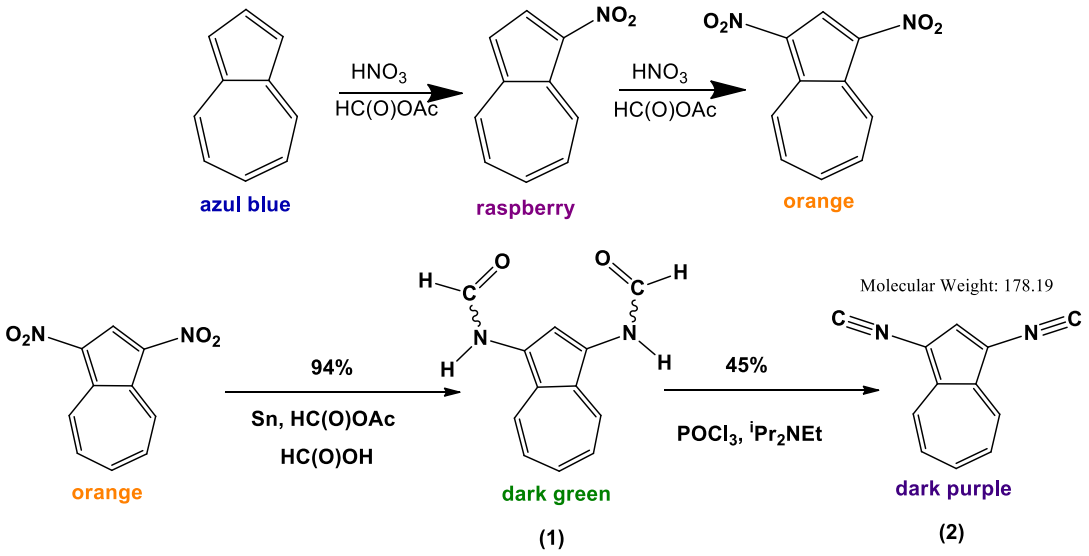

Scheme A.1 – Preliminary synthesis of 1,3-diisocyanoazulene

The preliminary synthesis of 1,3-diisocyanobiazulene (**2**), summarized in Scheme A.1, is based on the preparation of 1-isocyanoazulene previously reported by the Barybin group.[2] The author of this Thesis found the most challenging step to be the separation of 1-nitroazulene from 1,3-dinitroazulene after the second nitration. The preferred method is column chromatography on neural alumina, although even this procedure proved to have limited success at best because of very close R_f parameters for 1-nitroazulene and 1,3-dinitroazulene in all solvents tested. Soxlet extraction using $CHCl_3$ was also attempted but with little success. Upon obtaining a spectroscopically (^{1}H NMR, IR) pure sample of 1,3-dinitroazulene, the reductive formylation of the nitro groups afforded presumed 1,3-diformamidoazulene, which was immediately used in the next (dehydration) step without purification. Of note, attempts to reductively formylate a mixture of 1-nitroazulene and 1,3-dinitroazulene with the hope that the formamide products would be easier to separate from one another, resulted in poorer outcome with respect to the

desired diformamide product formation. Dehydration of the formamide was performed on an NMR scale to afford a crude sample of the diisocyanide **2**, the ^{1}H NMR spectrum of which was consistent with the presence of a symmetrically 1,2,3-substituted azulene scaffold but featured an additional resonance due to contamination with dichloromethane solvent.

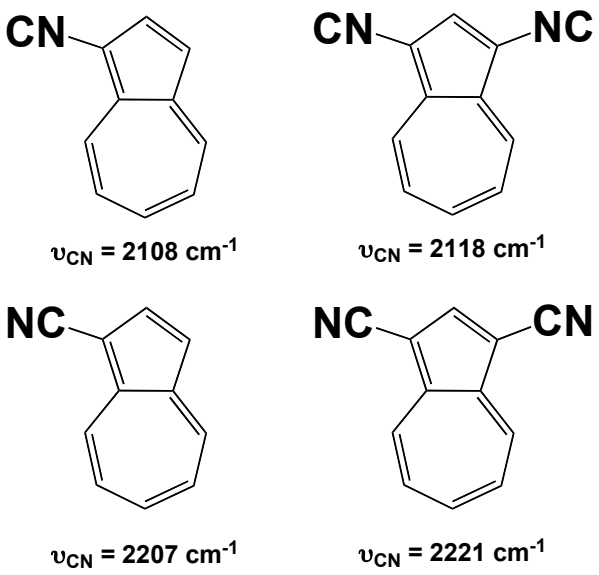

Figure A.1 - Comparison of the $\nu_{C\equiv N}$ values for 1-isocyano-, 1,3-diisocyano-, 1-cyano-, and 1,3-dicyano-substituted azulenes.

Interestingly, the $\nu_{C\equiv N}$ band for **2** occurs at a higher (*ca.* 10 cm^{-1}) energy than that for 1-isocyanoazulene. A similar trend can be noted for the nitrile stretching frequency documented for 1,3-dicyanoazulene versus 1-cyanoazulene.[2] In both cases, this can be rationalized by the electron-withdrawing effect of the second substituent on the strength of the other C≡N bond.

In order to make the synthesis of 1,3-diisocyanoazulene presented herein practical, the step involving isolation of 1,3-dinitroazulene will need to be substantially improved. Conducting the column chromatography of a 1-nitroazulene/1,3-dinitroazulene mixture under simple gravity

pressure may improve separation of the two components thereby increasing the yield of isolated pure 1,3-dinitroazulene. Optimization of the protocol (temperature, concentrations, reaction time, etc.) for double nitration of azulene to minimize the presence of 1-nitroazulene in the nitration product mixture should be attempted as well. In addition, the dehydration step converting diformamide **1** into diisocyanide **2** may benefit from conducting this reaction under air-free conditions to avoid product loss due to oxidation of the intermediates in solution.

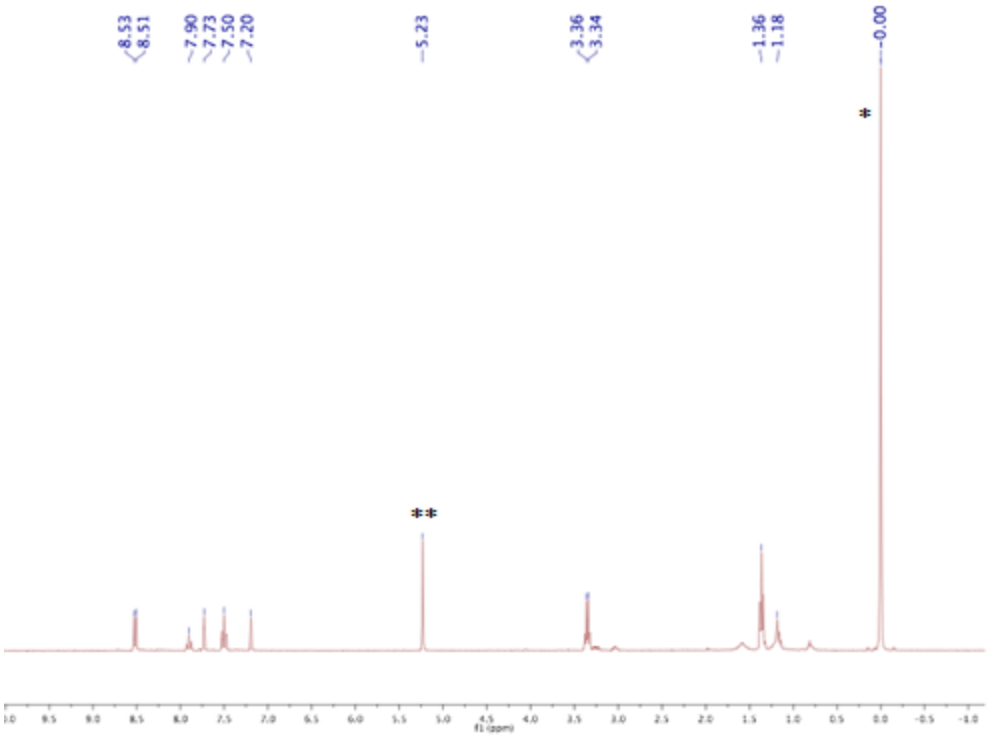

Figure A.2 – ^{1}H NMR spectrum of **2** in $CDCl_3$ at 25 °C. * Internal $SiMe_4$ resonance.

** Residual CH_2Cl_2 solvent that was used in the preparation of (**2**). The peak at 7.20 is a residual NMR solvent resonance ($CHCl_3$).

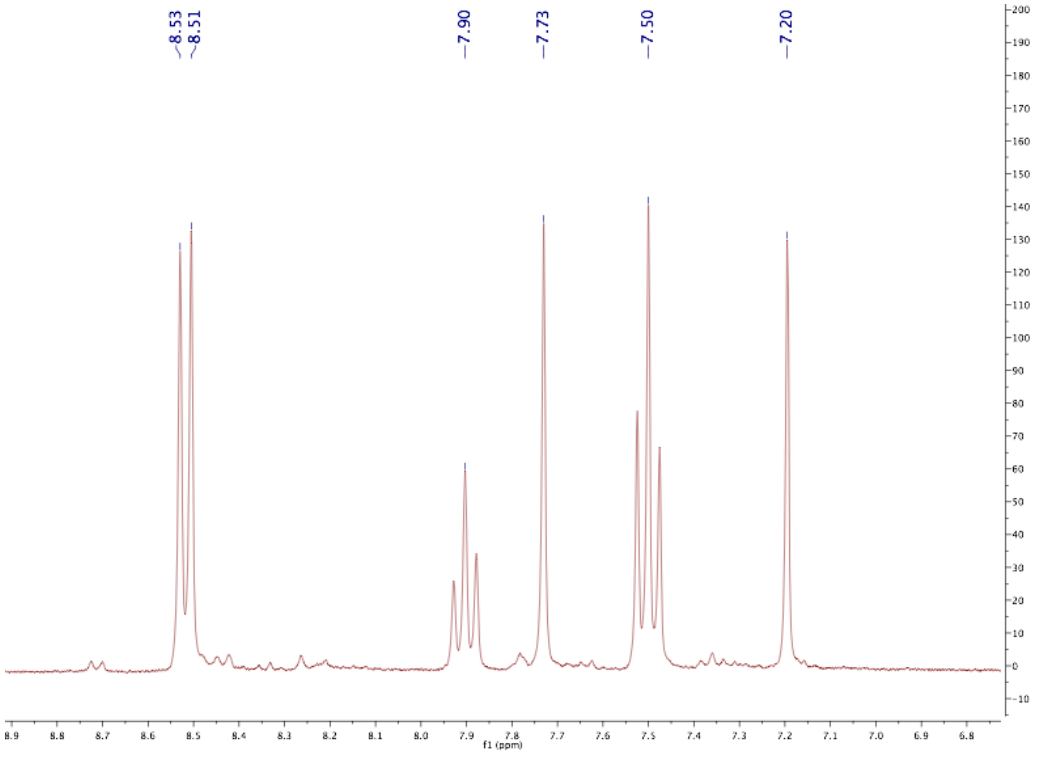

Figure A.3 – Aromatic region of the ^{1}H NMR spectrum of **2** in $CDCl_3$ at 25 °C.

A.4 References

1. McGinnis, David M. Synthesis and Coordination of Azulene- and Ferrocene-Based Isoyanide Ligands University of Kansas, 2011. UMI, Ann Arbor MI.

2. Robinson, R.E., Holovics, T.C., Deplazes, S.F., Powell, D.R., Lushington, G.H., Thompson, W.H., Barybin, M.V. Five Possible Isocyanoazulenes and Electron-Rich Complexes Thereof: A Quantitative Organometalic Approach for Probing Electronic Inhomogeneity of the Azulenic Framework. *Organometallics*, **2005**, *24*, 2386-2397.

3. Holovics, T. C., Robinson, R. E., Weintrob, E. C., Toriyama, M., Lushington, G. H., Barybin, M. V. The 2,6-Diisocyanoazulene Motif: Synthesis and Efficient Mono- and Heterobimetallic Complexation with Controlled Orientation of the Azulenic Dipole. *Journal of the American Chemical Society,* **2006**, *128*, 2300-2309.

4. Barybin, M. V., Chisholm, M. H., Dalal, N. S., Holovics, T. H., Patmore, N. J., Robinson, R. E., Zipse, D. J. Long-Range Electronic Coupling of MM Quadruple Bonds (M = Mo or W) via a 2,6-Azulenedicarboxylate Bridge. *Journal of the American Chemical Society,* **2005**, *127*, 15182-15190.